CHARACTERISTICS AND APPLICATION POTENTIAL OF AN ALCOHOL OXIDASE FROM THE HYDROCARBON - DEGRADING FUNGUS *ASPERGILLUS TERREUS*

A THESIS

submitted by

ADEPU KIRAN KUMAR

for the award of the degree

of

DOCTOR OF PHILOSOPHY

DEPARTMENT OF BIOTECHNOLOGY

INDIAN INSTITUTE OF TECHNOLOGY GUWAHATI

JANUARY 2009

Dedicated to my Beloved Parents & Puchyadal

Department of Biotechnology

INDIAN INSTITUTE OF TECHNOLOGY GUWAHATI

STATEMENT

I do hereby declare that the matter embodied in this thesis is the result of investigations carried out by me in the Department of Biotechnology, Indian Institute of Technology Guwahati, India, under the guidance of Dr. Pranab Goswami.

In keeping with the general practice of reporting scientific observations, due acknowledgements have been made wherever the work described is based on the findings of other investigators.

January, 2009. Adepu Kiran Kumar

DEPARTMENT OF BIOTECHNOLOGY

Indian Institute of Technology Guwahati
Guwahati 781 039, Assam, INDIA

Dr. Pranab Goswami

Associate Professor & Head

Tel: +91-(0)361 2582202
Fax: +91-(0)361 2582249/2690762
Email: pgoswami@iitg.ernet.in

CERTIFICATE

This is to certify that the thesis/dissertation entitled "**Characteristics and application potential of an alcohol oxidase from the hydrocarbon-degrading fungus *Aspergillus terreus***", that is being submitted by **Mr. Adepu Kiran Kumar** for the award of degree of Doctor of Philosophy is an authentic record of the results obtained from the research work carried out under my supervision in the Department of Biotechnology, Indian Institute of Technology Guwahati, India.

The results embodied in this thesis have not been submitted to any other University or Institute for the award of any degree.

January, 2009.

Dr. Pranab Goswami
Associate Professor
(Research Supervisor)

ACKNOWLEDGEMENTS

The thesis is ready… I look at this manuscript wondering how I managed to squeeze the last four years into 130 pages of text and figures. But then I look more carefully and I see all of what is written in between the lines. All the discussions we had, coffee (and dinner) breaks, games, "gossiping", group meetings, alcheringa, techniche, & manthan events but also my visits to the lab when all the others were sleeping, enjoying in the rain, little frustrations caused for instance during protein purifications that, for unknown reason, did not work for weeks, *etc*. All of it is an integral part of this thesis.

The thesis is ready… I am filled with pride but at the same time I realize it would not be possible without the help of many people. It is now the time to acknowledge you all.

First my guide, Dr. Pranab Goswami, I would like to thank him for giving me the opportunity to perform research in his lab and for all the support I got from him over these years. He showed me the guidelines I hope to follow in the future. Several people deserve special acknowledgements. Dr. Ghosh, Dr. Bora and Dr. Khijwania I thank for endless discussions, critical evaluations and all the support they gave me. I would like to thank Ms. Preety Vatsyayan, for her support and useful discussions in designing several critical experiments.

I would like to mention all the members of my research group, those who shared every small events: Shiva, Preety, Gopi, Lepakshi, Vishnu, Raju, the friendly atmosphere created in the lab and also in the hostel compensated for the separation with my family and friends. They all inspired me to become a Ph.D. student in this group. Also, colleagues that joined the group later: Naresh, Urmila, Seraj, Asim, and Vinod, each of them contributed to the fact that I felt really well in the group and they were always there to help. Thank you all. Our wonderful non-teaching staff members: Nurul, Anitha and Sharan, I would like to acknowledge their inestimable help in administrative works I had to go through during all these years.

My brothers, Nagraj (toppanagulu) and Rajesh, friends Shiva and Preety, the preparations for the seminars would be very difficult without them. Also, I would like to mention people without whom my life in the Guwahati would not be the same, Vijay Raj, Dr. Gopi, Dr. Ramaraju, Dr. Veerababu, they have been great friends. I would not get to this point without the support of my best friends, Raghavendra and Srilatha. It is a great honor to have in my life. Finally my beloved Parents, I thank for their patience and encouragement all the time. I am grateful for all the support and kindness I received from them.

Adepu Kiran Kumar

January 2009

ABSTRACT

A hydrocarbon-degrading *Aspergillus terreus* was isolated from the oil contaminated soil. The organism could degrade a wide range of petroleum hydrocarbons including the immediate oxidation products of hydrocarbons, like alkanols and alkanals. Among all the linear chain carbon substrates, highest growth of 39 ± 4 g l^{-1} (wet weight) was observed when *n*-hexadecane was used as the sole source of carbon and energy. Using SEM the morphological change of the hyphae during growth of the fungi on hydrocarbon substrates was demonstrated. In glucose-grown cells the hyphae were smooth with a thick cell wall, whereas, the cell wall of the *n*-hexadecane cells was uneven and thin. The adaptation of the cells for up taking the hydrophobic hydrocarbon substrates through sorption mechanism and accumulation of high lipid content in the cells, as evident from the nearly seven-fold more lipid production (4.4 g%) in the *n*-hexadecane-grown cells than the glucose-grown cells (0.62 g%), were attributed to the observed morphological change. Analyses of the fatty acid profile by ESI/MS in the isolated lipid showed that nine different fatty acids induced in the hexadecane-grown cells were void in the glucose-grown cells. The oleic acid and palmitic acid were the fatty acids with highest peak intensity in the spectral profile corresponding to the glucose-grown cells and hexadecane-grown cells, respectively. It was revealed by analyzing the percentage distribution of different fatty acids in each cell type that palmitic and stearic acids were the predominant fatty acids in the hexadecane-grown cells; whereas, oleic and linoleic acids were the predominant fatty acids observed in the glucose-grown cells. Unlike glucose-grown cells, considerably high amount of fatty acids with chain length C_{32} and C_{33} were present in *n*-hexadecane-grown cells and each accounted nearly 9% (based on peak intensity) of the total fatty acid content in the cells. A microsomal membrane bound alcohol oxidase enzyme was isolated from this fungus during its growth on *n*-hexadecane substrate. This oxidase could oxidize short chain alcohol-,

long chain alcohol-, secondary alcohol-, and aryl alcohol- substrates and was localized in the microsomes of the cell. The optimal pH and temperature of the enzyme were found to be 8.1 ± 0.5 and 27-33 ^{o}C, respectively. The stability of the alcohol oxidase was drastically decreased beyond 30 ^{o}C. The enzyme showed 33% enantiomeric excess for the *R*(-)2-octanol over *S*(+)2-octanol, which may be correlated with the lower K_m values of the enzyme for the *R*(-)2-octanol than the *S*(+)2-octanol. The fluorescence emission spectrum of the protein (at 443 nm excitation) was similar to that obtained with authentic FAD. In this flavoenzyme, flavin was non-covalently but avidly associated. The native protein molecular mass was 269 ± 5kDa and the subunit molecular masses were 85-, 63-, 43-, 27-, and 13-kDa. The enzyme showed highest affinity for *n*-heptanol (K_m = 0.498 mM, K_{cat} = 2.7 x 10^2 s^{-1}). The isoelectric point of the proteins was within 8.3-8.5. High aggregating property of the protein was demonstrated by AFM, DLS and TEM analyses. Chemical analysis showed the presence of oleic acid and palmitic acid at a ratio of 2:1 in the purified protein. The high aggregating property of the alcohol oxidase may be correlated with the observed lipoidic nature of these protein particles. Peptide mass fingerprinting studies showed the presence of two FAD binding domains in 63kDa protein. Among these two FAD binding domain sequences only the YPVIDHEYDAVVV**G**A**G**GA**G**LR peptide shows 45-50% sequence similarity with the reported N-terminal sequences of other known alcohol oxidases. Non-redundant database search of 63- and 43-kDa subunits peptide sequences showed no sequence similarity with the other alcohol oxidase protein reported till now. The aggregated multimeric alcohol oxidase protein when treated with *β*-mercaptoethanol (*β*-ME) at an optimum concentration of 0.74M for 8 h at 4 ^{o}C, the protein was dissociated to subunit level and also nearly 87% of the total flavin present in the native protein was simultaneously separated. This dissociation process had traversed through two intermediate protein (IP) stages, IP_1 and IP_2, which were associated with the FAD. The IP_1 (size 10 nm) that contained the subunits 85-, 63-, 43-, 25-, 13-kDa was functionally active, whereas, the IP_2 (size 9 nm) that contained 85-, 63-, 25-, 13-kDa was inactive, which indicates the critical role of the 43kDa protein for the alcohol oxidase activity. A functionally inactive reconstituted apoprotein (P_R) with molecular mass and subunits similar to IP_1 was generated upon removal of *β*-ME from the subunit level dissociated proteins. The P_R when mixed with FAD and incubated

prolong with substrate (minimum 12 hr), a catalytically active P_R was formed and is evident from the protein conformational change (at 280 nm) and FAD emission quenching (at 525 nm) studies. The solvent effect caused by the high concentration of β-ME is attributed to the observed dissociation and associated deflavination of these multimeric alcohol oxidase protein particles. The alcohol oxidase protein reported here was demonstrated as a green catalyst in several oxidation reactions due to its catalytic activity for high molar yield conversions of broad range of alcohols to the corresponding carbonyl compounds under room temperature, atmospheric pressure and aqueous environment. The application potential of this enzyme for kinetic resolution of secondary alcohols is also foreseen with further optimization of the reaction parameters for the conversion.

CONTENTS

LIST OF FIGURES

LIST OF TABLES

ABBREVIATIONS

AAO ……..	Aromatic alcohol oxidase
ABTS ……	2,2'-azino-bis[3-ethylbenzothiazoline-6-sulfonic acid] diammonium salt
ACN ……..	Acetonitrile
ADH ……..	Alcohol dehydrogenase
AOX ……..	Alcohol oxidase
BSA ……...	Bovine serum albumin
CBB ……...	Coomassie brilliant blue
CHAPS ……..	3-[(3-cholamidopropyl) dimethyl ammonio] propane-1-sulfonic acid
CLSM ……	Confocal laser scanning microscopy
Cyt P450 ……	Cytochrome P450
1,12DCD ……..	1,12 Dichlorododecane
DCPIP ……...	Dichlorophenol indophenol
DEAE ……	Diethyl amino ethyl
DLS ……...	Dynamic light scattering
DMSO ……...	Dimethyl sulfoxide
DNPH ……	Dintrophenyl hydrazine
DTNB ……	Dithionitro benzoic acid
DTT ……...	Dithiothretol
EC ……..	Enzyme commission
EDTA ……	Ethylenediamine tetraacetic acid
FAD ……...	Flavin adenine dinucleotide
FAO ……...	Fatty alcohol oxidase
FMN ……..	Flavin mononucleotide
FPLC …….	Fast performance liquid chromatography
x *g* ……..	Relative centrifugal force
GMC ……..	Glucose-methanol-choline
HPLC ……	High performance liquid chromatography
HRP ……...	Horse radish peroxidase
IP ……...	Intermediate protein

LCAO ……	Long chain alcohol oxidase
LC-ESI/MS …..	Liquid chromatography-Electrosray Ionization-Mass spectrometry
β-ME …….	*β*-Mercaptoethanol
MTCC ……...	Microbial type culture collection
NAD^+ ……	Nicotinamide adenine dinucleotide (oxidized)
$NAD(P)^+$ ……...	Nicotinamide adenine dinucleotide phosphate (oxidized)
PBO	Piperonyl butoxide
PCMB	*p*-Chloro mercuri benzoic acid
PEG	Polyethylene glycol
P_R	Re-associated protein
PUFA	Poly unsaturated fatty acid
R_f	Retention factor
SCAO	Short chain alcohol oxidase
SAO	Secondary alcohol oxidase
SDS-PAGE	Sodium dodecyl sulfate-polyacrylamide gel electrophoresis
SEM	Scanning electron microscope
TCA	Trichloro acetic acid
Tris	Tris(hydroxymethyl)aminomethane
TEM	Transmission electron microscopy
UPLC	Ultra performance liquid chromatography

INTRODUCTION

The microbial degradation of hydrocarbons is a subject of interest among the researchers from diverse areas such as, bioremediation of oil contamination, production of secondary metabolites, biocatalysis and biotransformation *etc*. The metabolic pathways involved in these degradations have been studied intensively since last several decades and is fairly understood in case of bacteria and yeasts. However, the knowledge on the metabolism of hydrocarbon by filamentous fungi is not yet sufficiently acquired, although the potential of this eukaryotic organism on bioremediation of hydrocarbon and production of industrially important secondary metabolites using hydrocarbon substrates have been widely acclaimed. While the group of enzymes involved in these metabolisms has been identified to a greater extent, the characteristics of these enzymes and their potential applications have not been studied deeply. We focus our attention on the redox enzymes induced to catabolize these highly hydrophobic aliphatic hydrocarbon substrates by filamentous fungi, speculating the existence of enzymes bearing novel characteristics to catalyze such substrates of extreme physical nature. The oxidation of alcohols is one of the critical steps occurred during the microbial degradation of aliphatic hydrocarbons. This oxidation process is largely catalyzed by alcohol oxidase enzyme in case of filamentous fungi. Considering the enormous importance of alcohol oxidase enzymes in the development of various industrial processes and products, we direct our investigation to explore the characteristics and application potential of the alcohol oxidase produced by filamentous fungi during its growth on long chain alkane substrates.

The study embodied in this thesis is categorized into the following chapters:

Chapter 1: Literature Review

The objective of this chapter is to summarize the progress of the work on the subject as a whole, focusing the gaps and important findings on the area. Current knowledge on the redox enzymes involved in the oxidation of alcohols to the corresponding aldehyde or ketone from different sources is also presented here. A brief introduction with relevant literature is also included in each of the chapters to facilitate the readers to understand the respective background works.

Chapter 2: Isolation and Identification of a Hydrocarbon-Degrading Filamentous Fungus

The work presented in this thesis is based on an indigenously isolated hydrocarbon-degrading filamentous fungus endemic to this geographical location**.** The organism is deposited in a national depository, Microbial Type Culture Collection (MTCC), Chandigarh, so that the strain would be available to other researchers of the world. The growth characteristics of the isolated fungus were studied in various hydrocarbons as well as in glucose, a readily assimilating substrate for comparisons. The metabolic consequence on assimilation of these high energy hydrophobic substrates by the fungus was also investigated by analyzing the cellular lipid and fatty acid profile and presented in this chapter.

Chapter 3: Studies on Substrate Specificity and Sub-cellular Location of the Alcohol Oxidase

This chapter describes the isolation and sub-cellular localization of the alcohol oxidase from the fungus. The substrate specificity and optimum physical and chemical parameters for enzyme activity are also presented.

Chapter 4: **Purification and Functional Characterization of the Alcohol Oxidase**

The purification of the isolated alcohol oxidase and the novel physical and chemical characteristics of the enzyme revealed from the investigation are illustrated in this chapter.

Chapter 5: Dissociation, Deflavination and Reconstitution Studies of the Alcohol Oxidase

To understand the structure-function relationship of the isolated broad substrate specific multimeric flavo-enzyme, study was conducted on dissociating the enzyme protein into subunit level followed by analyzing the generated subunits for their functional activities. Studies on the reconstitution of the dissociated subunits and flavin cofactor and subsequent catalytic reactivation of the reconstituted protein-flavin complex were also undertaken with an aim to understand the nature of this multimeric enzyme as well as to explore a reconstitution approach for developing enzyme electrode for bio-electronic devices. Detail findings on the above investigations are included in this chapter.

Chapter 6: Application Potential of the Alcohol Oxidase as Biocatalyst

The catalytic activity of the isolated alcohol oxidase for the production of aldehyde or ketones from the corresponding primary or secondary alcohols were investigated in aqueous and ambient environment with an aim to explore the potential of this biocatalyst for green chemistry applications. The catalytic activity of the enzyme was studied on a wide range of substrates and incorporated the detail findings in the present chapter.

Chapter 7: Conclusions and Scope for Future Work

Critical analyses on the findings embodied in this thesis along with the scope for further research work are forwarded in this concluding chapter.

Chapter 1

LITERATURE REVIEW

In nature the direct conversion of alcohol to the corresponding carbonyl compound is known to catalyze primarily by two different enzymes, namely alcohol dehydrogenase and alcohol oxidase. The mechanism of catalysis is different as shown in the scheme 1.1.

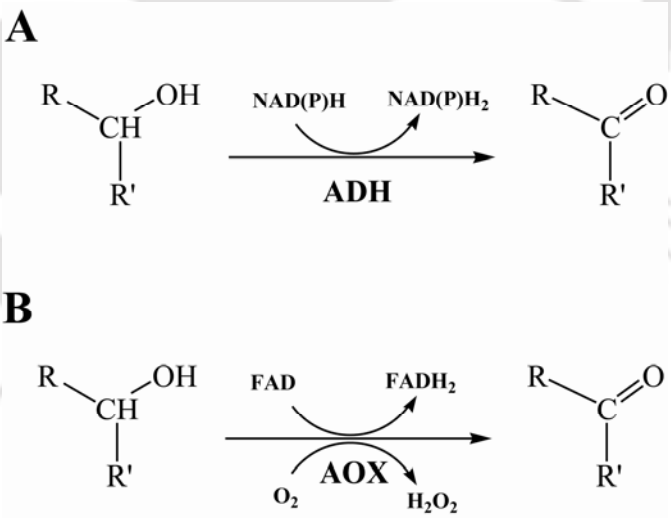

Scheme 1.1: [**A**] Alcohol dehydrogenase (ADH) as catalyst and [**B**] Alcohol oxidase (AOX) as catalyst. R' = -H or any other alkyl/aryl group.

Considering the focus of our work on alcohol oxidase we are presenting here only a brief description on the alcohol dehydrogenase followed by the literature review on the enzyme alcohol oxidase.

1.1. ALCOHOL DEHYDROGENASE

Alcohol dehydrogenases (Alcohol: NAD^+ oxidoreductase; EC 1.1.1.1) are widely distributed in animals, plants and lower microorganisms and are, by far, the most thoroughly studied of all the enzymes that catalyze this reaction as evident from the literatures reviewed in some of the selected papers on the subject [Radianingtyas & Wright 2003; Reid & Fewson 1994; Sofer & Presley 1987]. Humans have at least six slightly different alcohol dehydrogenases. These proteins exist in multiple forms as a dimer with a subunit mass of approximately 80 kDa and are encoded by at least seven different genes [Hammes-Schiffer *et al.,* 2006]. In humans and many other animals, they serve to breakdown alcohols which could otherwise be toxic; in yeast and several bacteria, some alcohol dehydrogenases catalyze the opposite reaction as a part of fermentation. Pyridine nucleotide-linked alcohol dehydrogenases from liver and yeast have been studied in great detail from both the structure and mechanism point of view as even evident from the comprehensive reviews on the topic published three decades ago [Dalziel 1975; Brandem *et al.,* 1975]. There are five classes (I-V) of alcohol dehydrogenases. The hepatic form that is primarily used in humans is class I. Class I consists of A, B, and C subunits that are encoded by the genes ADH1A, ADH1B, and ADH1C. The enzyme is present in the lining of the stomach and in the liver. The main alcohol dehydrogenase in yeast is larger than the human one, consisting of four rather than just two subunits. Together with the zinc-containing alcohol dehydrogenases of animals and humans, these enzymes from yeasts and many bacteria form the family of "long-chain"-alcohol dehydrogenases [Jornvall *et al.,* 1987]. Another family of alcohol dehydrogenase contains iron [Scopes 1983]. They occur in bacteria, and an apparently inactive form has also been found in yeast.

The alcohol dehydrogenase enzymes catalyze the inter-conversion between alcohols and aldehydes or ketones as shown in Scheme 1.1(A). This catalytic property of the enzyme is exploited for the biotransformation processes as well as for the function of many biofuel cells [Ernst *et al*., 2005; Nicolau *et al*., 2007; Kragl *et al*., 1996; Blacklock *et al*., 1993; Ramanavicius *et al*., 2005, 2008]. In the biotransformation processes these dehydrogenase enzymes are commonly used for the synthesis of enantiomerically pure chiral alcohols. In contrast to the chemical process, the enzymes yield directly the desired enantiomer of the alcohol by reduction of the corresponding ketone.

1.2. ALCOHOL OXIDASE

The alcohol oxidase activity was first reported by Janssen *et al.,* [1965]. Alcohol oxidase (Alcohol: O_2 oxidoreductase) catalyzes the oxidation of alcohols to the corresponding aldehydes or ketones in similar way to the ADH, where AOX requires molecular oxygen as a co-substrate as shown in Scheme 1.1B. During the oxidation process it does not require supplementation of any external cofactor unlike ADH, where external supply of NAD^+ is prerequisite to carry out the reaction. This makes the alcohol oxidase protein a high potential biocatalyst than the aldehyde dehydrogenase for several applications. Alcohol oxidase belongs to the group of glucose-methanol-choline (GMC) oxidoreductase family proteins [Cavener 1992], and are largely found in plants, fungi and yeasts [Banthorpe *et al.,* 1976]. Based on the substrate specificity, the alcohol oxidases (EC 1.1.3.x) are classified into different groups as described below:

1.2.1. Short chain alcohol oxidase (EC 1.1.3.13)

1.2.2. Long chain alcohol oxidase (EC 1.1.3.20)

1.2.3. Secondary alcohol oxidase (EC 1.1.3.18)

1.2.4. Aromatic alcohol oxidase (EC 1.1.3.7)

1.2.1. Short Chain Alcohol Oxidase (EC 1.1.3.13)

It is most commonly known as, alcohol oxidase, methanol oxidase, ethanol oxidase, *etc.* that catalyzes the oxidation of lower chain length alcohols in the range of C_1-C_8 carbons [Janssen & Ruelius 1968; Sahm & Wagner 1973; Tani *et al.,* 1972b]. It is the extensively studied enzyme among all the other alcohol oxidases as evident from voluminous publications and several reviews on this topic [Janssen *et al*., 1975; Yamada *et al*., 1979; Bringer *et al*., 1979; Nichols *et al*., 1980; Couderc & Barrati 1980; Patel *et al.*, 1980; Sahm *et al*., 1982; Geissler *et al.,* 1986; Van der Klei *et al.,* 1990; Cromartie 1981; Eriksson & Nishida 1988; Grewal *et al*., 2000; Danneel *et al*., 1994; Badea & Arsene 1996; Suye 1997; Stewart *et al*., 2001; Ozimek *et al*., 2005; Alvarado-Caudillo *et al*., 2002; Dienys *et al*., 2003; Gunkel *et al*., 2004; De Hoop *et al*., 1991; Kato *et al*., 1976; Evers *et al*., 1994; Segars *et al*., 2001; Szamecz *et al*., 2005]. Alcohol oxidase is the key enzyme of methanol metabolism in methylotrophic yeast species. It catalyses the first step of methanol catabolism, where methanol is converted to formaldehyde with concomitant production of hydrogen peroxide. The

generalized name "alcohol oxidase" is adopted from the fact that *in vitro* this enzyme also oxidizes other short chain aliphatic alcohols. The alcohol oxidase isolated from the leaves of *T. vulgare* primarily accepts C_6-C_{10} straight-chain primary alcohols and for which alcohols with chain length less than C_5 or more than C_{15} are very poor substrates [Banthorpe *et al.,* 1976]. The alcohol oxidase from is largely reported as octameric protein [Couderc & Baratti 1980; Kato *et al*., 1976; Suye 1997], with the exceptions of *C. tropicalis* [Dickinson & Wadforth 1992] and *T. vulgare* [Banthorpe *et al*., 1976], where the dimeric nature of the enzyme was demonstrated. The AOX protein and the regulation of the gene encoding AOX have been studied for decades for several reasons [Holzmann *et al*., 2002; Gurkan *et al*., 2004]. Firstly, the promoter that controls AOX expression is known to be one of the strongest promoters in nature and, at the same time, one of the most tightly controlled yeast promoters [Raschke *et al*., 1996; Romanos *et al*., 1992; Cregg *et al*., 1989; Cos *et al*., 2006]. Secondly, AOX protein itself is of high industrial interest. It constitutes, for instance, the main component of an alcohol sensor [Akyilmaz & Dinckaya 2000; Azevedo *et al.,* 2005] because of the various favourable properties of the enzyme such as, (i) the high affinity for primary alcohols, (ii) the high stability of the active form of the enzyme, and (iii) its easy availability, as AOX protein may comprised up to 30% of total cellular protein [Van Dijeken *et al*., 1976; Veenhuis *et al*., 1983; Guiseppin *et al*., 1988].

The biochemical and kinetic characteristics of short chain alcohol oxidase (SCAO) described in some prominent publications is given in table 1.1 and 1.2.

Table 1.1: Localization and protein chemical characteristics of SCAO from different sources

Source organism	Localization	Protein chemical characteristics		References
		Oligomeric nature and Molecular weight	Co-factor	
Peniophora gigantea	-----	576kDa, Homooctamer (72.5kDa)	FAD	Danneel *et al*., 1994
Achatina achatina	membrane bound	-----	-----	Grewal *et al*., 2000
Achatina fulica	membrane bound	-----	-----	Grewal *et al*., 2000
Arion ater	membrane bound	-----	-----	Grewal *et al*., 2000
Helix aspersa	endoplasmic reticulum membrane bound	-----	-----	Grewal *et al*., 2000
Basidiomycetes sp	-----	300kDa	FAD	Janssen & Ruelius 1968
Candida boidinii	-----	600kDa, Homooctamer (74kDa)	FAD	Bormann & Sahm 1978; Veenhuis *et al*., 1989; Nichols & Cromartie 1980
	microbody	-----	-----	Geissler *et al*., 1986
	peroxisome	-----	-----	Sahm *et al*., 1982
Candida methanosorbosa	-----	620kDa, Homooctamer (80kDa)	FAD	Suye 1997
Candida 25-A	-----	520kDa, Homooctamer (65kDa)	FAD	Yamada *et al*., 1979
Hansenula polymorpha	cytoplasm	600kDa, Homooctamer	FAD	Couderc *et al*., 1980
	peroxisome	-----	-----	Van der Klei *et al*., 1990
Phanerochaete chrysosporium	-----	310kDa, Homotetramer (75kDa)	FAD	Eriksson *et al*., 1988
Pichia pastoris	cytoplasm	675kDa, Homooctamer (80kDa)	FAD	Couderc *et al*., 1980
	chromosome	-----	-----	Hwang *et al*., 2000

Cont…

Source organism	Localization	Protein chemical characteristics		References
		Oligomeric nature and Molecular weight	Co-factor	
Pichia sp.	-----	300kDa, Homotetramer (76kDa)	FAD	Patel *et al.*, 1981
Polyporus obtusus	-----	------	FAD	Janssen *et al.*, 1975
Saccharomyces cerevisiae	chromosome, peroxisome	------	------	Hwang *et al.*, 2000
Chrysomela populi	extracellular	------	------	Bruckmann *et al.*, 2002
Phratora vitellinae	extracellular	------	------	Bruckmann *et al.*, 2002
Candida tropicalis	membrane	------	------	Dickinson & Wadforth 1992
Solea senegalensis	peroxisome	------	------	Komduur *et al.*, 2002

Table 1.2: Substrates and kinetic parameters of SCAO from different sources

Source organism	Substrate and K_m (mM) value	pH optima and range	Temperature optima and range (°C)	pH stability	Temperature stability (°C)	Inhibitors	References
Peniophora gigantea	1) Ethanol & 2.9 2) Methanol & 1.8	7.3-9.0	------	6.0-9.0	22	Cu^{2+}, $FeSO_4$, $NiCl_2$	Danneel *et al.*, 1994
Basidiomycetes sp.	1) Methanol & 1.52 2) Ethanol & 10	6.3-9.0	------	7.0-9.0	25	------	Janssen & Ruelius 1968
	------	------	------	5.0-6.5	------	------	Janssen *et al.*, 1975
Candida boidinii	1) Methanol & 3 3) 2-Propin 1-ol & 10 4) 1,4-Butynediol & 36						Nichols & Cromartie 1980
	-------	7.5-9.5	30	7.0-10.0	------	Cu^{2+}, PCMB H_2O_2,Ag^{+}	Sahm *et al.*, 1982

Cont…

Source organism	Substrate and K_m (mM) value	pH optima and range	Temperature optima and range (°C)	pH stability	Temperature stability (°C)	Inhibitors	References
Candida boidinii	-------	-------	------	-------	------	Diethyldicarbonate, Iodoacetate, PCMB, Sodium acetate	Geissler *et al.*, 1986
	------	------	------	6.5-8.5	------	------	Cromartie 1981
	------	------	------	------	------	Cyclopropanone	Cromartie 1982
Candida methanosorbosa	1) Methanol & 2.43 2) Ethanol & 8.23	6.0-9.0	50	------	30-65	Cu^{2+},Hg^{2+}, PCMB, Hydroquinone	Suye 1997
Candida 25-A	1)Methanol & 0.019 2) Ethanol & 0.13	7.5	37.5	6.0-8.0	30-60	1,10-Phenanthroline, KCN, PCMB, Phenylhydrazine	Yamada *et al.*, 1979
Hansenula polymorpha	1) Ethanol & 16.2 2) Methanol & 2.15	8.5 & 6.7-9.8	------	------	------	Formaldehyde, Hydroxylamine	Badea *et al.*, 1996
	------	5.5-8.5	------	5.5-8.5	20-45	------	Vanderklei *et al.*, 1990
	------	------	------	8.0-10.0	------	------	Couderc *et al.*, 1980
Helix aspersa	1) Butanol & 0.075 2) Propanol & 0.067	------	------	------	------	------	Grewal *et al.*, 2000
Phanerochaete chrysosporium	------	6.0-10.5	------	------	------	------	Eriksson *et al.*, 1988
	1) Methanol & 0.785 2)Ethanol & 1.97	6.0-10.5 & 5.5-11.0	------	------	30-50	------	Nishida & Eriksson 1987
Pichia pastoris	1) Methanol & 1-3.1 2)Ethanol & 1.4-3.1	7.5 & 6.5-8.3	37 & 18-45	7.0 & 9.0	------	H_2O_2	Couderc *et al.*, 1980
	------	7.3	30	------	------	-------	Dienys *et al.*, 2003

Cont…

Source organism	Substrate and K_m (mM) value	pH optima and range	Temperature optima and range (°C)	pH stability	Temperature stability (°C)	Inhibitors	References
Pichia sp.	1) Methanol & 0.5 2) Formaldehyde & 3.5	9.0 & 6.0-10	------	------	------	1,10-Phenanthroline, DTNB, Acetamide, H_2O_2, PCMB	Patel *et al.*, 1981
Polyporus obtusus	------	6.5-9.0	------	6.5	------	------	Janssen *et al.*, 1975
Poria contigua	1) Methanol & 0.2 2) Ethanol & 1	------	------	------	------	NaN_3, PCMB, Sodium azide	Bringer *et al.*, 1979
Fungus	1) Hexadecanol & 0.0005 2) Methanol & 89.58	------	------	------	------	------	Alvarado-caudillo *et al.*, 2002

1.2.2. Long Chain Alcohol Oxidase (EC 1.1.3.20)

It is also known as fatty alcohol oxidase, long chain fatty acid oxidase, long chain fatty alcohol oxidase. This enzyme catalyzes alcohol substrates with carbon chain length usually above C_{12}. The purification and properties of an alcohol oxidase that oxidizes not only long chain saturated alcohols but also unsaturated alcohol substrates from a plant source, *Tanacetum vulgare* was reported by Banthorpe *et al*., [1976]. In the cotyledons of *Simmondsia chinensis* (jojoba) seedlings fatty alcohols so formed from the hydrolysis of stored wax esters during the germination seeds are oxidized by two oxidizing enzymes, fatty alcohol oxidase (FAO) and fatty alcohol dehyrogenase [Moreau & Huang 1979]. Extensive study on fatty alcohol oxidases were carried out from *Candida* species, where it oxidizes monoterminal, diterminal and subterminal long chain alcohols [Blaisig *et al*., 1988; Kemp *et al*., 1988]. Although it is a membrane bound enzyme, the localization was in dispute due to the presence of enzyme activity in both mitochondrial and microsomal membrane fractions [Mauersberger *et al*., 1987; Sahm 1977; Krauzova *et al*., 1985]. The broad range of substrates utilized by the alkane induced alcohol oxidase distinguishes this enzyme from the alcohol (methanol) oxidases previously reported in yeasts [Tani *et al*., 1972a, 1972b; Veenhuis *et al*., 1976].

Fatty alcohol oxidase activities from *n*-alkane-grown *Candida tropicalis* and *Yarrowia lipolytica* rapidly decreased on exposure to light. The rate of inactivation of the enzyme depended upon the intensity and wavelength of the incident light (especially blue light of 405 nm), but was diminished under anaerobic conditions [Kemp *et al*., 1990]. Unlike short chain alcohol oxidases, the molecular mass and the subunit number of fatty alcohol oxidases were found to be different. In majority of the cases it was comparatively low mass. Recently two FAO genes from *C. cloacae* (FERM O-736) and a single FAO gene from *C. tropicalis* (NCYC 470) were cloned, and the DNA sequence was determined [Vanhanen *et al*., 2000]. The ORFs of FAO1 and FAO2 from *C. cloacae* were 2,094 and 2091 bp, respectively. The ORF of FAO from *C. tropicalis* (NCYC 470) was 2,112 bp. FAO shared 60.6 and 61.7% nucleotide identities and 74.8 and 76.2% amino acid sequence similarities with *C. cloacae* FAO1 and FAO2, respectively. The FAO1 gene but not the FAO2 gene was successfully cloned and expressed in *E. coli*. An international patent application utilizing this information has been filed [Slabas *et al.,* 1999].

The sub-cellular localization and protein chemical characteristics of long chain alcohol oxidase (LCAO) described in some prominent reports are given in table 1.3. Similarly, the substrates and kinetic parameters of LCAO from different sources are given in table 1.4.

Table 1.3: Localization and protein chemical characteristics of LCAO from different sources

Source organism	Localization	Protein chemical characteristics		References
		Oligomeric nature and Molecular Weight	Co-factor	
Candida bombicola	membrane bound	------	------	Hommel & Ratledge 1990
Candida cloacae	microsome membrane	73kDa, 77.3kDa	------	Vanhanen *et al.,* 2000
Candida tropicalis	membrane bound	145kDa, Homodimer (70kDa)	Flavin	Kemp *et al.,* 1988
	microsome	------	------	Kemp *et al.,* 1990
Simmondsia chinensis	glyoxysome membrane bound, oil body	------	NAD(P)+, riboflavin, 2,6DCPIP,Potassium ferricyanide, Cyt C	Moreau & Huang 1979, 1981

Cont…

Source organism	Localization	Protein chemical characteristics		References
		Oligomeric nature and Molecular Weight	Co-factor	
Tanacetum vulgare	------	180kDa, Heterodimer (94kDa, 75kDa)	FAD, FMN, NAD(P)+	Banthorpe *et al.*, 1976
Yarrowia lipolytica	membrane bound microsome	------	------	Kemp *et al.*, 1990
Arabidopsis thaliana	membrane	73kDa	------	Cheng *et al.*, 2004
Escherichia coli	membrane	------	------	Vanhanen *et al.*, 2000

Table 1.4: Substrates and kinetic parameters of LCAO from different sources

Source organism	Substrate and K_m (mM) value	pH optima and range	Temperature optima and range (°C)	pH stability	Temperature stability (°C)	Inhibitors	References
Candida cloacae	Dodecanol & 0.004	8.8-9.0	------	------	-------	-------	Vanhanen *et al.*, 2000
Candida bombicola	-------	7.6-8.8	30 & 18-38	------	25	------	Hommel & Ratledge 1990
Candida tropicalis	------	-------	------	------	-------	Light, O_2	Kemp *et al.*, 1988
	1) Dodecanol & 0.008, 0.0061, 40 2) Tetradecanol &0.0015 3) Hexadecanol & 0.005	------	20	------	-------	------	Kemp *et al.*, 1990; Kemp *et al.*, 1991
	-------	9.0	-------	6.0-9.0	25	Light	Dickinson & Wadforth 1992
Simmondsia chinensis	Dodecanol & 4	9.0 9.0 &	------	------	100	PCMB	Moreau & Huang 1981
	------	6.6-9.3	------	------	------	------	Moreau & Huang 1979
Tanacetum vulgare	1) *n*-Octanol & 0.49 3) Geraniol & 1.56	5.5-9.0 & 4.8-10.0	18-22 & 45	------	------	------	Banthorpe *et al.*, 1976
Yarrowia lipolytica	-------	9.3	------	------	-------	Light, O_2	Kemp *et al.*, 1990

1.2.3. Secondary Alcohol Oxidase (EC 1.1.3.18)

This category of alcohol oxidase catalyzes secondary alcohols to the corresponding ketones. Polyvinyl alcohol oxidase is also belongs to this category. Two different oxidative pathways, mediated by a secondary alcohol oxidase [Suzuki 1976; Morita & Watanabe 1977], were proposed for the enzymatic degradation of polyvinyl alcohol (PVA). It is mostly reported from *Pseudomonas* species. This category of alcohol oxidase is not adequately studied and the structure-function relationship properties of this group of enzymes are yet to be known. Until now very few literatures are available on the basic biochemical characteristics, purification and properties of this enzyme [Shimao *et al*., 1985; Kawagoshi & Fujita 1997]. PVA-degrading enzymes are monomeric in nature and are reported as both extracellular and periplasmic protein. Two secondary alcohol oxidase (SAO) isozymes have detected and denoted as SAO-I and SAO-II [Sakai *et al*., 1985]. The substrate specificities, electron acceptors, as well as some enzymatic properties like, optimum pH and thermal and pH stabilities of SAO-II were identical to those of SAO-I. These two enzymes are also similar in that they have a single polypeptide chain and contain a non-heme iron per molecule. Furthermore, they show similar absorption spectra. SAO-II is an acidic protein with the p*I* of 4.5. This is noteworthy since SAO-I is a basic protein with the p*I* of 10.3. In spite of the difference in the isoelectric points, the amino acid compositions of these enzymes are quite similar and no histidine is detected in them. The N-terminal amino acid of SAO-II, alanine, is identical to that of SAO-I. The molecular weight of SAO-II (about 40,000) is smaller than that of SAO-I (about 50,000). The two enzymes appear to have a common antigenicity according to the immunodiffusion and neutralization experiments. The common antigenicity may depend upon a peptide structure, since the enzyme contains no carbohydrate. This indicates the close relation of SAO-II to SAO-I in the polypeptide structure, suggesting that SAO-II may be derived from SAO-I during cultivation.

The localization, biochemical and kinetic characteristics of secondary alcohol oxidase (SAO) described in some prominent publications are summarized in the tabular form below.

Table 1.5: Localization and protein chemical characteristics of SAO from different sources

Source organism	Localization	Protein chemical characteristics	References
		Oligomeric nature and Molecular weight	
Bacterium	-------	50kDa, 40kDa, 38.5kDa, Monomer*	Sakai *et al*., 1985
Pseudomonas sp	cytoplasm	-------	Shimao *et al*., 1982
	extracellular	-------	Shimao *et al*., 1983
	intracellular	-------	Kawagoshi *et al*., 1977
	membrane periplasm	------	Shimao *et al*., 1985
	------	26kDa, 49.5kDa Monomer*	Suzuki 1976, 1978
	------	50kDa, 50.5kDa	Morita *et al*., 1979
Pseudomonas vesicularis	extracellular	75kDa, 85kDa Monomer*	Kawagoshi *et al*., 1977
Penicillium sp.	extracellular	------	Qian *et al*., 2004

*The molecular masses were determined by different methods like gel filtration, SDS-PAGE and sedimentation equilibrium analysis.

Table 1.6: Substrates and kinetic parameters of SAO from different sources

Source organism	Substrate and K_m (mM) value	pH optima and range	Temperature optima and range (°C)	pH stability	Temperature stability (°C)	Inhibitors	References
Bacterium	Hg^{2+}	7.0	45	5.0-9.0	45	------	Sakai *et al*., 1985
Pseudomonas putida	1) Polyvinyl alcohol & 1.0 2) 4-Heptanol & 11.0	8.0-9.6	45	------	------	$BaCl_2$, EDTA, $HgCl_2$, $MnCl_2$, $NiCl_2$	Shimao *et al*., 1983
Pseudomonas boreopolis	------	7.0 & 5.0-10	50 & 20-60	4.5-9.0	50	EDTA, Hg^{2+}, o-Phenanthroline, Pb^{2+}, Zn^{2+}	Morita *et al*., 1979

Cont…

Source organism	Substrate and K_m (mM) value	pH optima and range	Temperature optima and range (°C)	pH stability	Temperature stability (°C)	Inhibitors	References
Pseudomonas sp.	-------	6.5-7.5	45	------	------	------	Morita & Watanabe 1977
	-------	------	40	------	------	EDTA, Hg^{2+}	Kawagoshi *et al*., 1977
	-------	9.0	40 & 30-50	5.0-11	50	------	Suzuki 1976
	-------	-------	-------	-------	-------	Hydroxylamine, Ni^{2+},Salicylaldoxine	Suzuki 1978
Pseudomonas vesicularis	-------	10.0	40	6.0-10	45	Cu^{2+}, EDTA, Hg^{2+}, Fe^{2+}, Iodo acetamide	Kawagoshi *et al*., 1977

1.2.4. Aromatic Alcohol Oxidase (EC 1.1.3.7)

Aromatic alcohol oxidase (AAO) is a broad term used for some of the alcohol oxidases like veratryl alcohol oxidase and vanillyl alcohol oxidase that catalyzes a variety of aromatic alcohols is also belongs to this group of alcohol oxidase. The enzyme is mostly isolated and characterized from several lignin degrading fungal strains [Kim *et al*., 2001; Okamoto & Yanase 2002; Guillen *et al*., 1992]. Lignin is the most abundant renewable aromatic biopolymer. The degradation of lignin is a very slow process and the mechanism of degradation is not yet adequately known. There is a combination of enzymes involved in this degradation process. These lignin degrading enzymes do not function independently but mutually interact with each other as well as with other oxidases, including aryl alcohol oxidase. The important characteristics of the AAO are extra cellular production and monomeric glycoprotein, [Asada *et al*., 1995; Varela *et al*., 2000, 2001; Guillen *et al*., 1992; Okamoto & Yanase 2002] which makes this enzyme distinct from the other group of alcohol oxidases. The carbohydrate content is in the range 14-15% in all the reported AAO proteins [Bourbonnais & Paice 1988; Varela *et al*., 2000, 2001; Guillen *et al*., 1992]. The purified oxidase consisted of two isoforms with approximate molecular weight of 78 kDa and the p*I*s 4.25 and 4.35 [Bourbonnais & Paice 1988]. AAO genes from 30

fungal species have been screened using southern blotting. The protein sequence of the AAO from *Pleurotus eryngii* shows 33% sequence identity with the glucose oxidase from *Aspergillus niger* and lower homology with other oxido-reductases Varela *et al.,* [2000]. The AAO predicted to contain 13 putative α-helices and two major β-sheets, each of the putative β-sheets formed by six β-strands. The ADP binding site and the signature-2 consensus sequence of the GMC oxidoreductases were also present in the AAO. Moreover, residues potentially involved in catalysis and substrate binding were identified in the vicinity of the flavin ring. They include two histidines (H502 and H546) and several aromatic residues (Y78, Y92 and F501), as reported in other FAD oxidoreductases [Varela *et al*., 2000].

The biochemical and kinetic characteristics of aromatic alcohol oxidase (AAO) described in some prominent publications are given in tables 1.7 and 1.8.

Table 1.7: Localization and protein chemical characteristics of AAO from different sources

Source organism	Localization	Protein chemical characteristics		References
		Oligomeric nature and Molecular weight	Co-factor	
Arion ater	membrane bound	------	------	Mann *et al*., 1989
Bjerkandera adusta	extracellular	78kDa	FAD	Muheim *et al*., 1990a, 1990b
Pleurotus osreatus	extracellular		FAD	Marzullo *et al*., 1995
Pleurotus eryngii	extracellular	Monomer, 72.5kDa Glycoprotein 71.2kDa	FAD, non-covalently bound	Varela *et al.,* 2000, 2001
Penicillium simplicissimum	intracellular	Homooctamer, 510kDa (Each subunit contains 2 domains)	Flavin, covalently linked	Fraaije *et al.,* 1995
Pleurotus sajor-caju	extracellular	71kDa Glycoprotein	Flavin	Bourbonnais & Paice 1988
Geotrichum candidum	------	65.3kDa (SDS-PAGE)	Flavin	Kim *et al*., 2001

Cont…

Source organism	Localization	Protein chemical characteristics		References
		Oligomeric nature and Molecular weight	Co-factor	
Phanerochaete chrysosporium	------	Monomer 78kDa, p*I* 5.3	FAD	Asada *et al*., 1995
Pleurotus pulmonarius	extracellular	Monomer,70.5kDa p*I* 3.95, Glycoprotein	FAD	Varela *et al.*, 2000
Chrysomela populi	extracellular	Homotetramer, 79kDa, p*I* 5.4	------	Bruckmann *et al.*, 2002
Phratora vitellinae	extracellular	Homotetramer, 79kDa, p*I* 5.2	-------	Bruckmann *et al.*, 2002
Triticum aestivum	extracellular	-------	-------	Barrasa *et al*., 1998

Table 1.8: Substrates and kinetic parameters of AAO from different sources

Source organism	Substrate and K_m (mM) value	pH optima and range	Temperature optima and range (°C)	pH stability	Temperature Stability (°C)	Inhibitors	References
Bjerkandera adusta	1) 3,4 Dimethoxybenzyl alcohol & 1.5 2) Anisyl alcohol & 0.24	5.7	------	------	50	------	Muheim *et al*., 1990a, 1990b
Pleurotus eryngii	1) 3,4 Dimethoxybenzyl alcohol & 0.41, 0.56, 1.2 2) Benzyl alcohol & 0.63, 0.85 3) *m*-Anisyl alcohol & 0.22, 0.3, 0.03	------	------	------	------	Phenol	Varela *et al*., 2001
	-------	6.0-6.5 & 3.0-9.0	45-50 & 20-50	4.0-9.0	60 -70	Ag+, NaN_3, Pb_2^+	Guillen *et al*., 1990; 1992
Polystictus versicolor	4-Methoxy benzyl alcohol & 1.3	6.0-6.5	------	------	55	*p*-Methoxy benzyl alcohol	Farmer *et al*., 1960

Cont…

Source organism	Substrate and K_m (mM) value	pH optima and range	Temperature optima and range (°C)	pH stability	Temperature Stability (°C)	Inhibitors	References
Penicillium simplicissimum	Vanillyl alcohol & 290	10	30	-----	------	4-Allyl-2,6-dimethoxyphenol	Fraaijee *et al*., 1995
Geotrichum candidum	Veratryl alcohol & 1.7	5.5-7.5	45	6.0	30	------	Kim *et al*., 2001
Phanerochaete chrysosporium	Vanillyl alcohol & 0.02	6.0-7.0	45	5.0-8.0	35	$HgCl_2$, PCMB	Asada *et al*., 1995
Pleurotus pulmonarius	1) 3,4 Dimethoxybenzyl alcohol & 0.39	6.0	------	6.0-9.0	-----	------	Varela *et al*., 2000
Pleurotus sajor-caju	1) 3,4 Dimethoxybenzyl alcohol & 0.41, 0.46	5.0 & 3.5-8.0	------	------	------	------	Bourbonnais & Paice 1988
Coriolus versicolor	1) 2-Hydroxybenzyl alcohol & 63 2) 2-Hydroxybenzyl alcohol & 132	5.5 - 6.5	------	------	------	------	Bruckmann *et al*., 2002
Chrysomela populi	2-Hydroxybenzyl alcohol & 132	------	------	------	------	------	Bruckmann *et al*., 2002
Phratora vitellinae	2-Hydroxybenzyl alcohol & 63	------	------	------	------	------	Bruckmann *et al*., 2002

In general all the alcohol oxidases are FAD dependent enzymes, where flavin is either covalently or non-covalently bound [Janssen & Ruelius 1968]. One of the differentiating properties of these proteins into several classes is not only on the basis of substrate utilization but also from their difference in molecular masses, where SCAOs are high molecular weight in nature with four to eight subunits [Yamada *et al.,* 1979; Bringer *et al.,* 1979; Couderc & Baratti 1980; Sahm 1982; Van der Klei *et al.,* 1990; Danneel *et al.,* 1994; Suye1997], while LCAOs are dimeric [Banthorpe *et al.,* 1976; Dickinson & Wadforth 1992] and the SAO and AAOs are low molecular

weight proteins with single subunit [Shimao *et al.,* 1985; Morita *et al.,* 1979; Sakai *et al.,* 1985; Varela *et al.,* 2000, 2001; Asada *et al.,* 1995; Guillen *et al.,* 1992; Okamoto & Yanase 2002]. Cholesterol oxidase (EC 1.1.3.6) is considered to be one of the secondary alcohol oxidase that oxidizes sterols at the 3β-hydroxyl position to form Δ4-cholestenone and H_2O_2 [MacLachlan *et al.,* 2000; http://www.brenda.unikoeln.de/php/flat_result.php4?ecno =1.1.3.6].

All these alcohol oxidases are widely used in several fields and their application potentials are well known in different areas like biosensor, biofuel cell, and biocatalysis. Ethanol biosensor for the detection and quantification of alcohols with high sensitivity, selectivity and accuracy is required in clinical and forensic analysis in order to analyze human body fluids, *e.g.* blood, serum, saliva, urine, breath and sweat, among others, food, beverage (wine, beer and spirits), pulp industries and also in agricultural and environmental analysis, *e.g.* for the assessment of ethanol at a spill site or in ground waters [Davidsson *et al*., 2004; Korpan *et al*., 2000; Smith *et al*., 2000; Castillo *et al*., 2003; Johansson *et al*., 1993; Alhadeff *et al*., 2004; Hasunuma *et al*., 2004; Narvaez *et al*., 2000; Liden *et al*., 1998]. Cholesterol biosensors for the determination of total cholesterol in serum is required for clinical diagnosis, since the increased level of cholesterol is associated with atherosclerosis, myxoedema, nephrosis, diabetes mellitus and obstructive jaundice, while it's decreased level is observed in hyperthyroidism, certain anemia's, mal-absorption and wasting syndrome [Smith & Brooks 1977; Bokoch *et al*., 2004; Lin & Yang 2003; Ram *et al*., 2001; Pundir 2003; Sugiuchi *et al*., 1995]. The application of alcohol oxidase electrode for the construction of fuel cell has recently attracted much attention due to the possible application of this sustain energy generating device in areas like, biomedical instrumentation, space research, military applications *etc*. [MacLachlan *et al.,* 2000; Willner *et al*., 2001; Barton *et al*., 2004]. Apart from these, alcohol oxidases are also traditionally used in the organic synthesis, for example large scale synthesis of flavor compounds, like vanillin by vanillyl alcohol oxidase, which is generally regarded as a tasteful biocatalyst, and other carbonyl compounds of commercial importance [van den Heuvel *et al.,* 2001]. In some cases alcohol oxidase can also be used as a novel pathogenicity factor for *cladosporium fulvum* [Segers *et al*., 2001].

Oxidation of alcohol is one of the critical steps involved in the microbial degradation of wide range of aliphatic hydrocarbons as shown in the scheme 1.2, hence evolved as one of the process steps in the bioremediation of hazardous

petroleum contaminants [Morgan & Atlas 1989]. This oxidation step is largely catalyzed by alcohol oxidase when yeast [Dickinson & Wadforth 1992; Hommel & Ratledge 1990; Vanhanen *et al.,* 2000; Eirich *et al.,* 2004; Kemp *et al.,* 1990] or filamentous fungi are involved in the degradation process [Robelo *et al.,* 2004; Isobe *et al.,* 2007; Savitha & Ratledge 1991]. Research on these alcohol oxidases produced during the assimilation of hydrocarbon by filamentous fungi is in nascent stage and detail functional and physico-chemical characteristics of these oxidases are yet to be explored. Reports on the degradation of hydrocarbon by filamentous fungi are vast [Kirk & Gordon 1988; Annibale *et al.,* 2006; Juhasz & Naidu 2000; Muncnerova & Augustin 1994; April *et al.,* 2000]. During the biodegradation process, *Aspergillus* is considered as one of the potential microbial agents in comparison to other fungal species [Adekunle & Adebambo 2007; Santos *et al*., 2008]. The productions of different secondary metabolites and enzymes during the degradation of hydrocarbon by *Aspergillus* species have been reported [Radwan & Sorkhoh 1993; Vatsyayan *et al*., 2008; Kumar & Goswami 2006]. However, the basic studies on these metabolites for their potential applications are not adequately addressed so far. Presence of broad-substrate specific cytochrome P450 monooxygenase (Cyt P450) activity in the cells of *Aspergillus terreus* MTCC is reported recently from our laboratory [Vatsyayan *et al*., 2008].

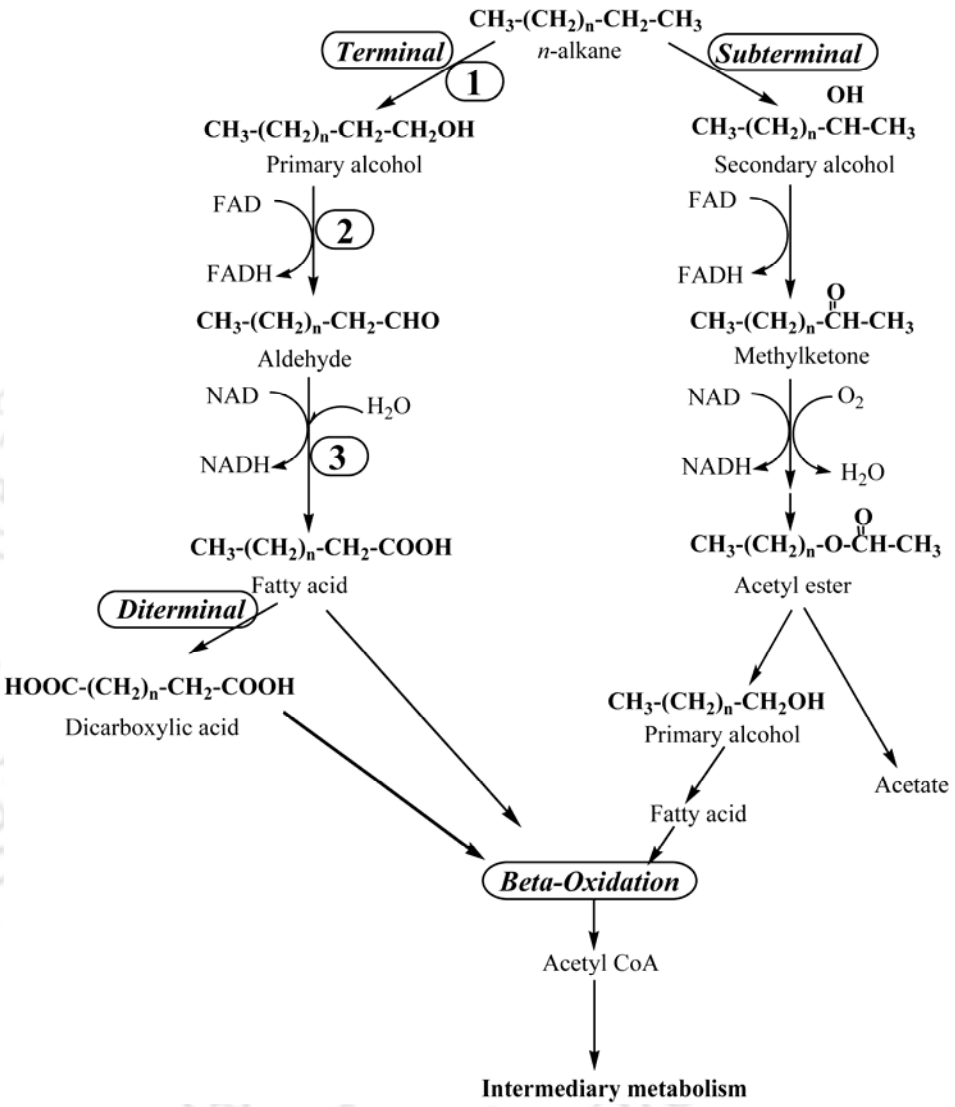

Scheme 1.2: Different hydrocarbon-degradation pathways of filamentous fungi. The main pathway is the terminal oxidation to fatty acids catalyzed by [**1**] alkane monoxygenase, [**2**] alcohol oxidase and [**3**] aldehyde dehydrogenase.

Chapter 2

ISOLATION AND IDENTIFICATION OF A HYDROCARBON-DEGRADING FILAMENTOUS FUNGUS

2.1 OVERVIEW

The microbial degradation of hydrocarbons is an area that has been continuously stimulating interest of the researchers since last several decades due to their scope for wide applications such as, bioremediation [Atlas 1981; Leahy & Colwell 1990; Yuan *et al*., 2000; Lanfranconi *et al.,* 2003; Miralles *et al.,* 2007], production of secondary metabolites [Dyal & Narine 2005; Radwan & Sorkhoh 1993] and enzymes [Kanwar & Goswami 2002; Vatsyayan *et al*., 2008; Goswami & Cooney 1999; Li *et al.,* 2004; Pedrini *et al.,* 2006], biotransformation [Santos *et al*., 2008] *etc*. The importance of fungal degradation of petroleum hydrocarbons is growingly recognized and attracts attention due to the widespread natural abundance of fungi in terrestrial ecosystem [Dashti *et al*., 2008; Britton 1984]. *Aspergillus* species has been identified as one of the potential fungal agents for the biodegradation process [Adekunle & Adebambo 2007; Santos *et al*., 2008]. The biodegradation of petroleum hydrocarbons by *Aspergillus* species have been largely studied from the environmental perspective, whereas the metabolic consequence and production of other important metabolites during the degradation is not adequately addressed so far. We report here isolation of a broad spectrum hydrocarbon-degrading *Aspergillus*

strain and increase induction of lipid during growth of the fungus on hydrocarbon substrates. Also the fatty acid profile of the lipids formed during the growth of the fungus on hydrocarbon substrates was also investigated and reported here.

2.2 EXPERIMENTAL APPROACHES

2.2.1. Sample collection and sampling

Petroleum contaminated soil samples from oil fields located near Digboi and Duliajan of Assam, India were collected in a sterile container. These were labeled and sealed, and then transported to the laboratory for analysis. A total number of twenty five soil samples were collected for the present study.

2.2.2. Isolation of fungi

The soil samples were transferred to test tubes containing 5.0 ml of sterilized distilled water. The test tubes were vigorously shaken, for approximately 60 sec, to release the fungal spores. Several serial dilutions were made and 1 ml portion from each dilution was pipetted on the surface of fungal agar (Himedia, India) plates and spread evenly throughout. The plates were kept at room temperature (± 28 ºC) until the development of colonies (3-4 days). The fungi were purified initially on the fungal agar plates. The fungal agar contained (g l^{-1}): papain digest of soyabean meal, 10; dextrose, 10; and agar, 15. The pure colonies formed in the plates were transferred to fungal agar slants and then incubated further at 28 °C. The organism was maintained on the fungal agar slants with periodic transfer to a new slant following each 15 days. For long term storage, the slants were sealed with paraffin and stored at 4 ^{o}C. For growth studies on different carbon substrates, the pure colonies were transferred to 500-ml Erlenmeyer flasks containing 2% (v/v) *n*-hexadecane in 50 ml of basal medium [Bushnell & Haas 1941] of the following compositions (g l^{-1}): $MgSO_4$ $7H_2O$, 0.2; NH_4NO_3, 1.0; $CaCl_2$, 0.02; KH_2PO_4, 1.0; K_2HPO_4, 1.0; $FeCl_3$, 0.002; and yeast extract, 1.0 as growth inducer. At this concentration yeast extract alone supported negligible growth. The pH of the medium was adjusted to 5.8 and the flasks were incubated at 28 °C under static condition. The media containing the substrate was sterilized at 15 lb for 15 min before inoculating the organism.

2.2.3. Identification of filamentous fungus

The identification of the filamentous fungal species was carried out through macroscopic observation of the colonies and examination of the micro-structural characteristics, and a comparative analysis with parameters established in the conventional taxonomy, by referring some of the books [Raper & Fennel 1977; Domasch *et al*., 1980]. The strain was then submitted to Microbial Type Culture Collection (MTCC), Chandigarh for species identification and accession number. After identification of the organism, the colonies were transferred to test tubes containing fungal agar medium for further study.

2.2.4. Growth of fungus in different carbon sources

Similar mineral media composition as mentioned previously for fungal isolation was used to study the growth of the microorganism in different carbon sources. A range of test carbon sources, alkanes, alkanols, alkanals and fatty acids were supplied separately in the mineral media as a sole source of carbon and energy. The optimum growth conditions of the fungi *A. terreus*, was studied using different concentrations of model carbon source, *n*-hexadecane.

2.2.5. Microscopic analysis of the fungus

The morphological characteristics of the hyphae were studied using scanning electron microscopy (SEM) (LEO model no 1430vp) following the general protocol for biological samples [Christian & Stadtlander 2005]. The cells were initially dehydrated using increasing concentration of ethanol (v/v) for different incubation periods at room temperature as follows: 50% for 5 min, 70% for 10 min, 80% for 10 min, 90% for 15 min and finally twice with 100% for 20 min. Since the samples were non-conductive, gold coating of the dried samples were done in a Polaron Sputter coater unit (Model SC 7620) after mounting on aluminum stubs fixed with double coated carbon tape for 90 sec. The vacuum chamber was maintained at 10^{-2} Torr and current 1mA at 1kV voltage and then analyzed through SEM using the following setting conditions: 10-15 kV EHT, 50 µm aperture, 500 X magnifications.

2.2.6. Lipid analysis from cells grown in different carbon sources

The harvested cells were washed thoroughly in a glass funnel covered with a filter paper (Whatman) with 50 mM Tris-HCl buffer, pH 8.0 to remove the mineral

salts of the medium and then briefly washed with *n*-hexane to remove the cell bound *n*-hexadecane. Finally the cells were washed with the similar buffer for several times. The washing step with organic solvent was omitted for glucose-grown cells. Total lipid content from the wet cells was extracted following the standard chloroform-methanol (2:1) method [Folsch *et al*., 1958]. Fatty acids were isolated by hydrolyzing the lipid with ethanolic KOH (6% KOH in 95% ethanol) at 70 ^{o}C for 3 hr and 150 rpm. The pH of the reaction medium was then reduced to 2 by adding 1N HCl and then kept standing overnight for phase separation. The fatty acid layer formed at the top was then extracted with chloroform. The solvent was evaporated by rota-vapor and the extracted fatty acids were stored at -20 ^{o}C until analysis.

Elecrospray ionization/ mass spectrometry (ESI/MS) (Q-Tof Premier, Waters) was used to identify the fatty acids. Before analysis the fatty acids were dissolved in 5 mM ammonium acetate in methanol. Identification of fatty acids was done with an ESI probe source in negative mode. ESI-MS was operated at spray voltage 2.5 kV, sample cone 60, extraction cone 4, and the heated capillary temperature at 250 ^{o}C. The fatty acids were identified from the corresponding *m/z* peaks using Masslynx 4.1 software provided with the instrument. This software includes both elemental composition and molecular mass calculator to determine the exact structure.

2.2.7. Statistical analysis

Results obtained were the mean of three or more determinations. Analysis of variance was carried out on all data at $p < 0.05$ with the help of Microsoft® Excel 2003 version 11 (USA). When '*F*' value was found to be significant, critical difference was calculated by multiplying the standard error of difference (SE_d) with the corresponding '*t*' values at 5% level of probability. Significant differences among the means were determined by using least significant difference test.

2.3 RESULTS AND DISCUSSION

Different hydrocarbon-degrading fungal strains were isolated from the oil contaminated soil samples collected from different locations of Digboi and Duliajan oil fields of Assam. (Fig 2.1). Among these the fastest growing strain was taken and

considered for the present investigation. Based on the morphological characteristics the organism was provisionally identified as *Aspergillus terreus* and subsequently confirmed its identity by using the identification service of the Microbial Type Culture Collection (MTCC), Chandigarh. The organism was deposited in the MTCC with accession number MTCC 6324. A single colony of the *Aspergillus terreus* grown on fungal agar is shown in figure 2.2A.

A. terreus MTCC 6324 could degrade a wide range of petroleum hydrocarbons, alcohol and long chain primary alkanols, secondary alcohols including cholesterol, and chlorinated aliphatic hydrocarbons as shown in table 2.1. There are many reports on the degradation of specific classes of hydrocarbon substrates by microorganisms [Dashti *et al.,* 2008; Adekunle & Adebambo 2007; Karlinski *et al.,* 2007; Pedneault *et al.,* 2007; Van Hamme *et al*., 2003; Widdel *et al*., 2006; Cerniglia & Perry 1974; Patrick & Dugan 1974]. However, specific microorganisms capable of degrading broad range of hydrocarbon substrates are rare and not adequately studied among filamentous fungi. The advantage ascribed to filamentous fungi over other microbial strains for cleaning polluted soil is that the hyphae of the filamentous fungi could penetrate several centimeter depths from the soil surface, thus able to degrade contaminants in sub-surface anaerobic environment. This indicates *A. terreus* may be a potential microbial agent for bioremediation of hazardous and toxic petroleum hydrocarbons and bioconversion processes. Among all the studied complex carbon sources maximum cell growth was observed in *n*-hexadecane with a wet weight cell mass 39 ± 4 g l^{-1}, which is closer to cell mass of 40 ± 2 g l^{-1} obtained by using glucose as the growth substrate. However, the growth of the organism on *n*-hexadecane substrate was significantly slow as evident from the requirement of nearly 96 hr of incubation to reach stationary phase of growth contrary to the glucose-grown cells that needs only 72 hr of incubation to reach the similar growth phase. A 2% (v/v) *n*-hexadecane substrate was found to be optimal for attaining maximum wet mass of the cells under the standard condition of cultivation used in this investigation (Fig 2.3).

Many microorganisms are known to produce surface active agent (biosurfactant) to facilitate degradation of water insoluble hydrocarbon substrate through emulsification that increases oil to water surface area for enhance assimilation/transport through the cell wall [Christovaa *et al*., 2004; Deziel *et al*., 1996; Goswami & Singh 1991]. No surface activity of the culture broth was observed

during growth of *A. terreus* on *n*-hexadecane or other similar hydrophobic hydrocarbon substrates used in this investigation. Hence, assimilation of such highly hydrophobic aliphatic hydrocarbon substrates by this filamentous fungus is appeared to occur only through the sorption mechanism, which is supported by the fact that the fungal hyphae were largely associated with the water insoluble top hydrocarbon layer during growth of the fungi on such hydrophobic hydrocarbon substrates (Fig 2.2B). Degradation of such highly hydrophobic substrates through sorption is expected to occur through special modification of the hyphal cell wall. Scanning electron microscopic studies of the cell hyphae obtained from the growth of the organism on *n*-hexadecane and glucose separately were conducted and found that there was a marked difference on the cell wall morphology of the hydrocarbon-grown cells from the glucose-grown cells as shown in figure 2.4. In glucose-grown cells the hyphae were smooth with a thick cell wall, whereas, the cell wall of the *n*-hexadecane cells was uneven and thin.

The metabolic consequence of assimilation of these high energy hydrophobic substrates by the fungus was investigated by analyzing the cellular lipid content. The lipid production (w/w wet biomass) in *n*-hexadecane- and glucose-grown cells were 4.4% and 0.62%, respectively, thus showing seven fold higher lipid content in *n*-hexadecane-grown cells than the glucose-grown cells. The fatty acid profiles in these lipids were examined by ESI/MS as shown in Fig 2.5. It is evident from the spectra in the figure 2.5 and also in the table 2.2 that nearly nine fatty acids induced in the hexadecane-grown cells were void in the glucose-grown cells. The oleic acid and palmitic acid were the fatty acids with highest peak intensity in the spectral profile corresponding to the glucose-grown cells and hexadecane-grown cells, respectively. It was revealed by analyzing the percentage distribution of different fatty acids in each cell type (Table 2.2) that palmitic and stearic acids were the predominant fatty acids in the hexadecane-grown cells; whereas, oleic and linoleic acids were the predominant fatty acids observed in the glucose-grown cells. Moreover, considerably high amount of unsaturated fatty acids with chain length C_{32} and C_{33} were present in *n*-hexadecane-grown cells that each account nearly 9% (based on peak intensity) of the total fatty acid content in the cells. These fatty acids were however either negligible or void in the corresponding glucose-grown cells as shown in table 2.2. Although reports on long chain fatty acids from microbial strains are available [Walker & Cooney 1973; Kinderlerer 1993; Nemec *et al*., 1997], presence of these fatty acids in *Aspergillus*

strains is not reported until now. The role of these fatty acids in the metabolism of hydrocarbons is not yet known.

Induction of very high amount of palmitic acid ($C_{16:0}$) in *n*-hexadecane-grown cells is expected and it is likely that this palmitate is the product of terminal oxidation of *n*-hexadecane substrate catalyzed by the cell membrane associated enzymes, namely, Cyt P450, alcohol oxidase and aldehyde dehydrogenase. The existence of the Cyt P450 and alcohol oxidase in the cells of this fungus have already been reported by us [Vatsyayan *et al*., 2008; Kumar & Goswami 2006]. The myristic acid that is void in glucose-grown cells is suggested to form from the palmitic acid by *β*-oxidation pathway. These long chain fatty acids directly derived from the substrate is thus stored as lipid in the cells. Although direct cellular transformation of aliphatic hydrocarbon substrate to the corresponding fatty acids has been described [Cerniglia & Perry 1974; Patrick & Dugan 1974], report on the cellular accumulation of such high level of lipid content with these fatty acids is not yet known in the filamentous fungi. This hydrocarbon-substrate induced production of lipid is envisaged to have potential application for the production of biodiesel and industrially important poly unsaturated fatty acids (PUFA), which were induced to a significant level (C_{13}-C_{33} in table 2.2) as compared to the glucose-grown cells.

2.4 FIGURES

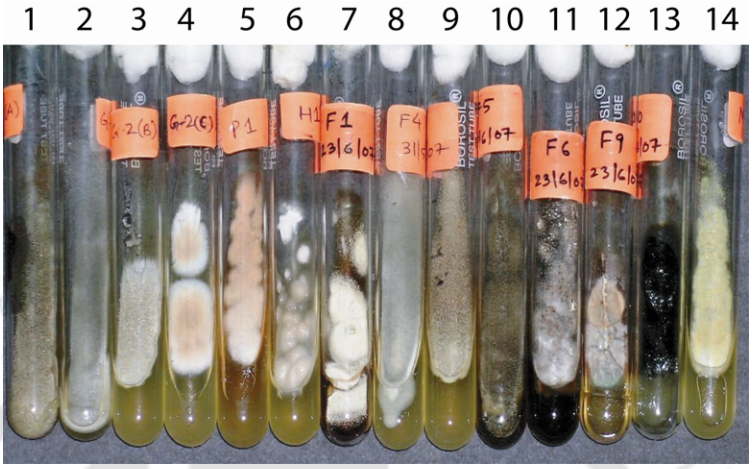

Figure 2.1: Fungal strains isolated from oil contaminated soil samples.

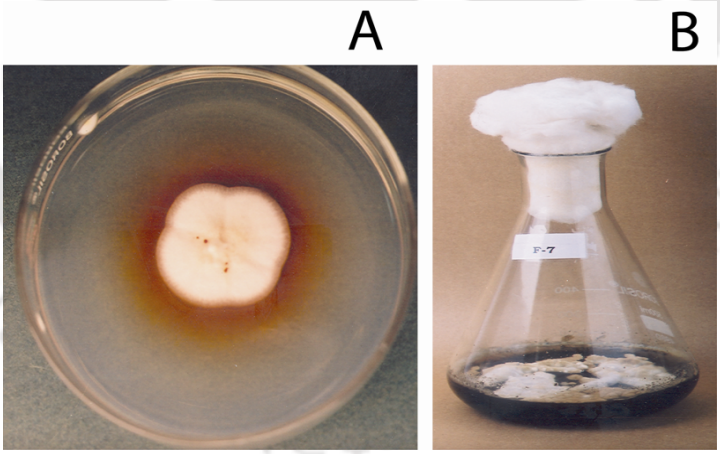

Figure 2.2: Growth of *Aspergillus terreus* on (**A**) fungal agar and (**B**) mineral media supplemented with petroleum sludge.

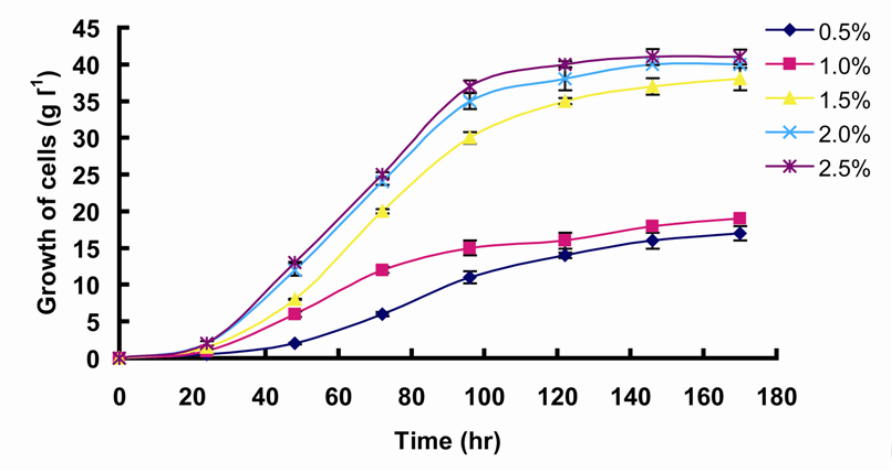

Figure 2.3: The growth of *A. terreus* in the culture media containing different *n*-hexadecane concentrations. The statistical analysis were done as described earlier in the methods section.

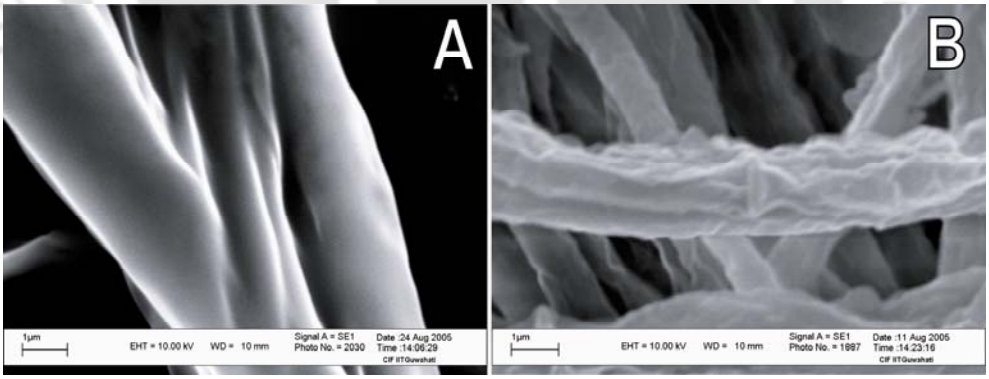

Figure 2.4: SEM analysis of *Aspergillus terreus*. The filamentous fungal hyphae present in the (**A**) glucose- and (**B**) *n*-hexadecane-grown cells.

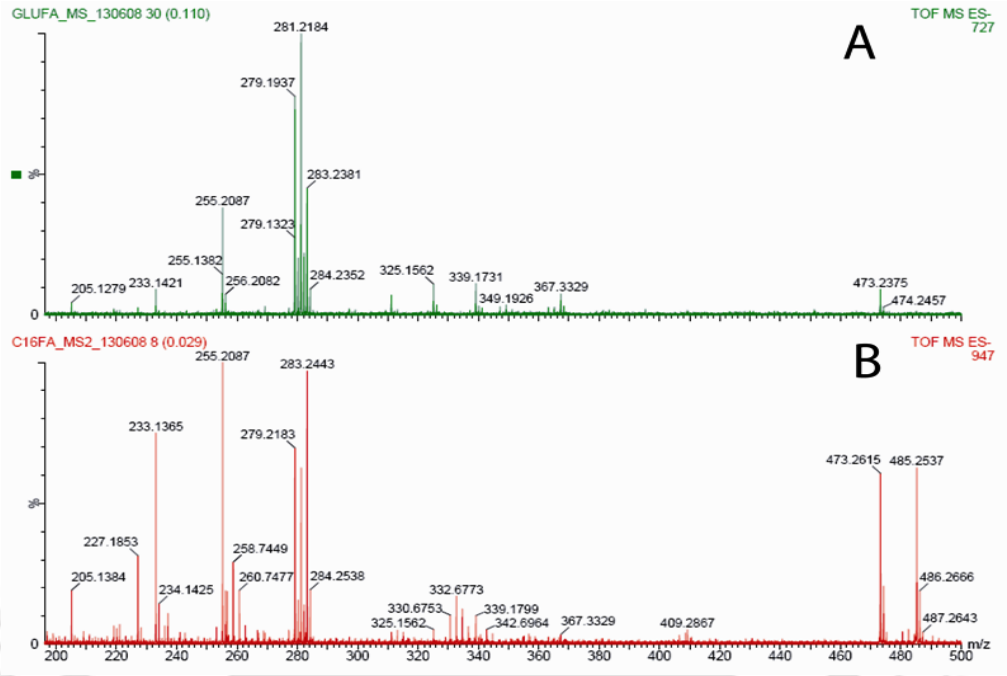

Figure 2.5: LC-ESI/MS fatty acid profile of (**A**) glucose and (**B**) *n*-hexadecane cells.

2.5 TABLES

Table 2.1: Growth of *A. terreus* in different carbon substrates

Substrate	Wet weight* ($g\ l^{-1}$)	Substrate	Wet weight* ($g\ l^{-1}$)
n-Octane	12.8 ± 1.9^{m}	Isoamyl alcohol	5.6 ± 1.1^{t}
n-Dodecane	15.4 ± 1.3^{l}	3-Butanol	3.0 ± 1.5^{w}
n-Hexadecane	39.1 ± 3.8^{b}	3-Octanol	3.2 ± 1.9^{v}
n-Octadecane	24.9 ± 1.2^{d}	2-Dodecanol	24.1 ± 2.2^{e}
n-Docosane	15.7 ± 1.6^{k}	2-Docosanol	21.8 ± 1.3^{h}
n-Tetracosane	8.1 ± 1.3^{q}	Cholesterol	10.2 ± 1.9^{p}
Methanol	14.8 ± 0.9^{l}	1-Dodecanal	15.9 ± 1.3^{j}
Ethanol	15.4 ± 1.5^{l}	1-Hexadecanal	17.9 ± 2.1^{h}
n-Butanol	15.8 ± 2.1^{k}	Pristane	5.3 ± 2.9^{t}
n-Heptanol	5.2 ± 0.8^{u}	Benzene	8.1 ± 3.1^{o}
n-Octanol	6.0 ± 1.4^{s}	Toluene	6.8 ± 2.2^{r}
n-Decanol	8.6 ± 1.3^{r}	Phenol	4.1 ± 2.7^{u}
n-Undecanol	21.9 ± 3.0^{g}	Naphthalene	10.6 ± 1.5^{o}
n-Dodecanol	25.5 ± 2.9^{c}	Testosterone	3.2 ± 1.1^{w}
n-Tetradecanol	24.7 ± 3.1^{e}	12-Hydoxydodecanoic acid	16.8 ± 1.6^{i}
n-Hexadecanol	23.3 ± 2.8^{f}	1,12-Dichlorododecane	12.7 ± 2.4^{m}
n-Octadecanol	23.8 ± 1.2^{f}	1,16-Hexadecadiol	10.9 ± 1.2^{n}
n-Tetracosanol	17.9 ± 1.9^{g}	Petrol	12.5 ± 1.8^{m}
n-Hexacosanol	15.4 ± 1.6^{k}	Kerosene	8.1 ± 2.0^{r}
n-Eicosanol	12.3 ± 0.4^{m}	Crude oil	13.4 ± 1.7^{m}
n-Docosanol	13.4 ± 1.8^{l}	Yeast extract	10.1 ± 2.9^{p}
Isopropanol	16.7 ± 1.1^{j}	Glucose	40.3 ± 2.1^{a}

***** Wet weight of the cells was determined after 96 hr growth (72 hr growth for glucose substrate) after supplementing each set of experiments with 2% (g/v for solid and v/v for liquid substrates) carbon source (final concentration) in the medium. Each value represents the mean ± standard error; with no common letter are significantly different at $p < 0.05$.

Table 2.2: The cellular fatty acid profile of *A. terreus* grown in glucose and *n*-hexadecane substrates

Name of fatty acid	Short cut name	*m/z* (M^+-H)	Relative Intensity (%)	
			Hexadecane cells	Glucose cells
Myristic acid	14:0	227.1	30	---
Palmitic acid	16:0	255.2	100	40
Stearic acid	18:0	283.2	97	47
Arachidic acid	20:0	311.5	5	4
Henicosanoic acid	21:0	325.1	5	7
Docosanoic acid	22:0	339.1	15	7
Tetracosanoic acid	24:0	367.3	2	5
Heptacosanoic acid	27:0	409.2	5	---
Oleic acid	18:1	281.2	62	100
Linoleic acid	18:2	279.2	70	80
Tridecatetraenoic acid	13:4	205.1	20	5
Pentadecatetraenoic acid	15:4	233.1	75	10
Heptadecatetraenoic acid	17:4	260.7	20	---
Nonadecahexaenoic acid	19:6	284.2	20	---
Henicosaheptaenoic acid	21:7	311.1	2	7
Docosaheptaenoic acid	22:7	325.1	5	12
Docosatetraenoic acid	22:4	332.6	20	---
Dotriacontatrienoic acid	32:3	473.2	60	5
Tritriacontatetraenoic acid	33:4	485.2	62	---
Unidentified	----	258.7	29	---
Unidentified	----	260.7	20	---
Unidentified	----	330.6	10	---

Chapter 3

STUDIES ON SUBSTRATE SPECIFICITY AND SUB-CELLULAR LOCATION OF THE ALCOHOL OXIDASE

3.1. OVERVIEW

The redox enzymes that catalyze the oxidation of alcohol to the corresponding aldehyde or ketone have potential application in the pharmaceutical, food, clinical, pulp and other industries [Azevedo *et al.*, 2005; Hargrove *et al.*, 2004; Hummel 1999]. These enzymes may be categorized into alcohol dehydrogenase and alcohol oxidase, on the basis of the mechanisms involved in the catalytic reactions. Alcohol dehydrogenases require nicotinamide (NAD^+ or $NADP^+$) co-factor as terminal electron acceptor, while, alcohol oxidases use molecular oxygen as electron acceptor that leads to the formation of hydrogen peroxide during the catalysis [Geissler & Hemmerich 1981; Kemp *et al.*, 1988]. The alcohol dehydrogenases have been studied extensively as evident from their voluminous publications, while, the hydrogen peroxide generating alcohol oxidases are not yet adequately studied. The alcohol oxidases (systematic name: alcohol: oxygen oxidoreductase) have been categorized into different classes, such as, short chain alcohol oxidase (SCAO), also known as, alcohol oxidase, methanol oxidase, ethanol oxidase, *etc*. (EC 1.1.3.13); secondary alcohol oxidase (SAO), also known as polyvinyl alcohol oxidase (EC 1.1.3.18); long chain alcohol oxidase (LCAO), also known as fatty alcohol oxidase, long chain fatty acid oxidase, long chain fatty alcohol oxidase, (EC 1.1.3.20); and aromatic alcohol

oxidase (AAO), also known as aryl alcohol oxidase, such as, veratryl alcohol oxidase (EC 1.1.3.7) and vanillyl alcohol oxidase (EC 1.1.3.38) based on the substrate oxidized. Research on alcohol oxidases from filamentous fungi is limited. Among different alcohol oxidases, AAO and SCAO have been studied to a greater extent, while, only limited studies with this microorganism have been done on LCAO and SAO as revealed from the available literature [Savitha & Ratledge 1991; Alvarado-Caudillo *et al*., 2002].

Alcohol oxidase is reported as one of the inducible enzymes formed during microbial degradation of aliphatic hydrocarbons. Majority of the reports described on alcohol oxidase are from yeasts, such as, *Candida* species [Dickinson & Wadforth 1992; Hommel & Ratledge 1990; Vanhanen *et al*., 2000; Eirich *et al*., 2004], *Yarrowia* species [Kemp *et al*., 1990]. Report on the alcohol oxidase from hydrocarbon-grown filamentous fungi is limited and appears to be available only with *Cladosporium* species [Goswami & Cooney 1999], *Aspergillus* species [Savitha & Ratledge 1991], and YR-1 strain [Robelo *et al*., 2004]. All these reports largely deal with fatty alcohol oxidase. Systematic investigation on the functional characterization of an alcohol oxidase induced during degradation of different hydrocarbons by filamentous fungi is not reported till. The only report on the location of the alcohol oxidase from filamentous fungi appeared so far is from *Cladosporium resinae*, where light mitochondrial fraction was indicated as the sub-cellular location of the enzyme [Goswami & Cooney 1999]. In this chapter we describe the sub-cellular localization and functional characterization of an intracellular alcohol oxidase produced by the aliphatic hydrocarbon-degrading *Aspergillus terreus* with broad substrate specificity in oxidizing different classes of alcohols.

3.2. EXPERMINTAL APPROACHES

3.2.1. Organism and Culture Conditions

The culture conditions and the maintenance of the *A. terreus* MTCC 6324 used in this study were described in detail in chapter 2.

3.2.2. Preparation of Microsomes

For microsome preparation, the *n*-hexadecane-grown cells were harvested from the early stationary phase of growth of the static culture. The harvested cells were separated from the culture broth and then washed with 50 mM Tris-HCl buffer, pH 8.0 and *n*-hexane to prepare substrate-free cell mass following the procedure described by Goswami & Cooney [1999]. The cells were suspended in 50 mM Tris-HCl buffer, pH 8.0 containing EDTA (10 mM); $MgCl_2$ (1 mM) and PMSF (1 mM) and then disrupted by using mechanical cell disruptor (Constant Systems Ltd, UK) at 30 kpsi. The cell homogenate formed after disruption was then immediately mixed with DTT (1 mM) and then centrifuged at 10000 x *g* for 15 min to pellet the undisrupted cells and nuclei. The supernatant (Sup-1) was collected and subjected to 20000 x *g* for 30 min. The supernatant (Sup-2) collected was again centrifuged at 114000 x *g* for 3 hr (Beckman Ultracentrifuge, USA) to sediment the microsomal fraction. The microsomes were separated and suspended in 50 mM Tris-HCl buffer, pH 8.0. The supernatant (Sup-3) formed was retained for enzymatic study. All the steps in the procedure were performed at 4 ^{o}C unless specified.

3.2.3. Enzymatic Assay of Alcohol Oxidase

The alcohol oxidase was assayed by measuring substrate dependent oxygen consumption using Biological Oxygen Monitor (5300A, YSI USA) using Clark-type polarographic oxygen electrodes following the method described by Blasig *et al*., [1988]. Calibration of the oxygen electrode was done by Xanthine oxidase assay [Billiar *et al*., 1970]. The reaction mixture consists of 50 mM Tris-HCl buffer, pH 8.0, sodium azide (6 mM), and the test alcohol substrate (10 mM) dissolved in 0.1 ml dimethyl sulfoxide (DMSO). The reaction was carried out at 30 ^{o}C immediately after addition of approximately 0.3 ml of the enzyme sample. The final volume of the reaction mixture was maintained at 3 ml. The alcohol oxidase activity was simultaneously confirmed for each datum using the spectrophotometric assay method of Kemp *et al* [1988] using 2,2'-azino-bis[3-ethylbenzothiazoline-6-suphonic acid] diammonium salt (ABTS) as the chromogenic agent. The molar extinction co-efficient of 18.4 at 405 nm was used for the radical cation of ABTS [Werner *et al*, 1970] in the method. The stoichiometric equivalence of 1 mM ABTS with 0.5 mM oxidized substrate was considered to measure the product. One unit of enzyme

activity for both the assay methods was finally expressed as the amount of enzyme required to consume 1 μM O_2 min^{-1} at 30 ^oC.

3.2.4. Analyses of the Alcohol Oxidase in Native PAGE

Native PAGE analysis of the protein was done at 4 ^oC following the method of Laemmli [1970] by using various concentrations of separating gels at 20 mA and 25 mA for stacking and resolving gel, respectively. The enzyme in the gel was detected by biological staining using ABTS and horseradish peroxidase following the method of Kemp *et al*., [1988]. The exact replica of the same gel was also stained with coomassie brilliant blue (CBB) R-250. The standard protein markers used to determine the approximate molecular mass (M_r) of the sample protein were urease, BSA, and chicken egg albumin.

3.2.5. pH and Temperature Optima of the Alcohol Oxidase

The optimum pH and temperature of the enzyme was determined after incubating the enzyme sample in different pH buffers of pH 6 to 10 and for temperature optima studies the enzyme activity of the alcohol oxidase was measured at different reaction temperatures and assayed following the similar spectrophotometric assay method stated earlier.

3.2.6. Analytical Methods

Protein estimation was done following the Hartree's modification of Lowry method using BSA as standard [Hartree 1972]. All the data presented here were the mean of three or more experiments with a variation within 10%. Analysis of variance was carried out for the statistical data with the help of Microsoft Excel as described in chapter 2.

3.3. RESULTS AND DISCUSSION

A. terreus could grow on basal medium containing *n*-hexadecane as the sole source of carbon and energy. The alcohol oxidase activity in the culture broth of *A. terreus* during growth on *n*-hexadecane was nearly proportional to the cell protein (about 6.5 U g^{-1} cell protein) till the early stationary phase (96 hr) of growth.

However, the activity was declined in the late stationary phase where fungal sporulation started. The enzyme was localized in the microsomal membranes as majority of the alcohol oxidase activity was observed in this sub-cellular fraction. All the studies were performed using enzyme bound microsomal membranes. This fraction was collected and stored until further analysis. The flow chart on differential centrifugation and sub-cellular location of the alcohol oxidase is shown in scheme 3.1.

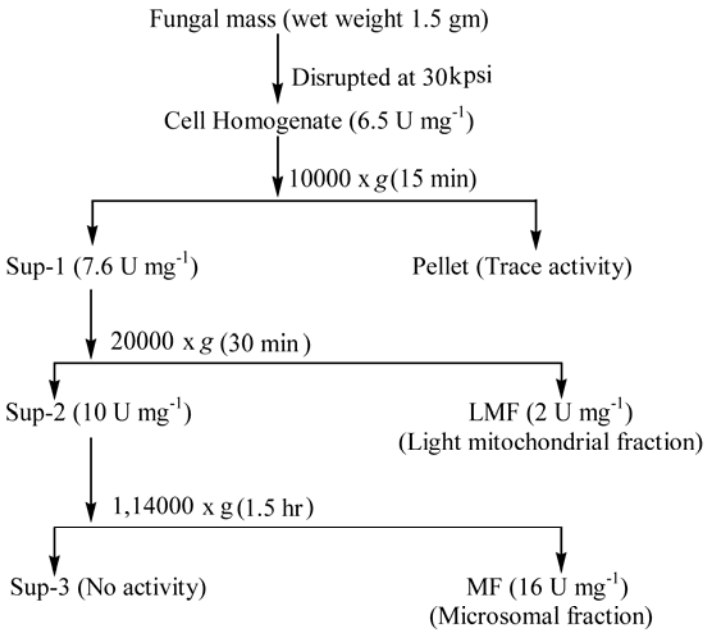

Scheme 3.1: Flow chart on localization of alcohol oxidase enzyme.

The alcohol oxidase activities were studied separately in the sub-cellular fractions of *n*-hexadecane-, glucose-, and ethanol-grown cells of *A. terreus* (Table 3.1). In all these activity studies the alcohol oxidase was localized only in the microsomal fraction of the cells. In *n*-hexadecane-grown cells the alcohol oxidase oxidized a broad range of alcohols, namely, SCAO-, LCAO-, SAO-, and AAO substrates. Whereas, in glucose- and ethanol-grown cells the enzyme was not active against AAO-, and LCAO-substrates, respectively. Moreover, the levels of induction on other substrates were also poor in the glucose- and ethanol-grown cells. Among various short chain-, long chain-, and secondary alcohol substrates highest alcohol oxidase activity in the *n*-hexadecane-grown cells were detected with the substrates *n*-heptanol (15.01 ± 0.06), *n*-hexadecanol (15.26 ± 0.09), and 3-octanol (17.06 ± 0.02), respectively. Similar results with short chain alcohols were obtained with glucose- and ethanol-grown cells, albeit, the level of activities were low. Our findings on the

detection of a broad substrate specific alcohol oxidase activity in the same enzyme provoking further investigation on the protein chemical natures of the enzyme, the results of which may be useful to establish the structure-function relationship of this protein.

The alcohol oxidase isolated from the *n*-hexadecane-grown cells showed 33% enantiomeric excess activity for the *R*(-)2-octanol over *S*(+)2-octanol (Table 3.1). Higher enzyme activities for the *R*(-)2-octanol over *S*(+)2-octanol were also observed in glucose- and ethanol-grown cells. Kinetic studies of the alcohol oxidase catalysis of *n*-hexadecane-grown cells were carried out for different substrates and the corresponding Michaelis-Menten constants (K_m) were calculated. Lowest K_m for the short chain-, long chain- and secondary alcohol substrates were found for *n*-heptanol (0.005 mM), *n*-hexadecanol (0.008 mM) and 3-octanol (0.006 mM), respectively.

Zymogram analysis of the microsome of *n*-hexadecane-grown cells in 7% gel (run time 5 hr) using mixed alcohol substrates containing *n*-heptanol, *n*-dodecanol, 2-dodecanol, and benzyl alcohol showed a broad green color band with alcohol oxidase activity (Fig 3.1B). Preliminary investigation of the alcohol oxidase protein in native PAGE showed that the M_r of the alcohol oxidase was more than 250 kDa. These observations on the very high molecular weight and broad substrate activity of the alcohol oxidase prompted us to suggest that this enzyme-protein is oligomeric in nature containing different sub-units bearing different functional (catalytic) properties. In all microorganisms and plants studied so far on the alcohol oxidase as a whole, the enzyme is largely reported as octameric [Couderc & Baratti 1980; Kato *et al.*, 1976; Suye 1997], with the exceptions of *C. tropicalis* [Dickinson & Wadforth 1992] and *T. vulgare* [Banthorpe *et al*., 1976], where the dimeric nature of the enzyme was demonstrated.

The enzyme activity was not inhibited by iron chelating agents, taxifolin and piperonyl butoxide (PBO), indicate the lack of heme iron in these isozymes. The alcohol oxidase activity was inhibited to 86 ± 3 % and 57 ± 1 % with 5 mM of *p*-chloromercuribenzoic acid (PCMB) and tetraethylthiuram disulphide, respectively. The activity was strongly inhibited by PCMB and tetraethylthiuram disulphide. Although, no quantitative conclusion could be drawn with the results on the strong inhibition the involvement of sulfahydryl group of the enzyme in the catalysis may be implicated. Lack of inhibition by taxifolin and piperonyl butoxide, which usually inhibit the heme-enzymes, indicates the lack of heme iron in this protein (Fig 3.2).

The optimum pH for the alcohol oxidase activity was found to be 8.1 ± 0.5 (Fig 3.3 A). The optimum temperature for the alcohol oxidase activity was found to be in the range of 27-33 ^{o}C as shown in Fig 3.3 B. Statistical analysis showed that there were no significant differences among the activity data obtained within the temperature range of 27 to 33 ^{o}C.

No difference in the alcohol oxidase activity was observed upon addition or non-addition of FAD, FMN, $NADP^{+}$ and NAD^{+} in the reaction mixture. The fluorescence emission spectra of the DEAE sepharose column eluted protein with authentic FAD were compared by using excitations at 443 nm. The excitation gave similar emission spectra for both alcohol oxidase and FAD with emission peaks at around 527 nm for both the samples (Fig 3.4). Thus the alcohol oxidase appears to contain FAD as reflected from the similar fluorescence emission spectra obtained by excitation at 443 nm.

Although, primary alcohol is a common metabolic intermediate formed during microbial degradation of normal alkanes, formation of secondary alcohol through sub-terminal oxidation of long chain *n*-alkanes in fungi is also documented [Britton 1984]. We have demonstrated the involvement of hydroxylase enzyme in the sub-terminal oxidation of carbon chain during growth of *A. terreus* on hydrocarbon [Vatsyayan *et al.*, 2008]. Hence the induction of alcohol oxidase protein capable of oxidizing secondary alcohols may be attributed to its role on the metabolism of secondary alcohols formed as metabolic intermediates during the assimilation of *n*-hexadecane by *A. terreus*. High selectivity of the alcohol oxidase for the *R*(-)2-octanol (33% ee) over *S*(+)2-octanol may be correlated with the lower K_m value (0.012 mM) of the enzyme for the *R*(-)2-octanol than the K_m value (0.02 mM) obtained for the *S*(+)2-octanol. The activity of the alcohol oxidase with many other substrates also could be correlated with the corresponding K_m values as reflected from table 3.1.

3.4 FIGURES

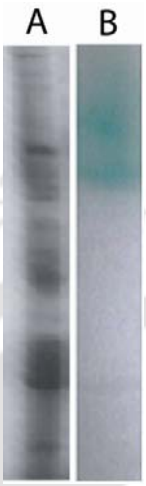

Figure 3.1: Zymogram analysis with mixed substrates namely *n*-heptanol, *n*-dodecanol, 3-octanol and benzyl alcohol. (**A**) CBB R-250 staining gel were recorded as B/W using Gel Documentation systems (Bio-Rad, USA). (**B**) Gel stained with ABTS dye to detect alcohol oxidase bands in PAGE. Photograph was recorded with CCD camera (Nikon, Japan).

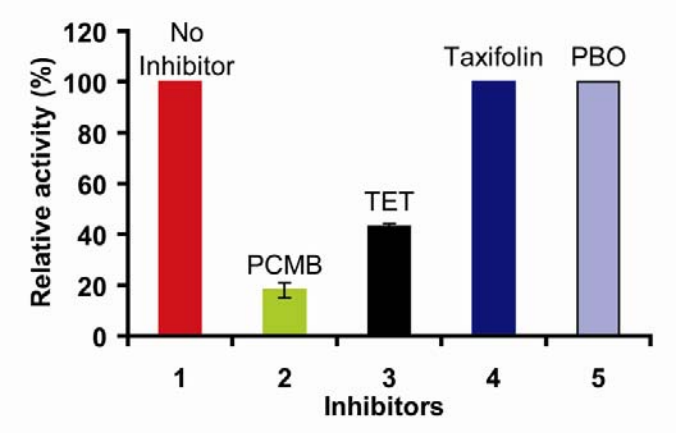

Figure 3.2: Alcohol oxidase inhibition assay with different effectors. PCMB: *p*-chloromercuribenzoic acid, TET: tetraethyl thiuram disulfide, taxifolin and PBO: piperonyl butoxide.

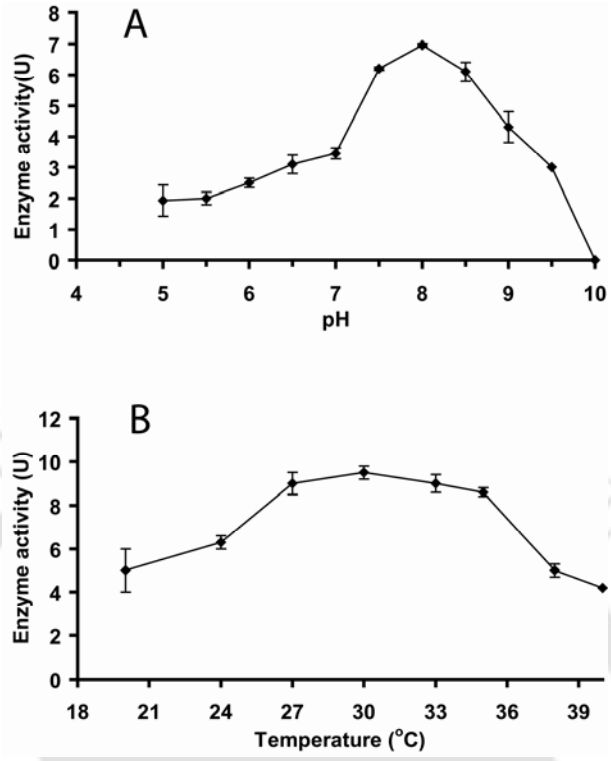

Figure 3.3: Alcohol oxidase enzyme activity studies. (**A**) Optimum pH was 8.1 ± 0.5 at an (**B**) optimum temperature 27-33 °C.

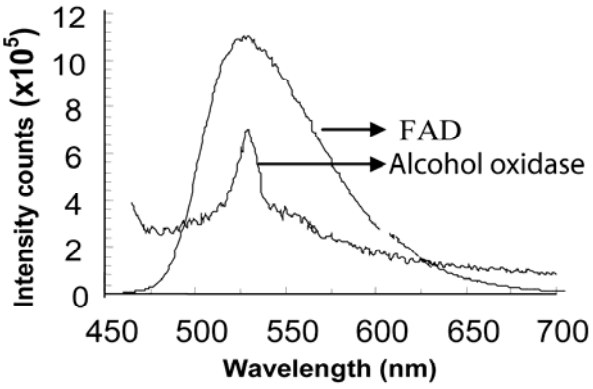

Figure 3.4: Fluorescence emission spectra of alcohol oxidase and FAD obtained by excitation at 443 nm.

3.5 TABLES

Table 3.1: Detection of alcohol oxidase activity (μM O_2 consumed per min) in the cells of *A. terreus* during growth on different carbon substrates

Alcohol substrate	Enzyme activity in different growth substrates			K_m[a] (mM)
	Hexadecane	Glucose	Ethanol	
Short chain alcohols				
Methanol	trace (< 2)	nil	nil	ND
Ethanol	trace (< 2)	nil	nil	ND
1- Butanol	10.9 ± 0.06	6.2 ± 0.04	3.1 ± 0.08	0.028
1- Heptanol	15.0 ± 0.02	7.6 ± 0.09	4.8 ± 0.01	0.005
1- Octanol	11.6 ± 0.06	5.3 ± 0.03	2.8 ± 0.09	0.050
Long chain alcohols				
1- Decanol	10.6 ± 0.17	trace (< 2)	nil	0.060
1- Undecanol	10.5 ± 0.14	trace (< 2)	nil	0.050
1- Dodecanol	11.2 ± 0.11	trace (< 2)	nil	0.028
1- Tetradecanol	11.6 ± 0.06	nil	nil	0.020
1- Hexadecanol	15.3 ± 0.09	nil	nil	0.008
12-Hydroxydodecanoic acid	2.0 ± 0.15	nil	nil	ND
1,16-Hexadecanediol	8.9 ± 0.05	nil	nil	0.028
Secondary alcohols				
Isopropanol	8.9 ± 0.04	nil	nil	0.030
Isoamyl alcohol	4.8 ± 0.23	trace (< 2)	nil	0.100
R(-)2-Octanol	14.3 ± 0.06	2.3 ± 0.05	2.1 ± 0.09	0.012
S(+)2-Octanol	9.5 ± 0.19	trace (< 2)	trace (< 2)	0.020
Cyclooctanol	8.8 ± 0.11	nil	nil	0.030
2-Octanol	12.1 ± 0.02	ND	ND	ND
3-Octanol	17.0 ± 0.09	nil	2.8 ± 0.02	0.006
2-Dodecanol	15.7 ± 0.11	nil	nil	0.008
Aromatic alcohols				
Benzyl alcohol	8.7 ± 0.06	nil	trace (< 2)	0.030

ND, not determined

[a] The K_m was determined with the alcohol oxidase activities of *n*-hexadecane-grown cells using the spectrophotometric assay method of Kemp *et al*., [1988]. The mean of the three values is given in the table. Each value represents the mean ± standard error at $p < 0.05$.

Chapter 4

PURIFICATION AND FUNCTIONAL CHARACTERIZATION OF THE ALCOHOL OXIDASE

4.1 OVERVIEW

The importance of alcohol oxidases in the metabolic processes and their possible utilization in various products and processes have been reviewed as revealed from some of the selected recent publications [Fernando *et al.,* 2007; Azevedo *et al.,* 2005; Hargrove *et al.,* 2004; Segers *et al.,* 2001; Van den Heuvel *et al.,* 2001; Hack *et al.,* 2000]. Research on these membrane bound enzymes has been primarily dealt with the morphological, protein chemical and functional aspects due to highly complex molecular and biophysical nature of this group of enzymes [Ozimek *et al.,* 2005; Tahallah *et al.,* 2002; Mattevi 1998; Ghisla & Massey 1989]. Among these various alcohol oxidases, methanol oxidase and aryl alcohol oxidases have been studied to a greater extent [Ozimek *et al*., 2005; Sahm *et al*., 1982; Varela *et al*., 2000, 2001; Guillen *et al*., 1992]. Research on other groups of alcohol oxidases has not received adequate attention although, preliminary findings gathered so far on those oxidases may be the basis for unfolding many interesting facts, and thus, advancing the scope for their applications.

The research on these alcohol oxidases produced during the assimilation of hydrocarbon by filamentous fungi is in nascent stage and detail functional and physico-chemical characteristics of these oxidases are yet to be explored. In the

earlier chapter we have described the detection, localization and preliminary functional characterization of a broad substrate specific alcohol oxidase able to oxidize short chain-, long chain-, aromatic- and secondary alcohols in the microsomal membrane of *n*-hexadecane-grown *Aspergillus terreus* MTCC 6324. In this chapter we present the purification and novel structural features on this broad substrate specific alcohol oxidase present in the said fungal species.

4.2 EXPERIMENTAL APPROACHES

4.2.1. Organism and Culture Conditions

The culture conditions and maintenance of *A. terreus* MTCC 6324 used in this study were described previously as in the chapter 2.

4.2.2. Isolation of Alcohol Oxidase from Microsomal Membrane

The 20000 x *g* supernatant of the disrupted *n*-hexadecane-grown cells was prepared according to the method described previously as in chapter 3. A floating protein layer containing alcohol oxidase activity was fractionated from the supernatant using ammonium sulfate at a saturation of 35% (w/v). The enzyme layer was separated by 10000 x *g* and re-suspended in a minimum volume (10-13 ml) of 50 mM Tris-HCl, pH 8.0, and then desalted by dialyzing for 4 hr against the same buffer (500 ml x 2) containing 0.1 mM PMSF. The membrane bound protein was solubilized following the method described by Hjelmeland & Chrambach [1984]. The desalted enzyme solution was mixed with a suitable concentration of 3-[(3-cholamidopropyl) dimethyl ammonio] propane-1-sulfonic acid (CHAPS) and 0.15 M KCl, and vortexed for 1 hr at 4 ^{o}C to solubilize the enzyme. The membrane was then separated by pelleting at 114000 x *g* for 1 hr and the clear supernatant was collected for enzymatic study. All the steps of purification were performed at 4 ^{o}C, unless it is specified.

4.2.3. Purification of Alcohol Oxidase by Ion Exchange Chromatography

The membrane-free soluble enzyme was dialyzed against ice cold 20 mM Tris-HCl, pH 9.0, (500 ml x 2) containing 0.1 mM PMSF for 4 hr. Hitrap DEAE-sepharose FF (1.6 x 2.5 cm, 90 μm) weak anion exchanger connected to FPLC ACTA system (GE Healthcare) was equilibrated with 20 mM Tris-HCl, pH 9.0. The enzyme

sample was filtered through 0.45 μm filter and loaded on to the pre-equilibrated column at a flow rate of 1 ml min^{-1}. The bounded proteins were eluted with 20 mM Tris-HCl, pH 9.0, containing 400 mM NaCl, in a linear gradient (0-400 mM) at flow rate of 5 ml min^{-1}. The tubes containing protein peak were pooled, and then concentrated by using either 40% PEG 6000 or lyophilization. The concentrated samples were re-suspended in minimal volume (0.2-0.8 ml) of 50 mM Tris-HCl, pH 8.0, and stored at 4 ^{o}C.

4.2.4. Enzymatic Assay of Alcohol Oxidase

Alcohol oxidase activity was assayed using HRP (10 μg ml^{-1}) coupled assay method monitoring H_2O_2 production at 405 nm for ABTS radical at 30 ^{o}C (ε_{405} = 18400 $\mu M^{-1}.cm^{-1}$) [Werner *et al.,* 1970]. The enzyme activities were simultaneously confirmed for each datum using biological oxygen monitor assay method with Clark-type polarographic oxygen electrodes following the similar protocol described previously in chapter 3. As the enzyme was able to oxidize a broad range of alcohol substrates as reported earlier in chapter 3, we have analyzed all the experiments with a representative substrate bearing highest activity from each class of alcohol group. The representative alcohol substrates of short chain-, long chain-, aryl-, and secondary-alcohol for enzymatic assays and kinetic studies were *n*-heptanol, *n*-dodecanol, phenyl-3-propanol, and *R*(-)2-octanol, respectively. Stock solutions of all the substrates were prepared in DMSO.

4.2.5. Molecular Mass Determination of Alcohol Oxidase by Native and SDS-PAGE Analysis

Native and SDS-PAGE analysis of the purified protein were done following the method of Laemmli [1970]. Zymogram analysis of the native PAGE was done after incubating the gel with assay reaction mixture containing 100 mM *n*-heptanol, 70 U HRP, 7 mg ml^{-1} ABTS in 50 mM Tris-HCl, pH 8.0 for 15 min. Gels were stained either with standard CBB R-250 or silver staining methods. PAS staining of SDS-PAGE was done following the method of Matthieu & Quarles [1973]. Different percentages of native PAGE gels (4, 5, 6 and 7.5%) were run to determine the molecular weight of the native protein. The slope of the line (-log K_r) is plotted against molecular weight of the standards. The holoenzyme molecular mass was determined through native PAGE following the standard Ferguson plot method

[Hedrick & Smith 1968]. The final slope value obtained in the graph between slope against molecular weight of the standards (r^2 = 0.9872) was used to calculate the native protein molecular weight. The protein markers used were horse spleen apoferritin (443 kDa), jack bean urease (272 kDa), bovine liver catalase (250 kDa), sweet potato amylase (200 kDa), yeast alcohol dehydrogenase (150 kDa), BSA (66 kDa, 132 kDa). The SDS-PAGE protein markers used were BSA (66 kDa), ovalbumin (45 kDa), glyceraldehyde-3-phosphate dehydrogenase (36 kDa), carbonic anhydrase (29 kDa), trypsinogen (24 kDa), and trypsin inhibitor (20.1 kDa).

4.2.6. Measurement of Isoelectric Point (p*I*)

The p*I* was determined by isoelectric focusing, using immobiline pH gradient gel strips of 3-10 linear range (GE healthcare, Sweden) following the instruction manual supplied with the Multiphor II gel apparatus (Hoefer Pharmacia). The p*I* markers used were *Aspergillus niger* amyloglucosidase (3.6), soybean trypsin inhibitor (4.6), bovine milk *β*-lactoglobulin A (5.1), bovine erythrocytes carbonic anhydrase II (5.9), human erythrocytes carbonic anhydrase I (6.6), horse heart myoglobin (6.8, 7.2), *lens culinaris* lectin (8.2, 8.6, 8.8), and bovine pancreas trypsinogen (9.3).

4.2.7. Mass Spectrometry

LC-MS/MS identification of the protein was carried out by ProtTech, Inc. (Norristown, PA). In brief, proteins in each gel band were digested in-gel with modified sequencing grade trypsin (Promega), and the resulting peptide mixture was subjected to tandem mass spectrometry for peptide sequencing. A Finnigan ion trap mass spectrometer LCQ coupled with an HPLC system running a 75 μM inner diameter C_{18} column was used. Data were acquired in a data dependent mode. MS/MS spectra were used to search the most recent non-redundant protein data bases, including the Protein Information Resources data base and GenBankTM using ProtQuest software suite from ProtTech. The output of the data base search was manually analyzed and validated to verify proper protein identification.

4.2.8. Lipid Staining

Nile red, a specific dye for lipids and hydrophobic domains in proteins, was prepared from nile blue sulfate following the method of Greenspan & Fowler [1985]

with a slight modification, where instead of flash evaporation xylene was evaporated by lyophilization to obtain the product. Nile red fluorescence was examined under Confocal laser scanning microscopy (CLSM) (Zeiss LSM 510) using similar spectral settings of Fowler & Greenspan [1985].

4.2.9. Structural Analysis of Alcohol Oxidase by AFM and TEM

The size, aggregation pattern and surface properties of the protein particles were studied by Atomic force microscopy (AFM) and Transmission electron microscopy (TEM). AFM was performed using an ambient air scanning probe microscope (Picoscan 2500, Molecular Imaging). Images were recorded with typical contact force loads of 0.5 nN using pyramidal Si_3N_4 probe tips mounted on triangular 0.03 (± 0.01) nm^{-1} Au-coated cantilevers. 10 μl of 0.8 mg ml^{-1} purified protein was deposited on a freshly prepared thin layer of mica film and dried under nitrogen for 2 hr.

For TEM (JOEL model TEM-2100) analysis 5 μl of 0.06 mg ml^{-1} purified protein was mixed with equal volume of 1% ammonium molybdate and then deposited on a 300-mesh copper coated carbon grid. The sample was allowed to air dry under laminar hood for 4 hr. The TEM was operated at an accelerating potential of 80kV - 200kV and in a magnification range of 40k X – 1500k X.

4.2.10. DLS Analysis of Alcohol Oxidase

Experiments were carried out in a 201 Spectroscatter Dynamic light scattering (DLS) instrument (RiNA GmbH, Berlin). Data were acquired at 20 ^oC, repeated 20 times and averaged. The viscosity was set to 1 cP at a scattering angle of 90^o and measured at 685 nm. The resulting autocorrelation function was analyzed by the integrated control software to obtain size, radius or shape distributions.

4.2.11. Fatty Acid Analysis by LC-ESI-MS

Purified protein (1.9 mg) was treated with 2M HCl in 83% methanol and refluxed at 100 ^oC for 4 hr. The sample was allowed to cool and then mixed with chloroform to a final ratio of water/methanol/chloroform (1:2:0.8). After 10 min incubation at room temperature, the ratio was increased to 2:2:1.8 for the formation of two separate layers. Chloroform layer was separated by 10000 x *g* for 15 min at 4 ^oC. The lipid was then collected by removing the chloroform using vacuum evaporator

and then stored at 4 ^{o}C. LC-ESI-MS analysis (Q-Tof Premier, Waters) was done in a UPLC BEH RP18 column (1.7 μm x 2.1 x 50 mm). Samples were diluted to picogram concentration using 50% (v/v) acetonitrile containing 0.1% (v/v) formic acid before injecting into the column. Solvents used for the elution were *A*: 5 mM formic acid in water, and *B*: acetonitrile. The column was washed initially for 3 min with *solvent A*, and then fatty acids were eluted with increasing the concentration of *solvent B* in the following order: 20% (8 min), 40% (5 min), 50% (6 min), 60% (3 min), 80% (1 min), and 100% (10 min), respectively. The flow rate was 0.1 ml min^{-1}. Auto sampler was maintained at 15 ^{o}C and the separation was performed at ambient temperature. Identification of fatty acids was done with an ESI probe source in negative mode. ESI-MS was operated at spray voltage 2.5 kV, and the heated capillary temperature at 250 ^{o}C.

4.2.12. Cofactor Analysis using Reverse Phase HPLC and SDS-PAGE

Alcohol oxidase (100-140 μg in 80 μl) was mixed with 40 μl of 15% TCA (5% final concentration) and incubated at 4 ^{o}C for 30 min in dark. The mixture was then centrifuged at 15000 x *g* for 10 min, and the supernatant was applied to an HPLC (Perkin Elmer) Chromatopak RP18 column (0.4 x 25 cm, 5 μm). Isocratic elution was carried out with 5 mM ammonium acetate buffer, pH 5.6, supplemented with 35% methanol, at $UV_{254\ nm}$ with a flow rate of 0.5 ml min^{-1}.

For SDS-PAGE analysis, protein was denatured in SDS sample buffer without bromophenol blue dye. After electrophoresis, the flavin was detected in the gel using UV transilluminator. Gel was excised and crushed with glass homogenizer in distilled water and then centrifuged twice at 12000 x *g* for 10 min to remove the gel matrix. The supernatant was then analyzed for flavin using spectrofluorometer under similar parameters as mentioned earlier. A control containing gel portion devoid of flavin was analyzed separately.

4.2.13. Studies on the Stability of the Alcohol Oxidase

In order to analyze the pH stability the enzyme samples were treated with the test pH [phosphate buffer (pH 6.0 and 7.0); tris buffer (pH 8.0); ethanol amine buffer (pH 9.0 and 10.0); and piperazine buffer (pH 11.0)] separately, for minimum 30 min to maximum 120 min and then analyzed for residual activity following the spectrophotometric assay method stated above. The temperature stability of the

enzyme was studied by treating the enzyme samples in test temperatures (4 ^{o}C to 40 ^{o}C) for different time periods and then analyzed for the residual activity following the same spectrophotometric assay method stated earlier.

4.2.14. Analytical methods

Protein estimation was done following Bradford method using BSA as standard [Bradford 1976]. The carbohydrate content was estimated by Anthrone method [Scott & Melvin 1953] as well as Phenol-sulfuric acid method [Hounsell *et al.,* 1997] using glucose as standard.

All the data presented in this study were the mean of three or more experiments with a variation within 10%. Analysis of variance was carried out for the statistical data with the help of Microsoft® Excel 2003 as described in chapter 2.

4.3 RESULTS

The ammonium sulfate fractionated (35% w/v) proteins (Fig 4.1) from the 20000 x *g* supernatant of cell homogenate were solubilized with CHAPS and then the microsomal membranes were separated by ultracentrifugation. The optimum concentration of CHAPS for maximum solubilization and activity of the enzyme was 0.5% (w/v) (Fig 4.2).

The membrane free soluble proteins were then adsorbed on DEAE-sepharose column and then purified to a single sharp peak containing alcohol oxidase activity using 0-400 mM linear NaCl gradient (Fig 4.3).

The purification steps and degree of purification is shown in table 4.1. The purified enzyme exhibited a broad substrate tolerance towards oxidation of short chain-, long chain-, secondary- and aryl-alcohols, respectively. The substrates with highest specific activities obtained for short chain-, long chain-, secondary- and aryl-alcohols were *n*-heptanol (305 ± 0.3 U mg^{-1}), *n*-dodecanol (62 ± 0.1 U mg^{-1}), *R*(-)2-octanol (62 ± 0.3 U mg^{-1}), and phenyl-3-propanol (250 ± 0.2 U mg^{-1}), respectively. The apparent kinetic constants determined for the representative substrates for each class of alcohols are given in table 4.2. Comparison of the catalytic efficiencies

(K_{cat}/K_m) among the alcohol substrates indicates that *n*-heptanol (K_m = 0.498 mM, K_{cat} = 2.7 x 10^2 s^{-1}) is the preferred substrate for this alcohol oxidase.

The homogeneity of the purified protein was demonstrated from a single protein band in native PAGE (Fig 4.4A). Zymogram analysis of the native PAGE showed the alcohol oxidase activity in the protein band (Fig 4.4B).

The native protein molecular mass 269 ± 5kDa was calculated using native PAGE. The purified protein, however, could not be resolved by size exclusion column (TSK G3000SW) with cut off size 15 to 300 kDa, since the protein was eluted in the initial void volume. It implies that the purified native protein was likely to be in aggregated form with molecular mass was more than 300 kDa (Fig 4.5).

SDS-PAGE of the pure protein stained with CBB R-250 showed four different bands with molecular mass of 85-, 63-, 43- and 27-kDa, respectively and a weak band corresponding to 13kDa (Fig 4.6A). PAS staining of the SDS-PAGE gel did not show any band except in the position of the dye front, thus ruled out the possibility of glycoprotein nature of the enzyme (Fig 4.6C). Glyco band appeared in the dye front was ascribed to the ribitol sugar present in the FAD. The presence of FAD in the dye front (Fig 4.7) and detection of sugar in the purified FAD were demonstrated. Result showed that the FAD was detached from the protein during the SDS-PAGE of the native enzyme and moved in the dye front irrespective of running the gel under non-reducing condition that void *β*-ME in the sample preparation (Fig 4.6B) or reducing condition (Fig 4.6A). The FAD was not separable from the protein by simple ion exchange or gel filtration chromatography. This indicates that the FAD is non-covalently but avidly associated with the alcohol oxidase protein.

There was no difference in number and position of the bands in the gel when SDS-PAGE of the protein was run in presence (Fig 4.6A) or absence of *β*-ME (Fig 4.6B), which implied that the subunits in this multimeric protein were not linked by disulfide bonds.

The isoelectric point of the subunit proteins of the enzyme was found within the pH range of 8.3-8.5. The effects of pH on the stability of the enzyme were studied at different buffer pH ranging from 6-11 using a treatment time of 3 hr for each sample and then assayed for residual enzyme activity. The optimum stability was detected at pH 9 where the residual activity of the enzyme was more than 95% and is significantly different from pH 7 and pH 8 with a $p < 0.05$ (Fig 4.8A). The enzyme protein was found to be temperature sensitive. Although the enzyme was highly stable

at 4 ^{o}C and more than 50% of the original activity was retained even after 1 month, the enzyme activity was lost to nearly 20% of the original value when the protein was incubated at 32 ^{o}C for 2 hr (Fig 4.8B).

Peptide sequencing of two intense SDS-PAGE protein bands with corresponding molecular masses of 63- and 43-kDa subunits were done by LC-MS/MS. Peptide sequencing of 63kDa protein showed the presence of two FAD binding domains (**G**x**G**xx**G**) (YPVIDHEYDAVVV**GA**G**G**A**G**LR and SAFV**G**A**G**AG**G**TVLESLK), whereas in 43kDa protein no FAD binding domain was detected within the resolved sequences. Homology studies revealed that among the two FAD binding domain sequences of 63kDa protein, only the YPVIDHEYDAVVV**GA**G**G**A**G**LR sequence (Figure 4.9) shows 45-50% similarity with the N-terminal sequences of reported alcohol oxidases from methylotropic yeasts and other organisms. The multiple sequence alignment of these peptides using ClustalW software is shown in table 4.3. Non-redundant database search of these peptides showed that the protein subunits belong to a novel class of alcohol oxidase as they did not show any sequence similarity with the alcohol oxidase protein sequences available until now.

DLS analysis of the purified protein solution (0.24 mg ml^{-1}) at highest soluble state (clear solution obtained at 20,000 x *g*) showed the average mean radius distributions of the native protein particles 180 ± 23 nm (Fig 4.10). The aggregation was found to be not uniformly formed as evident from the poly-dispersed protein particles of different sizes observed under AFM (Fig 4.11A). The sizes of the bigger particles, however, were found to be nearly multiples of the smallest protein particle size. Aggregating tendency of the protein particles was also evident from the micrograph as indicated by an arrow in figure 4.11A. High inter protein particle adhesion property was also revealed from the TEM images (Fig 4.11B). The smallest native protein particle size observed was 10.2 nm. The surface topology of the protein was studied with ImageJ software using interactive 3D surface plot (software to view and export electron microscopy image files [http://rsb.info.nih.gov/ij/]). The top view and side view of the 3D images showed globular shape of the protein particles with uneven surface morphology (Fig 4.11C-D).

The purified protein was studied under CLSM using nile red staining and examined red fluorescence at 515-560 nm excitation. Native protein showed intense red fluorescence (Fig 4.12A). A control protein, HRP (M_r = 45kDa), that does not

have any hydrophobic domains and contains uniformly distributed medium size protein particles, did not show any excitation in similar to the Fig 4.12B.

The presence of fatty acids in the pure alcohol oxidase protein was investigated to address the issue related to high staining ability of the protein with nile red and high aggregating properties of this alcohol oxidase protein. Two fatty acids namely, oleic acid ($C_{18:1}$) and palmitic acid ($C_{16:0}$) at a ratio of nearly 2:1, were found in the purified native protein as evident from LC-MS analysis (Fig 4.13). This implies the lipoprotein nature of the protein entity. The ratio of these fatty acids was calculated from the mass spectra obtained by injecting the samples through infusion method, where samples were injected directly into the ESI/MS without passing through the liquid chromatographic column.

$MgCl_2$ at a concentration of 1 mM increased the enzyme activity to nearly 50% for both short chain-, and long chain alcohol substrates; whereas, ferrocene at the similar concentration increased the alcohol oxidase activity only for the short chain alcohol substrate to 47% of the original activity. There was complete loss of enzyme activity with 1 mM $AgNO_3$ or 5 mM PCMB, while >70% original activity was lost with 5 mM tetraethylthiuram disulphide. The complete list of effect of different effectors on the alcohol oxidase enzyme activity is shown in figure 4.14.

We identified for the first time the 1,12dichlorododecane (1,12DCD) as competitive inhibitor for long chain alcohol substrate (Table 4.2). The K_i for 1,12DCD was found to be 2.46 μM for *n*-dodecanol. There was no inhibitory effect of 1,12DCD on the oxidation of short chain- and aromatic alcohols, while, it was found to be an activator for secondary alcohols. We also found that the β-ME acted as competitive inhibitor for the alcohol oxidase substrates as evident from the increased K_m in presence of β-ME (Table 4.2). The K_i values calculated for the β-ME inhibition for representative alcohol substrates *n*-heptanol, *n*-dodecanol, phenyl-3-propanol and *R*(-)-2-octanol were 1.57-, 0.63-, 3.62-, and 0.014- μM, respectively. Whereas, ethylene glycol that is structurally similar to the β-ME did not act as inhibitor even at higher concentrations. The findings indicate that –SH group of the β-ME was critical for the inhibition.

4.4 DISCUSSION

The reports on oxidation of different classes of alcohol substrates from filamentous fungi is limited and the research on these oxidases is yet to get momentum as compared to other alcohol oxidases as evident from some of the selected reviews and publications on the subject [Fernando *et al.,* 2007; Ozimek *et al.,* 2005; Van Der Klei *et al.,* 1991; Siebum *et al.,* 2006; Luxova & Svatos 2006; Cheng *et al.,* 2005; Szamecz *et al.,* 2005; Ferreira *et al.,* 2005; Ko *et al.,* 2005; Hortencia & Roberto 2005; Qian *et al.,* 2004; Eirich *et al.,* 2004; Dienys *et al.,* 2003; Grewal *et al.,* 2000; Kondo *et al.,* 2008; Isobe *et al.,* 2007; Daniel *et al.,* 2007]. In all these reports either methanol oxidase (EC 1.1.3.13) or aryl alcohol oxidase (EC 1.1.3.7) were studied extensively, while oxidation of a wide range of alcohol substrates by a single enzyme are rare. This is the first report on the broad substrate specific alcohol oxidase activity present in a single protein entity from filamentous fungi. The preferred substrate range among all the alcohol substrates is C_7-C_9 primary aliphatic alcohols with highest affinity for *n*-heptanol. The alcohol oxidase showed poor activity for C_1-C_4 alcohol substrates thus appeared different from the methylotropic alcohol oxidases. In chapter 3, the alcohol oxidase activities on different classes of substrates, namely, short chain-, long chain-, secondary-, and aromatic alcohol groups were described to a great extent. The native protein molecular mass was found to be similar with *Aspergillus ochraceous* alcohol oxidase [Isobe *et al.,* 2007], whereas the subunit molecular weight profile detected by us is different from this report. The holoenzyme and subunit molecular weight profile of alcohol oxidase obtained by us is distinct from other reports on various alcohol oxidases from methylotropic yeasts [Ashin & Trotsenko 2000; Suye 1997; Veenhuis *et al.,* 1989], *Penicillium, Peniophora* and *Poria contigua* species [Tahallah *et al.,* 2002; Cheng *et al.,* 2005; Qian *et al.,* 2004; Danneel *et al.,* 1994; Bringer *et al.,* 1979]. Similarly, the high isoelectric point of alcohol oxidase from *A. terreus* observed by us is also found to be entirely different from other organisms, where it was reported as below neutral pH [Isobe *et al.,* 2007; Daniel *et al.,* 2007]. The preliminary identification of the alcohol oxidase protein following peptide mass fingerprinting using LC-MS/MS analysis was done based on two subunits with high intensity in the SDS-PAGE gel. Further investigation on detail sequence analysis of all the subunits is warranted to elucidate the structure-function relationship of this novel alcohol oxidase protein.

Application of specific inhibitor 1,12DCD, non-specific inhibitor *β*-ME, activators like ferrocene and $MgCl_2$ has been envisaged in industrial processes involving alcohol oxidase catalyzed conversion of broad range of alcohols to the corresponding aldehydes or ketones with high catalytic efficiencies for maneuvering the production of desired industrial products. The selective inhibition and activation of the alcohol oxidase activity with respect to the substrates by different activators and inhibitors is intriguing. These results raised query on the number of active sites in this multimeric protein entity for different substrates.

The strong aggregating property of this multimeric enzyme through non-covalent interaction among different proteins demonstrated through this investigation may be an appealing finding in the field of protein-protein interaction and aggregation. The remarkable aggregation size (average size of 180 nm radius) of these protein particles demonstrated by us is the first report of its kind to the best of our knowledge until now. Peroxisomal small proteinaceous aggregates containing alcohol oxidase [Evers *et al.,* 1994] and aggregation of alcohol oxidase protein under high local concentrations during native PAGE [Ashin & Trotsenko 2000] are the extent of findings reported so far. Highly aggregating property of this alcohol oxidase protein entity is suggested to be caused by the hydrophobic interactions between the subunits that contain these fatty acids namely, oleic acid and palmitic acid. This is the first report on the lipoprotein nature of alcohol oxidase enzyme from any sources. This investigation has opened up new avenue on the research to explore the architecture of alcohol oxidase proteins from different sources including their structure-function relationship and their potential applications.

4.5 FIGURES

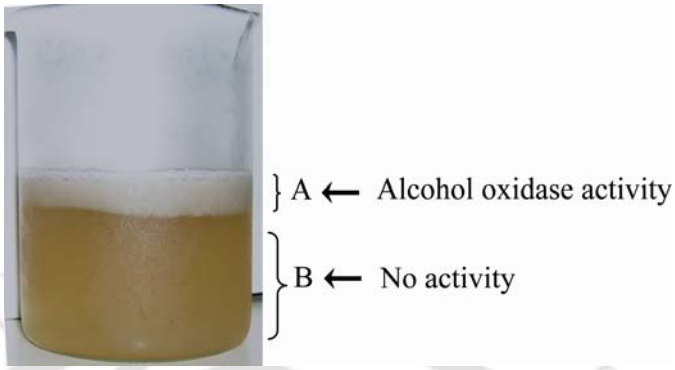

Figure 4.1: Ammonium sulfate precipitation of alcohol oxidase protein. The floating top layer [**A**] formed after precipitation largely contained the alcohol oxidase activity and accounted 12% of the total protein present in the supernatant. The clear supernatant [**B**] in the botton account 88% of the total protein of the supernatant but did not contain the activity.

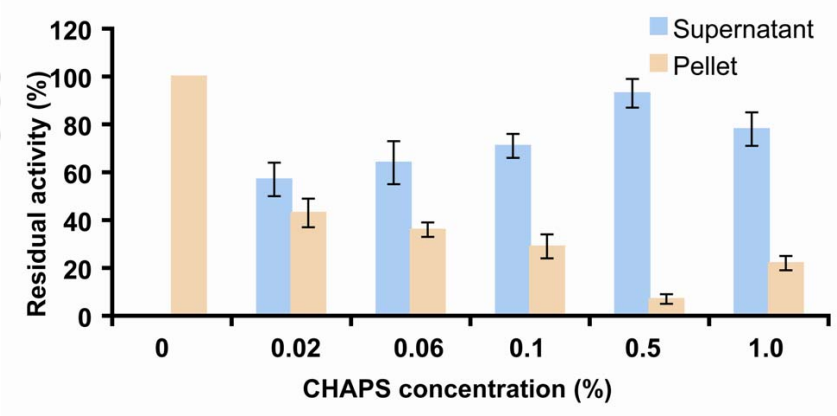

Figure 4.2: Membrane solubilization of alcohol oxidase protein using CHAPS detergent. After treating the membrane bound proteins with 0.5% (w/v) CHAPS for 1 hr majority of the alcohol oxidase protein was released into the supernatant devoid of membranes were obtained.

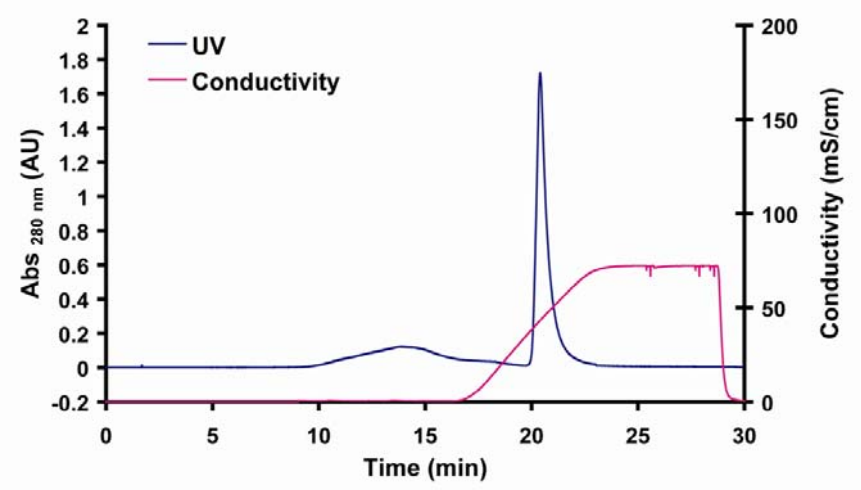

Figure 4.3: DEAE sepharose anion exchange chromatogram of alcohol oxidase. The membrane free supernatant containing alcohol oxidase activity was absorbed on to a pre-equilibrated DEAE sepahrose FF column at a flow rate of 1 ml min^{-1}. The protein was eluted with NaCl (0-400 mM) in linear gradient at flow rate of 5 ml min^{-1}.

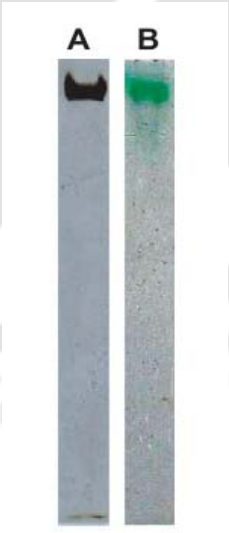

Figure 4.4: Native PAGE analysis of alcohol oxidase protein. (**A**) Native PAGE stained with silver staining. (**B**) Zymogram analysis was done after incubating the gel with the assay reaction mixture containing *n*-heptanol substrate as mentioned in methods section. The molecular mass was calculated using Ferguson plots and it was found to be 269 ± 5kDa.

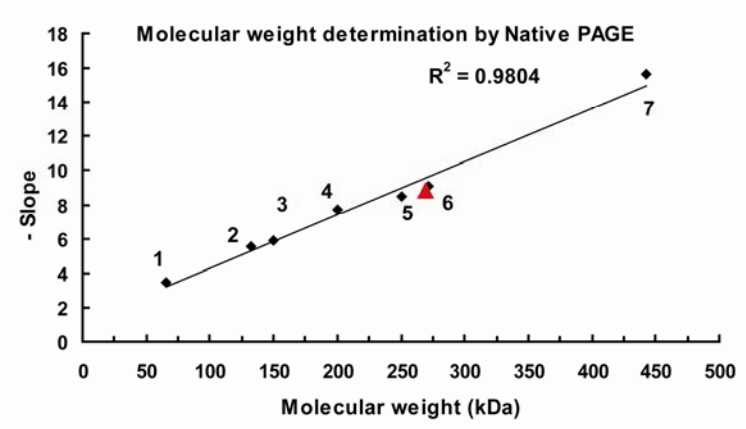

Figure 4.5: Native PAGE molecular mass determination using Ferguson plots. The slope of the line (-log K_r) is plotted against molecular weight of the standards. The final slope value obtained in the graph between slope against molecular weight of the standards (r^2 = 0.9872) was used to calculate the native protein molecular weight (marked triangle). The standard native PAGE protein markers used for molecular weight determination were [1,2] bovine serum albumin (66kDa, 132kDa); [3] yeast alcohol dehydrogenase (150kDa); [4] sweet potato amylase (200kDa); [5] bovine liver catalase (250kDa); [6] jack bean urease (272kDa); and [7] horse spleen apoferritin (443kDa), respectively.

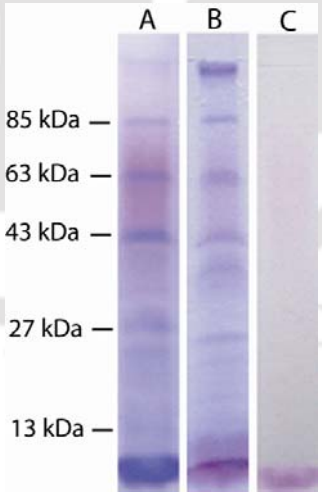

Figure 4.6: SDS-PAGE analysis of alcohol oxidase. SDS-PAGE of native protein under (**A**) reducing conditions, (**B**) non-reducing conditions and (**C**) SDS-PAGE stained with Periodic acid Schiff (PAS) for glycoprotein. The dye front at the bottom of the gels is also shown, which was stained with both PAS and CBB R-250.

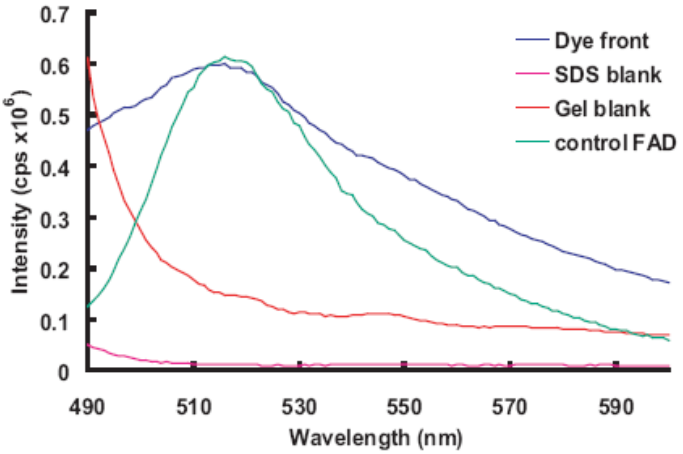

Figure 4.7: FAD fluorescence emission spectra of the gel portion (dye front) excised from SDS-PAGE. Two controls, one containing SDS in de-ionized water for base line correction and other containing aqueous extraction from non-lane gel portion, were also analyzed similarly to nullify any background noise. An authentic FAD sample was also analyzed for comparison.

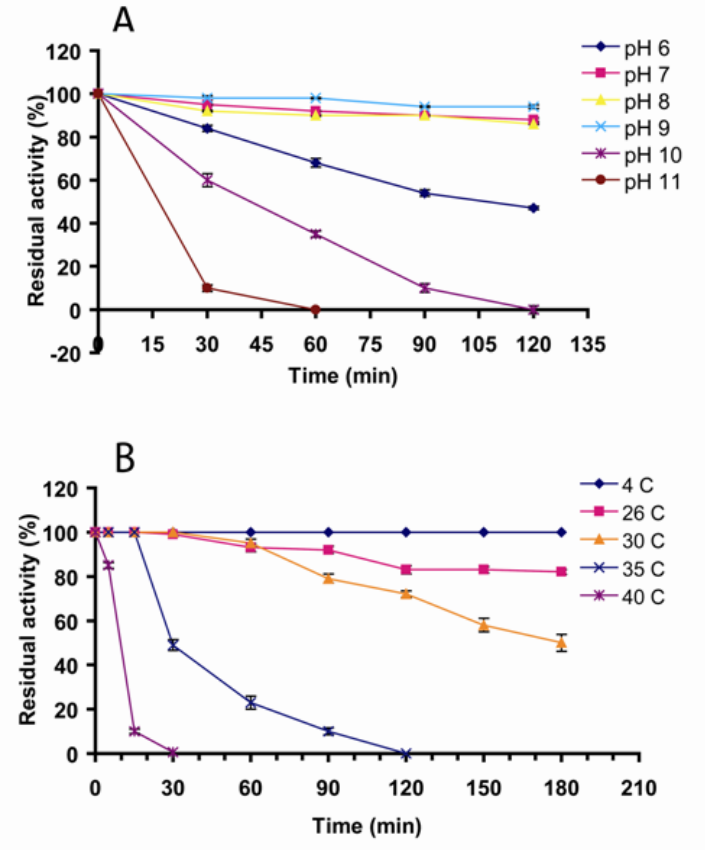

Figure 4.8: pH (**A**) and Temperature (**B**) stability of alcohol oxidase: Buffer system used for pH stability studies were: phosphate buffer (pH 6.0 and 7.0); tris buffer (pH 8.0); ethanol amine buffer (pH 9.0 and 10.0); and piperazine buffer (pH 11.0). The activity corresponding to 100% residual activity was 15.01 ± 0.06 U.

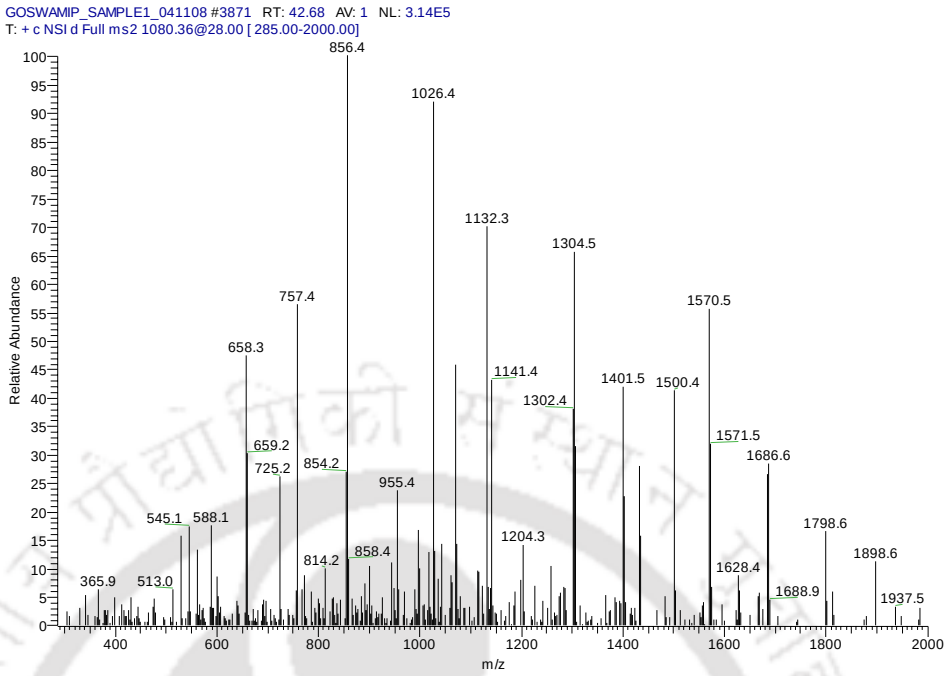

Figure 4.9: LC-MS/MS tandem mass spectra of "YPVIDHEYDAVVV**G**A**G**GA**G**LR" peptide. The raw MS/MS spectra of the above peptide containing FAD binding domain (**G**x**G**xx**G**) is shown here. The peptide was obtained from 63kDa subunit protein.

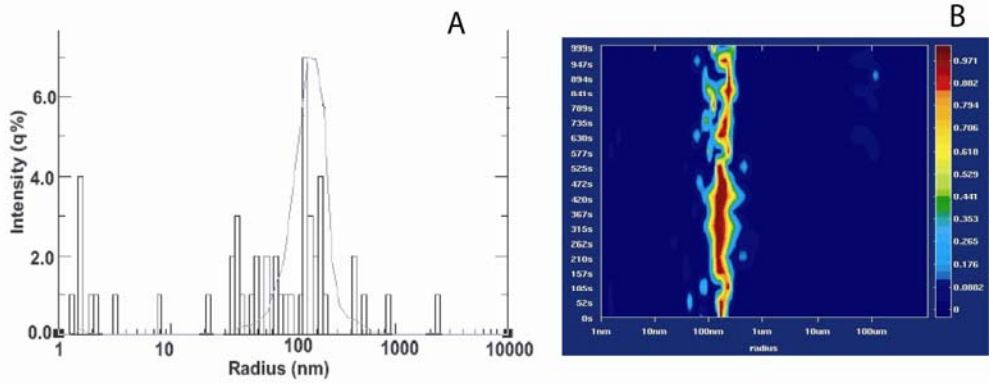

Figure 4.10: DLS studies on the particle size distribution of the purified protein solution. (**A**) The mean radius distribution was found to be 180.54 ± 26.22 nm. (**B**) DLS plot of native purified protein. The line indicates the purity of the samples and the blue patches are dust particles. The axis of the plot is as follows: x-axis indicates the radius (μm), y-axis the analysis time (sec), and secondary y-axis indicates the purity of the samples.

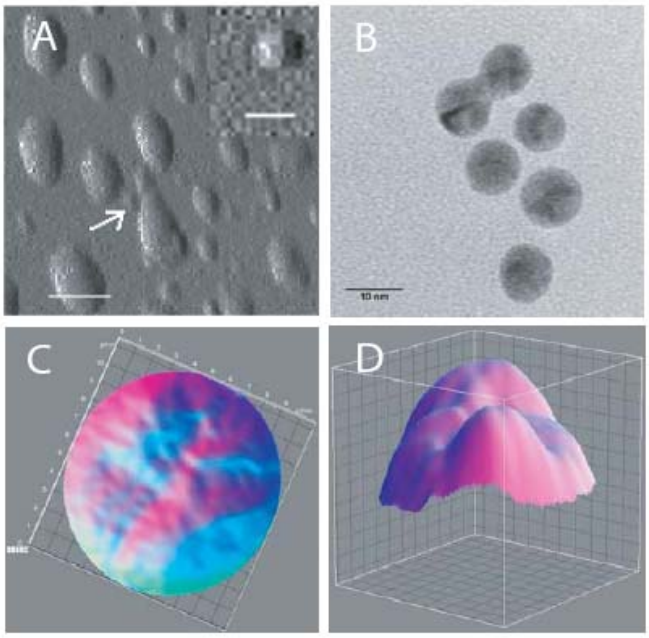

Figure 4.11: Aggregation profile and shape of alcohol oxidase protein entity. (**A**) AFM image. The poly-dispersity of the aggregated particles of different sizes is evident. Inlet shows a single protein particle (Bar = 20 nm). Protein particles tending to aggregate with other smaller protein particles are shown by arrow (Bar = 130 nm). (**B**) TEM image of the protein particles (Bar = 10 nm). (**C-D**) Top view and side view of 3D surface plot derived from a single protein in TEM image using ImageJ software. The TEM images show globular shape of the protein particles with uneven surface morphology.

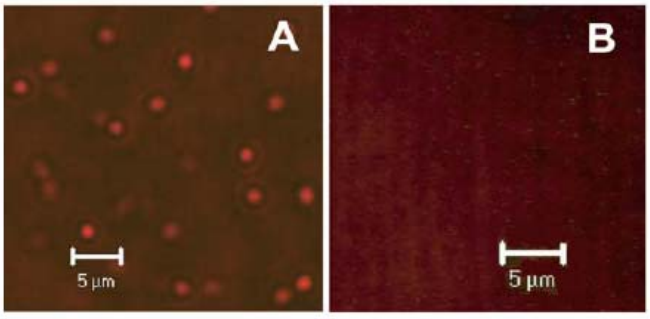

Figure 4.12: CLSM images of purified protein after staining with nile red. (**A**) Purified protein shows the nile red fluorescence. (**B**) A reference protein, HRP. Bar = 5 μm.

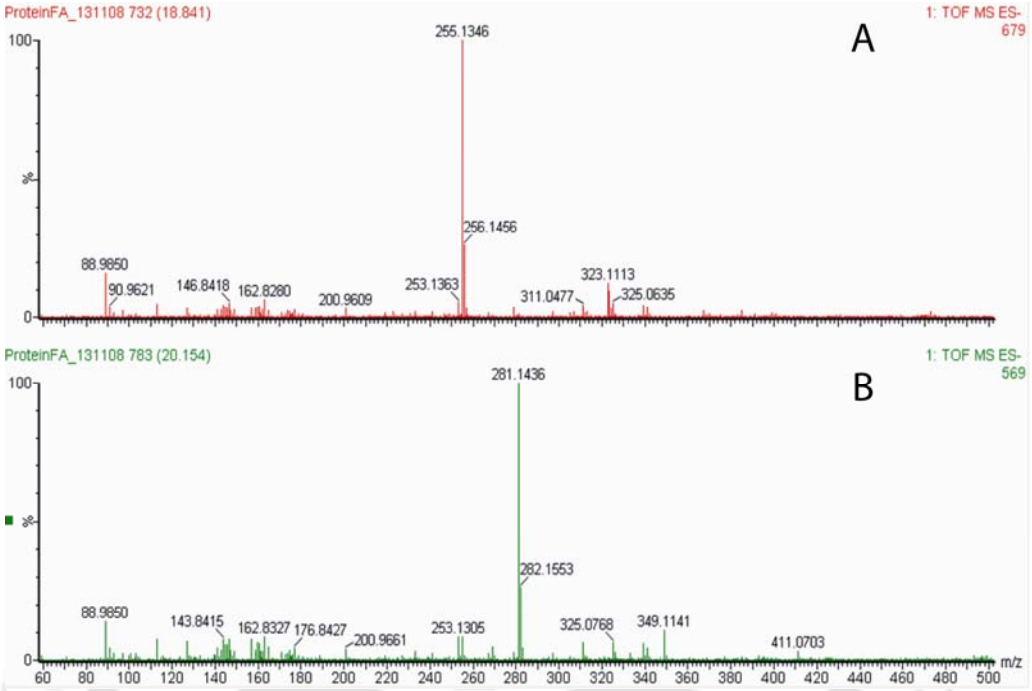

Figure 4.13: LC-ESI-MS spectral analysis of fatty acids. Two fatty acids were present in the protein sample. These were identified as (**A**) palmitic acid ($C_{16:0}$), *m/z* 256.2402 [M^+ (the molecular ion)], 255.1346 (M^+–H) and (**B**) oleic acid ($C_{18:1}$), *m/z* 282.2559 [M^+ (the molecular ion)], 281.1436 (M^+–H).

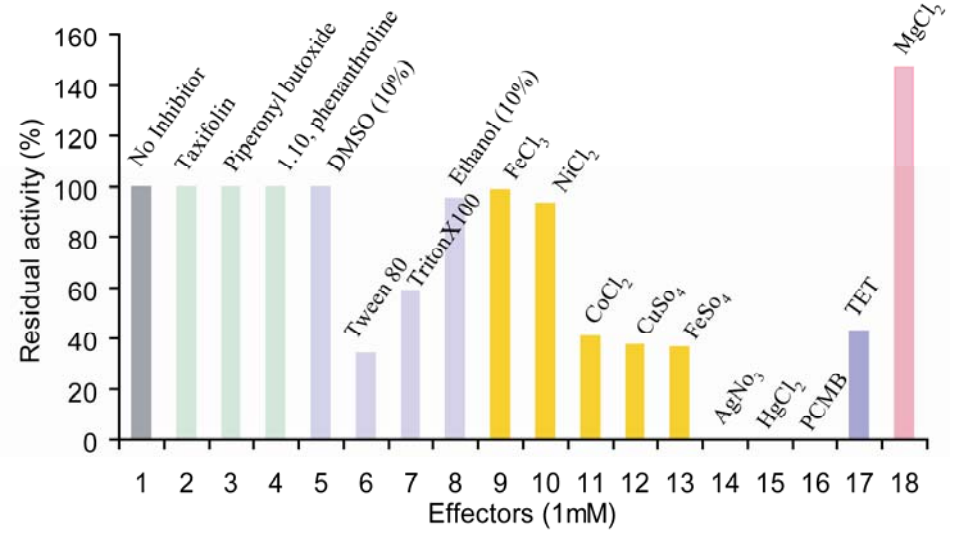

Figure 4.14: Effect of different chemical agents on the alcohol oxidase activity.

4.6 TABLES

Table 4.1: Purification table of alcohol oxidase

Fractions	Enzyme activity (U ml^{-1})	Protein (mg ml^{-1})	Specific activity	Purification fold (U mg^{-1}-Protein)
20000 x *g* supernatant	53.05 ± 0.5	2.80 ± 0.3	19 ± 0.1	1.0
Ammonium sulfate fractionated protein	56.18 ± 0.8	2.31 ± 0.5	26 ± 0.9	1.4
Membrane-free fractions*	169.12 ± 9.0	1.32 ± 0.1	128 ± 8.0	6.7
DEAE purified protein	256.22 ± 0.5	0.84 ± 0.1	305 ± 0.3	16.0

*Membrane free fraction was obtained by CHAPS solubilization of ammonium sulfate fractionated protein and then collected the supernatant after subjecting to ultracentrifugation. Each value represents the mean ± standard error at $p< 0.05$.

Table 4.2: Kinetic analysis of alcohol oxidase with different effectors

Substrate	K_m (mM)[a]			K_{cat}/K_m ($s^{-1}mM^{-1}$)[b]
	No Effector	Effectors		
		β-ME	1,12DCD	
n-heptanol	0.49	3.7	1.3	5.42×10^2
n-dodecanol	1.86	5.4	4.6	0.26×10^2
Phenyl-3-propanol	2.3	8.9	3.6	0.52×10^2
R(-)-2-octanol	18.3	25.3	2.6	0.08×10^1

[a]The K_m was calculated using Lineweaver-Burk plot. The concentrations of *β*-ME and 1,12DCD were 10 *μ*M and 10 mM, respectively, except for SAO substrate where 5 *μ*M of *β*-ME was considered to calculate the K_m. [b]Calculated in absence of any effectors.

Table 4.3: Multiple sequence alignment of alcohol oxidase protein FAD binding domain (GxGxxG) with other known alcohol oxidases

Alcohol oxidase source	Amino acid sequence
Aspergillus terreus MTCC 6324	YPVIDHEYDAVVVGAGGAGLR
Candida pignaliae	MAIPDEFDIIVVGGGSTGCC
Candida boidinii	MAIPEEFDIIVCGGGSTGCV
Candida sonorensis	MAIPDEFDIIVVGGGSAGCA
Pichia angusta	MAIPDEFDIIVVGGGSTGCC
Cladosporium fulvum	MTIPDEVDIIVCGGGSCGCV
Cochliobolus victoriae	MTIPDEVDIIVCGGGSCGCV
Penicillium chrysogenum	MTIPEEVDIIICGGGSSGCV
Pichia methanolica	MAIPDEFDIIVVGGGSTGCA
Aspergillus niger	MTIPDEVDIIVCGGGSTGCV
Aspergillus fumigatus Af293	WSDSHYKGPAFKVGAGVMGFQ
Arabidopsis thaliana	DNVYIIRCDAVVVGSGSIGLV
Oryza sativaJaponica	RNVCIVECDIAIVGSGCIGLV
Pleurotus pulmonarius	ANLPTAIFDYIVVGAGNAGNV

The multiple sequence alignment was done using ClustalW software. The alcohol oxidase from *A. terreus* MTCC 6324 showed identity with the N-terminal regions and also internal peptide sequences of reported alcohol oxidases.

Table 4.4: Characteristics of alcohol oxidase from *A. terreus* and its comparison with other origins

Origin	K_m value (mM)[a]	pH optima	Temp optima	Molecular mass (kDa)	SDS-PAGE band M_r	Isoelectric point
A. terreus	ND[b]	8.5	30	269	85, 63, 43, 27, 13	8.3-8.5
A. ochraceus	12.0	5.5-7.0	50-55	262	68	5.35
Kloeckera sp.	2.5	8.0	35	673	83	ND
P. pastoris	11.9	7.0	37	675	80	6.30
C. boidinii	4.2	8.0	30	600	74	ND
H. polymorpha	4.4	8.0-9.0	45	669	83	6.20
T. aurantiacus	10.2	8-11	---	560	75, 59	6.08

[a]The K_m was determined using ethanol substrate. The enzyme has different substrate specificity with less affinity for C_1-C_3 carbon substrates in comparison to other reported source organisms.

[b]The activity of alcohol oxidase from *A. terreus* on ethanol as observed by us was trace (<2 U ml^{-1}), hence K_m could not be determined. M_r, molecular mass. ND, not determined.

Chapter 5

DISSOCIATION, DEFLAVINATION AND RECONSTITUTION STUDIES OF THE ALCOHOL OXIDASE

5.1 OVERVIEW

The alcohol oxidases are known as complex multimeric proteins [Ozimek *et al.,* 2005]. Considering the importance of these oxidases for biocatalytic and biosensor applications research on these redox enzymes has been accelerated to unveil the mechanism on biogenesis and assembly of the subunits in these multimeric protein complex [Dmytruk *et al.,* 2007; Dienys *et al.,* 2003; Gunkel *et al.,* 2004; Evers *et al.,* 1994; Ozimek *et al.,* 2003]. The short chain alcohol oxidase, commonly known as alcohol oxidase, reported from the methylotrophic yeasts is studied to a greater extent and described mostly as octameric protein complex [Bringer *et al.,* 1979; Suye 1997; Couderc & Baratti 1980; Van der Klei *et al.,* 1990; Danneel *et al.,* 1994]. The information on protein chemical characteristics of the alcohol oxidases produced by filamentous fungi is limited and, among theses limited reports hetero-oligomeric characteristics of these oxidases have been reported [Alvarado-Caudillo *et al.,* 2002; Robelo *et al.,* 2004]. The molecular mass of the alcohol oxidases are largely varied from 145 kDa to 600 kDa [Van der Klei *et al.,* 1990; Banthorpe *et al.,* 1976; Dickinson & Wadforth 1992; Isobe *et al.,* 2007; Ko *et al.,* 2005]. We have also isolated a hetero-oligomeric alcohol oxidase [Kumar & Goswami 2008], which however contained five different non-covalently bound subunits, from *Aspergillus*

terreus as reported in the chapter 4 and accordingly the finding was published [Kumar & Goswami 2008]. Intriguingly this multimeric alcohol oxidase bears the catalytic activity for different short chain-, long chain-, secondary-, and aromatic alcohol substrates. Very high aggregating tendency of the protein stands as hindrance on elucidating the structure-function relationship of this broad substrate specific alcohol oxidase. To investigate the functional role of the individual subunit proteins and their nature of assembly, developing a benign technique to dissociate this aggregated multimeric protein into the subunit level and subsequent investigation on the dissociated proteins on their function and reasemblance may be an useful approach as reported for few other cases [Rangel-Aldao & Roseno 1976; Henderson & Henderson 1970; Recny & Hager 1982; Raibaud & Goldberg 1976; Mainwaring *et al.,* 1986]. Usually dissociation of the aggregated or multimeric protein into stable soluble forms has been a challenging task. Although few dissociating agents have been reported [Evers *et al.,* 1995; Visser *et al.,* 2007] the degree of dissociation is strongly dependent on the conditions applied and property of the proteins. Hence, searching a suitable dissociating agent for this fungal enzyme is warranted to augment understanding on the structural and functional insight of these alcohol oxidase proteins. In this chapter we are describing a simple and highly efficient method for dissociation and simultaneous separation of FAD of this flavin dependent multimeric alcohol oxidase protein produced by *A. terreus*. Further, reconstitution of the apoprotein and subsequent assembling of the reconstituted apoprotein with the cofactor flavin to a functionally active enzyme have also been demonstrated and reported here.

5.2 EXPERIMENTAL APPROACHES

5.2.1. Isolation and Purification of Alcohol Oxidase

The culture conditions of *A. terreus* MTCC 6324 used in this study and the procedure for isolation of the alcohol oxidase from the microsomal membrane by differential centrifugation are described earlier in chapter 2 and 3, respectively. The enzyme was separated and solubilized from the microsomal membrane using 0.5% (v/v) CHAPS. The protein was then purified initially by 35% (w/v) ammonium sulfate precipitation followed by DEAE sepharose ion exchange chromatography. The steps

for purification and functional characterization were described in detail in chapter 4. The purified native protein was used through out this investigation.

5.2.2. Enzymatic Assay of Alcohol Oxidase

Alcohol oxidase activity was assayed using HRP coupled assay method monitoring H_2O_2 production at 405 nm for ABTS radical at 30 ^oC (ε_{405} = 18400 $\mu M^{-1}cm^{-1}$) [Werner *et al.,* 1970] and also by measuring substrate dependent oxygen consumption using biological oxygen monitor with Clark-type polarographic oxygen electrodes as described in the chapter 3.

5.2.3. Dissociation, Deflavination and Re-association Studies

5.2.3.1 Gel Filtration Chromatographic Analysis

Enzyme protein (150-170 μg in 100 μl) was treated with a suitable concentration of the chemical (dissociating or deflavinating) reagents for different time periods (1 min-8 hr) at 4 ^oC under either static or agitation condition, except KBr treatment, where the reaction mixture was dialyzed against KBr buffer (2 M KBr in 0.25 M potassium phosphate, pH 7.5, 0.3 mM EDTA, 5 mM β-mercaptoethanol, and 20% glycerol) for 4 days at 4 ^oC [Casalin *et al.,* 1991]. The mixture was applied to HPLC gel filtration column TSK G3000 SW (0.75 x 30 cm, 10 μm, Tosoh corp. Japan) and then eluted isocratically with 50 mM Tris-HCl buffer, pH 8.0 at flow rate 1 ml min^{-1}. The eluted fractions were scanned simultaneously at UV_{280nm} for protein and at 525 nm emission filter for flavin (at 450 nm excitation). A control devoid of the chemical reagent was also run and analyzed to compare the results.

5.2.3.2 Dynamic Light Scattering (DLS) Analysis

Experiments were carried out in a 201 Spectroscatter DLS instrument (RiNA GmbH) to measure the mean radius particle size distribution of the protein samples for investigating the aggregation and dissociation profile of the sample protein. Before analysis the sample was subjected to 20000 x *g* for 20 min, to remove any turbidity. Data were acquired at 20 ^oC, repeated 20 times and averaged.

5.2.3.3 Confocal Laser Scanning Microscopic Analysis

The protein subjected to dissociation or re-association was stained with nile red, a specific fluorescent dye for lipids and hydrophobic patches of proteins and then

observed under CLSM (Zeiss LSM 510, UK). The fluorescent images were photographed using similar spectral settings as described earlier in chapter 4.

5.2.3.4 Native PAGE and SDS-PAGE Analysis

Native PAGE and SDS-PAGE analysis of the dissociated and re-associated proteins were done following the method of Laemmli [1970]. The holoenzyme molecular mass was determined through native PAGE following the standard Ferguson plot method [Hedrick & Smith 1968]. Different percentages of native PAGE gels (4, 5, 6 and 7.5%) were run to determine the molecular weight of the native protein. The final slope value obtained in the graph between slope (-log K_r) against molecular weight of the standards (r^2 = 0.9872) was used to calculate the native protein molecular weight. Gels were stained with standard silver nitrate staining method. The SDS-PAGE protein markers used were rabbit muscle phosphorylase b (97.4 kDa), rabbit muscle fructose-6-phosphate kinase (85 kDa), human transferrin (76.1 kDa), BSA (66 kDa), rabbit muscle lactate dehydrogenase (36.5 kDa), respectively.

5.2.4. Re-association Studies of the Alcohol Oxidase

The dissociating agent was removed from the treated protein sample by dialysis and then examined the re-association of the proteins following the similar Gel filtration, CLSM, native PAGE and SDS-PAGE methods as stated above. For Gel filtration chromatographic analysis the dissociated protein fractions were pooled, dialyzed against 50 mM Tris-HCl buffer, pH 8.5 for 4 hr at 4 ^{o}C (100 ml x 2) to remove the chemical reagent and again run gel filtration column separately under similar conditions as stated above to investigate the re-association process. The tubes containing protein peaks from this filtration were pooled, concentrated and assayed for alcohol oxidase activity. In gel filtration chromatography the dissociation and re-association of the protein were demonstrated on the basis of the retention times of the eluted protein peaks.

5.2.5. Absorbance and Fluorescence studies of Proteins

Reaction mixtures containing 50 mM Tris-HCl buffer, pH 8.0 with varying re-associated protein concentration (5-25 μg ml^{-1}) were prepared. The protein sample was incubated with 10 mM *n*-heptanol and then absorbance at UV_{280nm} (Cary 100Bio,

Varian) was recorded for different time periods. The fluorescence study was carried out using spectrofluorometer (Fluoromax Jobin Vyon, Horiba) equipped with 450 nm excitation filter and 465-600 nm emission filter (excitation slit width 3 nm and emission slit width 6 nm, scan rate 0.5 nm sec^{-1}). For fluorescence quenching study the re-associated protein samples was incubated with *n*-heptanol and FAD at 25 ^{o}C. A control without the substrate was also studied simultaneously.

5.2.6. Analytical Methods

Protein estimation was done following Bradford method using BSA as standard [Bradford 1976]. All the data presented in this study were the mean of three or more experiments with a variation within 10%.

5.3 RESULTS AND DISCUSSION

The microsomal alcohol oxidase protein purified through DEAE sepharose anion exchanger was reported in the previous chapter as lipoprotein in nature with high aggregating property to an average mean radius particle size of 180 nm. The aggregated multimeric protein when treated with *β*-mercaptoethanol (*β*-ME) at an optimum concentration of 0.74M for 8 h at 4 ^{o}C, the protein was dissociated into smaller molecular masses as evident from the longer retention times of the eluted proteins P_2, P_3, and P_4 from the HPLC gel filtration column while untreated protein (marked as P_1) was eluted at low retention time (Fig 5.1). Hereafter, the untreated protein in all the analysis is termed as native protein. The dissociation was also evident from the loss of 180 nm (radius) protein particles in the treated fractions observed through DLS analysis. No significant distribution of particles with mean radius higher than 4 nm was detected in the *β*-ME treated protein samples (Fig 5.2). The purified native protein, which is basically a lipoprotein, when stained with nile red and observed under CLSM showed intense red fluorescent particles (Fig 5.3A). However, no fluorescent particles were detected when the protein was treated with *β*-ME, indicating the dissociation of the native protein particles (Fig 5.3B). No interference of *β*-ME on the fluorescence caused by the nile red was observed. A control protein, HRP (M_r = 45kDa), which do not have any hydrophobic domains and

contains uniformly distributed medium size protein particles, did not show any fluorescence staining similar to the Fig 5.3B.

FAD fluorescence recorded simultaneously during elution of the proteins through gel filtration with and without treatment with *β*-ME clearly showed deflavination of the dissociated proteins (Fig 5.1). A sharp fluorescent peak was observed when FAD was associated with the native protein, whereas, the free FAD formed by deflavination of the protein showed a broad trailing fluorescence peak due to lack of its globular nature. After collecting the protein peaks the FAD fluorescence intensity of the dissociated protein fractions (pooled fraction from P_2 to P_4) and the un-dissociated protein (P_1) was recorded and found that nearly 87% of the total FAD of the native protein was detached while incubated with the *β*-ME. These results showed that the aggregated multimeric protein entity was simultaneously dissociated and deflavinated when incubated with *β*-ME at the concentration and time stated above.

At a low incubation time (< 8 hr) of the protein with *β*-ME, two additional intermediate dissociated protein peaks, IP_1 and IP_2 were detected (Fig 5.4). Concomitant increase in peak heights of P_2 to P_4 with the reduction of IP_1 and IP_2 height upon increasing the *β*-ME treatment time was observed. This indicates that the aggregated multimeric protein was first dissociated into two intermediate states corresponding to the protein IP_1 and IP_2. The intensity of P_2 was increased at a rate of 0.06 mAU min^{-1} while incubated with the *β*-ME at the concentration stated above; whereas, the intensity of the IP_1 and IP_2 were decreased with increasing treatment time and vanished completely. We also observed that FAD was associated with these two intermediate protein peaks. Distribution of FAD in IP_1 and IP_2 were 72% and 28%, respectively, out of the total FAD (cps units) detected in these two proteins obtained after incubating the native protein with *β*-ME for a period of 5 min.

The dissociated protein fractions (P_2 to P_4) were pooled and dialyzed to remove *β*-ME and then concentrated. The concentrated fraction was loaded on the gel column and run under similar parameters as stated earlier. A single re-associated protein peak (P_R) was obtained and no additional peaks were detected in the subsequent elution (Fig 5.5). This indicates that upon removal of *β*-ME, the dissociated proteins were re-associated to a single multimeric protein entity. The inhibitory role of *β*-ME on re-association was confirmed by the fact that when the dissociated proteins were pooled, concentrated and then filtered through the gel

column without removing the *β*-ME no protein peak corresponding to P_R was obtained, instead the peaks with retention time similar to P_2 to P_4 were regenerated. The re-association process was confirmed by CLSM study using nile red staining, where intense red fluorescent protein particles were regenerated after removing *β*-ME from the dissociated protein fractions (Fig 5.3C). Sequential removal of *β*-ME concomitantly increased the re-associated protein particles in the sample observed under CLSM following nile red staining.

The dissociation and re-association process of the alcohol oxidase protein were also demonstrated by analyzing the protein samples in native PAGE at 7% gel concentration (Fig 5.6). The retention factor (R_f) values of the protein bands corresponding to IP_1, P_R, and purified native protein were nearly similar (approx. 0.10). The R_f value of the IP_2 protein band (0.46) was comparatively higher than the above proteins thus indicated lower molecular mass of the IP_2 protein than IP_1 and native proteins. The R_f values of the pooled protein fractions, P_2 to P_4, (0.98) were far higher than the native protein and appeared immediately before the dye front due to the movement of these small protein masses together at low gel concentration. Results showed that the protein P_2 to P_4 are the dissociated proteins formed from the purified native protein by the action of *β*-ME.

While computing the subunit masses of 85-, 63-, 43-, 27- and 13-kDa for the total native protein molecular mass of 269 ± 5kDa, probability of the presence of two 43kDa subunits in the native protein was indicated. The molecular mass of the IP_1 was 267kDa. The P_R protein is equivalent to IP_1 protein in native PAGE and gel filtration. These P_R and IP_1 showed enzyme activity as shown later, whereas, IP_2 did not show any activity. The dissociated proteins were analyzed by SDS-PAGE using molecular markers separately with each gel for determination of subunit molecular masses (Fig 5.7). The *β*-ME treatment time for collecting the intermediate proteins entities, IP_1 and IP_2, was 5 min, and for the dissociated protein peaks (P_2 to P_4) was 8 hr. The protein IP_1 contained all except the 27kDa along with an additional intense band at 25kDa. Among these bands 85kDa protein band was very weak and clearly visible only when the concentration of the loaded protein is high. The most likely reason for the formation of 25kDa is the partial degradation of 27kDa protein at the high *β*-ME concentration used for the incubation. The exact cause of this partial degradation is not yet known. The re-associated protein (P_R) also contained similar protein subunits like IP_1. The IP_2 fraction, which contained 85-, 63-, 25- (weak), 13-

kDa (weak) bands, did not contain 43kDa band. Thus, unlike IP_1, IP_2 did not contain all the subunit proteins present in the native protein; this is attributed as the possible cause for the lack of enzyme activity in this intermediate IP_2 protein. The band profile of the peaks is P_2: 66- and 25-kDa, P_3: 85kDa, and P_4: 43- and 13-kDa. During the process of elution through the gel column the concentration of β-ME goes down, which to a certain extent resuscitate native environment, thus likely to promote partial re-association of the dissociated proteins due to their inherent high aggregating tendency. As a result, the dissociated proteins were not entirely resolved in the fractions into single protein level. This dissociation study could not be accomplished through either cation or anion exchange chromatography due to the interference of the high concentration of β-ME on protein binding to the resins. While with hydrophobic interaction chromatography, all the β-ME dissociated proteins were eluted as an unresolved broad peak.

Both IP_1 and P_R had the enzyme activity, however, the activity of the P_R was obtained only when the protein was mixed with 50 μM FAD (since P_R was reconstituted from the pooled fractions P_2 to P_4 that nearly void FAD) and incubated at 4 ^oC with the respective substrates (10 mM) for at least 12 hr. No enzyme activity was detected in IP_2 and other individual fractions P_2 to P_4 (after collecting the central fractions of each and removing the β-ME by dialysis) even after prolong incubation with the FAD and substrates. It may be inferred from the above findings that the catalytic activity of this multimeric protein is lost upon dissociation. A comparative enzyme activity of the native protein, IP_1 and P_R with different substrates are shown in table 5.1. The partial degradation of 27kDa protein, as detected in IP_1 and P_R, did not completely arrest the enzyme activity of these proteins, though, the activity was reduced significantly. Above results also implied that the β-ME mediated dissociation is nearly a reversible process since the alcohol oxidase activity of the re-associated protein was regained, though, albeit lower than the native protein.

The flavin in flavoenzymes is known to mediate the transfer of electron from the redox centre to the terminal electron acceptor, which is oxygen in the present case, through its isoalloxazine ring during the catalytic process as reported in case of cholesterol oxidase [Pollegioni *et al.,* 1999]. The event involves change of FAD emission fluorescence, which may be linked to the functional activity of this enzyme. When the native or IP_1 protein was treated with the substrate (10 mM *n*-heptanol), the emission intensity of FAD was quenched to nearly 90% with quenching rate, $K_{obs} \approx$

2.7-3 min^{-1} immediately after addition of the substrate to the reaction media. However, when the FAD emission of P_R was studied by mixing it with FAD (50 μM) (since P_R was prepared from the fractions that nearly void FAD) and substrate a prolong incubation time (minimum 12 hr) was required to exert the similar changes ($K_{obs} \approx 0.03$ min^{-1}) (Fig 5.8). No such change of FAD fluorescence emission of P_R was observed in absence of the substrate. This showed that reconstitution of the FAD to the apoenzyme (P_R) is induced by the substrate and this induction is a slow process. To investigate the conformational change of the alcohol oxidase during substrate induced reconstitution of FAD, UV_{280nm} absorptions were recorded by varying protein concentration at a saturated substrate concentration and FAD (50 μM). The absorbance was decreased at a level of 0.0038 AU μg^{-1} protein when incubated the mixture for 30 min. and at 25 ^oC. No significant change of native protein absorption upon incubating with the substrate was observed. This change in UV_{280nm} absorbance is probably due to the change in conformations evolved in the proper reorganization of the subunits during the substrate induced reconstitution of the FAD that resulted catalytically active alcohol oxidase protein. The drastic change of conformation of alcohol oxidase protein during FAD release was also demonstrated by other [Massey & Curti 1966]. Contrary to the decrease in absorbance during the reactivation, many folds increase in the absorbance during the process of dissociation was observed (Fig 5.4). For instance the UV_{280nm} absorbance of the dissociated protein P_2 was nearly five fold higher than IP_1 at their respective highest absorbance. This dissociation process likely to expose the UV-absorbing polar aromatic amino acid residues of the subunits in this membrane bound multimeric protein thus increased the absorbance; whereas, substrate induced reconstitution process buried these polar aromatic amino acids to the core of this hydrophobic protein that resulted in decrease the absorbance. Highly hydrophobic nature of this membrane protein is demonstrated earlier in chapter 4.

Deflavination and dissociation of the protein entity were studied separately using deflavinating agents, KBr [Casalin *et al.,* 1991], and TCA [Massey & Curti 1966], and dissociating agents, glycerol [Evers *et al.,* 1995], and DMSO [Visser *et al.,* 2007], following the similar parameters reported in these protocols. The extent of deflavination of the purified native protein obtained with KBr and TCA was 24-, and 60%, respectively. DMSO was ineffective in dissociating this alcohol oxidase, rather, 50% DMSO was inhibitory to this enzyme as no residual activity of the native enzyme was detected after treatment with this reagent (Fig 5.9). Ethylene glycol, a

structurally similar compound to *β*-ME, could not dissociate the protein even at its molar concentrations. Unlike *β*-ME, no inhibitory effect of ethylene glycol on the enzyme activity was observed. Thus, we are reporting the role of *β*-ME as both dissociating and deflavinating agent for this multimeric protein. *β*-ME treatment could dissociate nearly 87% flavin from the purified protein entity as demonstrated by us. That the subunit proteins of this multimeric alcohol oxidase are not linked by disulphide bond was demonstrated by us in chaper 4 since the SDS-PAGE separated the subunits of the protein alike with or without treating the sample with *β*-ME. Thus, breakage of inter-peptide disulphide bonds is not the cause for the dissociation of this multimeric protein. The *β*-ME likely to destabilize the multimeric protein under the anaerobic and partially non-polar microenvironment created by its high concentration used in this investigation that promote the sub-unit detachment and eventual dissociation of this lipoprotein. The solvent effect of *β*-ME at high concentration is an established fact demonstrated in several cases [Kirley 1990; Ahmed *et al.,* 1996]. This assumption is justified by the findings that removal of the *β*-ME from this dissociated fraction triggers the re-association of the subunit protein that led to the formation of the P_R protein. Expulsion of the solvent led to the preferential hydration and interaction among the subunits that simultaneously promote the re-association of the subunit proteins. Sequential removal of the *β*-ME by dialysis concomitantly increase the re-association as evident from the CLSM studies of the protein stained with nile red.

5.4 FIGURES

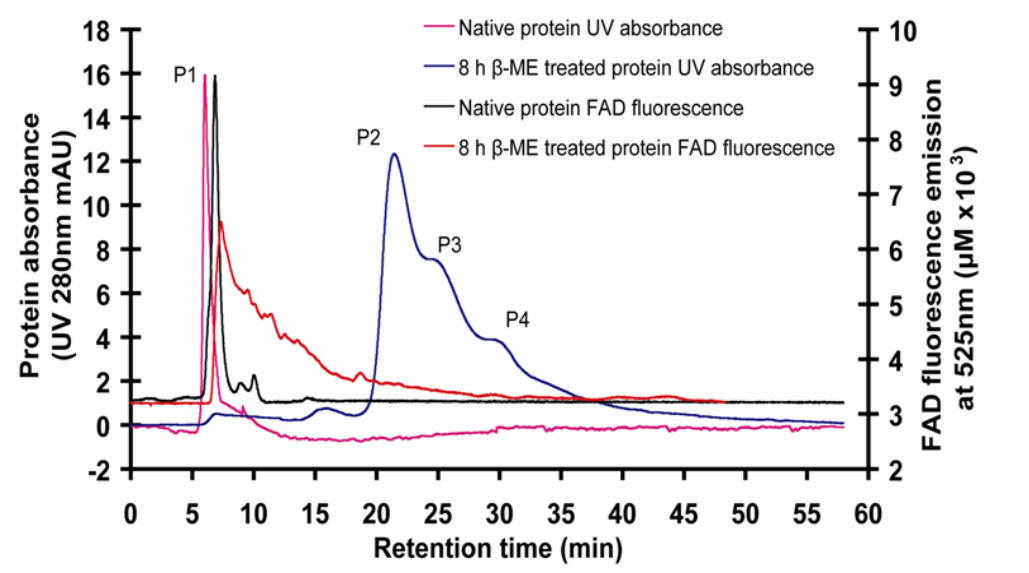

Figure 5.1: Gel filtration chromatograms of native protein with and without treatment with *β*-ME. Primary (Y) axis: protein absorbance and secondary (Y) axis: FAD fluorescence intensity. P_1: untreated native protein, P_2 to P_4: *β*-ME dissociated protein peaks.

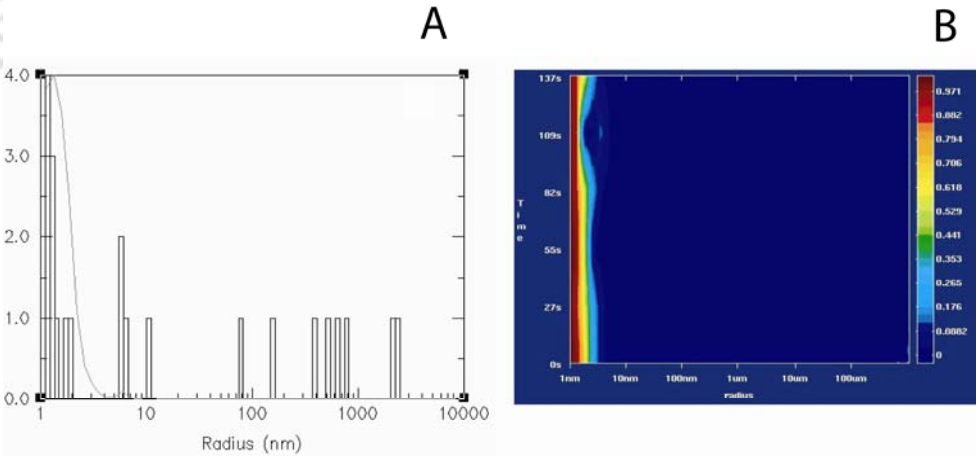

Figure 5.2: Dynamic light scattering analysis of *β*-ME treated protein particles. (**A**) The mean radius distribution of *β*-ME treated was less than 4 nm. (**B**) The red line in the corresponding graphs indicates the purity of the samples and the blue patches around the red line are impurities from dust particles. The axis of the plot is as follows: on x-axis the radius (*μ*m) of the protein particles; y-axis the analysis time (sec); and secondary y-axis indicates the extent of purity of the samples.

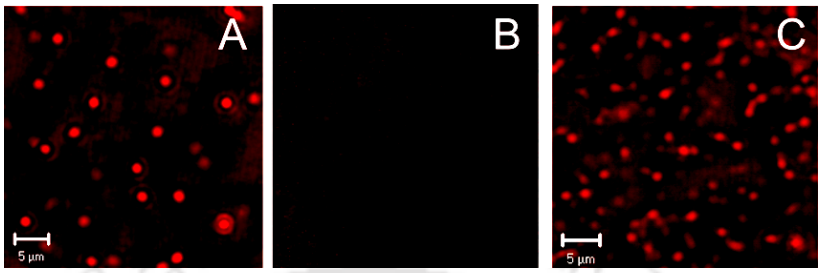

Figure 5.3: Dissociation and re-association studies of the protein particles with CLSM using fluorescence staining. (**A**) The native protein. (**B**) Native protein incubated with β-ME. (**C**) Re-associated protein formed after removal of β-ME. Bar = 5 μm.

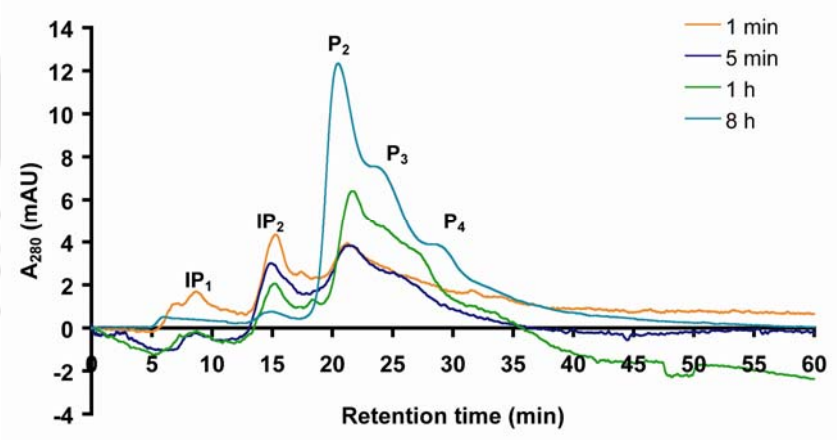

Figure 5.4: β-ME mediated dissociation of alcohol oxidase at different incubation periods. IP_1 and IP_2: intermediate dissociated protein peaks. P_2 to P_4: dissociated protein peaks. The intensity of 8 hr treated sample was consciously multiplied by a factor of 0.2 to visualize other peaks of different incubation periods (1 min-1 hr).

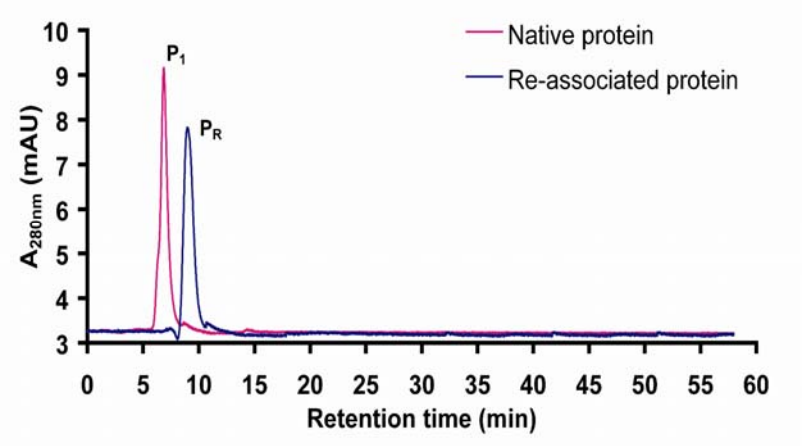

Figure 5.5: Re-association studies of dissociated protein peaks using gel filtration chromatography. The dissociated peak fractions (P_2 to P_4) obtained by *β*-ME mediated dissociation were pooled, dialyzed and concentrated, and then loaded on HPLC gel filtration column, a single peak (P_R) with lower retention time was generated.

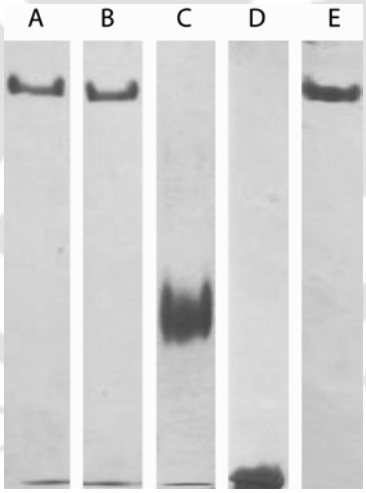

Figure 5.6: Native PAGE analysis of alcohol oxidase proteins. The R_f values of the proteins are as follows: Lane A. Native purified protein (0.09); lane B. IP_1 (0.11); lane C. IP_2 (0.46); lane D. The pooled protein peaks (P_2 to P_4) (0.98), and lane E. P_R (0.10). The treatment time of the native protein with *β*-ME to collect separately the IP_1, IP_2 was 5 min and dissociated protein fractions (P_2 to P_4) from gel filtration chromatography was 8 hr.

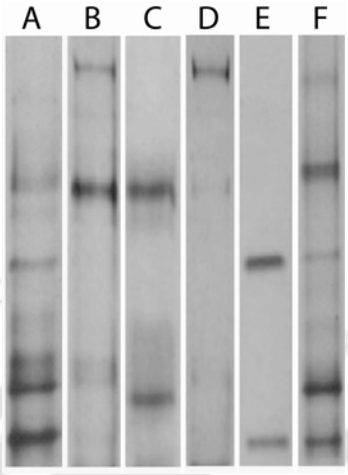

Figure 5.7: SDS-PAGE analysis of alcohol oxidase proteins. lane A. IP_1, lane B. IP_2, lane C. P_2, lane D. P_3, lane E. P_4 and lane F. P_R. The subunit proteins were analyzed using molecular markers separately with each gel for determination of subunit molecular masses.

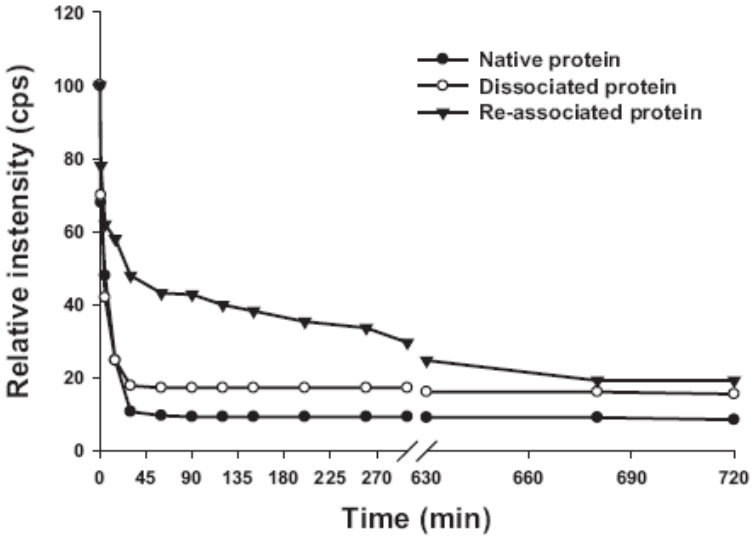

Figure 5.8: FAD fluorescence quenching study of native protein, IP_1 and P_R proteins after incubating with the substrate. P_R was additionally pretreated with 50 μM FAD.

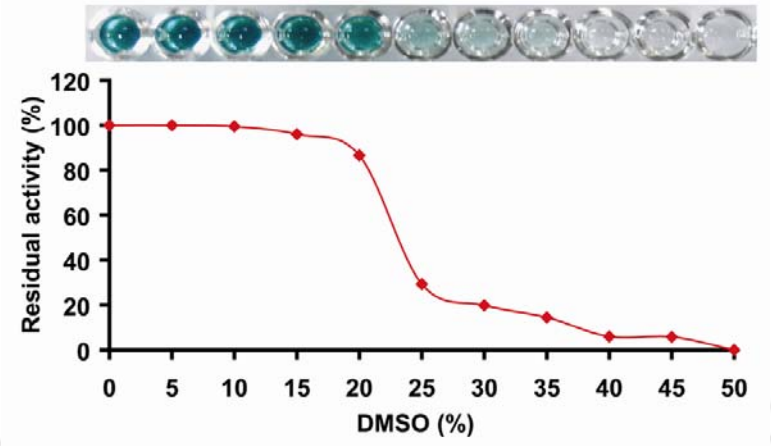

Figure 5.9: Effect of DMSO on alcohol oxidase activity. The figure embedded in the graph represents the alcohol oxidase activity at different concentrations of DMSO as shown in x-axis. The ABTS assay method was described in the material and methods section. The activity corresponding to 100% residual activity was 17.2 ± 0.2 U ml^{-1}.

5.5 TABLES

Table 5.1: Comparison of alcohol oxidase specific activity of the native, intermediate dissociated protein (IP_1) and re-associated protein (P_R)

Alcohol substrate	Specific activity (U mg^{-1})		
	Native protein	IP_1 protein	P_R protein
n-heptanol	305 ± 0.3	190 ± 0.8	96 ± 1.3
n-dodecanol	62 ± 0.1	49 ± 0.3	42 ± 0.5
phenyl-3-propanol	250 ± 0.2	183 ± 1.0	45 ± 0.2
R(-)2-octanol	63 ± 0.3	37 ± 0.1	Trace

Chapter 6

APPLICATION POTENTIAL OF THE ALCOHOL OXIDASE AS BIOCATALYST

6.1 OVERVIEW

A large number of carbonyl compounds available in the global market are produced traditionally from alcohol substrates following chemical oxidation methods. These methods mostly utilize harmful organic solvents, stoichiometric equivalent of toxic metal catalysts, or a large amount of energy consumption with high pressure and/or high temperature [Zhan & Thompson 2004; Hirano *et al.,* 2008]. Several methods related to the biocatalytic oxidation of alcohols have been published during recent past [Lahtinen *et al.,* 2007; Thomas *et al.,* 2002; Kroutil *et al.,* 2004]. Due to the obvious advantages of biocatalysts over the chemical catalysts from the environmental and selectivity point of view researchers have growingly focused their attention on the utilization of redox enzymes for such conversions [Kroutil *et al.,* 2004]. These alcohol oxidizing enzymes may be categorized into alcohol dehydrogenase (ADH) and alcohol oxidase (AOX), on the basis of the mechanisms involved in the biocatalytic reactions as shown in scheme 1.1.

Alcohol oxidase (systematic name: alcohol: oxygen oxidoreductase, EC 1.1.3.x) uses molecular oxygen as electron acceptor that leads to the formation of hydrogen peroxide or water as a by product during the catalysis [Faber 2000]. The redox active prosthetic compounds (flavin or its derivatives) in alcohol oxidase is

tightly bound to the protein matrix and hence not required to supplement them for the catalysis. Although the biocatalytic conversions of alcohols to carbonyl compounds are largely studied by using ADH [Molinari 2006], the need of external cofactors (e.g. $NAD(P)^+$, NAD^+) for these catalyses is the stumbling block for developing economically viable ADH-based process. The exploitation of alcohol oxidase enzymes as catalyst for such conversions is rare, the reasons being attributed to the low availability and supply, and inadequate study on this group of enzymes. We have demonstrated broad alcohol oxidizing activities in the microsomes of *A. terreus* as described in chapter 3. Further we have purified and studied the structural and functional properties of these nano-size alcohol oxidase protein particles (chapter 4). We report here the application potentials of this alcohol oxidase in the production of a broad range of carbonyl compounds from the corresponding alcohols.

6.2 EXPERMINETAL APPROACHES

6.2.1. Preparation of Hydrazone Derivatives

Isolation and purification of alcohol oxidase from *A. terreus* and characterization of the purified enzyme was described earlier in detail in the chapters 3 and 4. Dintrophenyl hydrazine (DNPH) reagent (0.35 mg ml^{-1}) was prepared in 1 M HCl solution. Stock solutions of the substrates were prepared in DMSO to increase the solubility in aqueous reaction mixture. All the reactions were carried out in 50 mM Tris-HCl, pH 7.5. The total reaction volume was maintained 10 ml containing the following components: 9.89 ml 50 mM Tris-HCl buffer, pH 7.5; 10 μl (10 mM) of corresponding substrate; and 100 μl (0.15 mg) alcohol oxidase protein. The enzyme protein was used as a biocatalyst in all these reactions. The reaction mixture was taken in a 50 ml round bottom flask caped with a teflon cork. The mixture was then incubated at 25 ^oC and 150 rpm for different time periods. At the end of the reaction time 5 ml DNPH reagent was added to the reaction mixture and incubated at 20 ^oC under static conditions in complete dark for 2 hr. The hydrazone derivatives so formed were extracted twice with 14 ml of ethyl acetate and then concentrated by evaporating the solvent using speedvac ($\leq$ 35 ^oC). The products were dissolved in acetonitrile and then analyzed immediately by LC-ESI/MS and UV-VIS spectrophotometer. Several control experiments containing DNPH reagent, alcohol

oxidase protein and both DNPH reagent and alcohol oxidase protein in the reaction mixtures were also analyzed separately for accurate estimation and blank corrections.

6.2.2. Measurement of Yield of the Carbonyl Compounds

The yield of the extracted carbonyl compounds was measured based on the molar absorption coefficients of their hydrazone derivatives obtained at $UV_{360\ nm}$. To determine the molar absorption coefficients for precise estimation of different categories of the carbonyl compounds, acetaldehyde, *n*-hexanal, *n*-dodecanal, cyclooctanone, benzaldehyde, and cholestenone were used as the representative carbonyl compounds for the short chain- (C_1-C_4), medium chain- (C_7-C_8), and long chain-aldehydes or ketones (C_{10}-C_{16}), cyclooctanone, aromatic aldehydes, and cholestenone, respectively. A calibration curve for the representative carbonyl hydrazone derivatives in acetonitrile was recorded in the concentration range 10-50 mM ml^{-1}. Molar absorption coefficients of the hydrazones were measured based on the calibration graph obtained by plotting absorbance (at UV_{360} nm) verses concentration with an $r^2 > 0.975$. The concentration and hence, the yield of the carbonyl compounds in the reaction mixture were calculated by computing the absorptions of the derivatives with the respective molar absorption coefficients of the representative hydrazone derivatives.

6.2.3. LC-ESI/MS Analysis of Hydrazone Derivatives

All separation and purification steps of products were performed using Q-Tof LC-MS/MS system (Waters) equipped with UPLC BEH RP18 column (250 mm x 4.6 mm x 5 μm). Chromatographic separation of carbonyls was conducted by using a mixture of acetonitrile (ACN), water and 1 mM L^{-1} ammonium acetate solution as mobile phase, constant 50% ACN and 50% water during 0-10 min, then changes of 50-90% ACN, 50-0% water and 0-20% ammonium acetate solution in 30 min was used. Constant 90% ACN with 20% ammonium acetate in 60 min and changes of 15-35% water, 20-0% ammonium acetate solution and constant 50% ACN in 60-65 min were used, and then followed by a 5 min equilibration time. A constant flow rate of 0.6 ml min^{-1} was maintained during the entire separation process. The injection volume was 10 μl. Detection of the hydrazone derivatives was carried out at $UV_{360\ nm}$ absorbance.

All mass spectrometric measurements were recorded using electro spray ionization (ESI) in the positive mode using the following conditions: nebulizer gas flow (N_2), 2 L min^{-1}; capillary voltage, 4 kV; temperature of the ESI probe, 100 ^oC; curve; CDL temperature, 350 ^oC; deflection voltages, 55 V; detector gain, 1.7 V; collision energy, 5. For scan measurements, a mass range from 100 to 1000 *m/z* was chosen; the integration time was 1 sec. High resolution mass spectra was calculated based on the calibration of the instrument with standard leucine enkaphalin using a lock mass *m/z* 556.2771. The spectra obtained were processed and analyzed with the MassLynx V4.1 integrated software.

6.3 RESULTS AND DISCUSSION

We have reported in the earlier chapters (chapter 3 & 4) regarding the purification and partial characterization of a broad substrate specific nano-size alcohol oxidase protein entity isolated from the microsomes of hydrocarbon-degrading *A. terreus*. In brief, the enzyme was purified by DEAE sepharose anion exchanger. The size and molecular mass of the alcohol oxidase protein were 10.2 ± 2 nm and 269kDa, respectively. This alcohol oxidase was found to be highly active and stable in aqueous reaction mixture at pH 7 to 9 and room temperature. These nano-size alcohol oxidase protein particles were utilized as biocatalyst for the conversion of different classes of alcohols to the corresponding carbonyl compounds as shown in table 6.1. Since the yield was estimated based on the molar absorption coefficient of the hydrazone derivatives of the corresponding carbonyl compounds (Fig 6.1), the mass spectra of the hydrazone derivatives were also recorded to confirm the formation of the respective products (Fig 6.2-6.24). The yields of the carbonyl compounds were found to be 96% or more when long chain primary and secondary alcohols bearing carbon chain length C_7 and above within the studied group of substrates and cyclohexanol were used as substrates. This yield could be achieved at a maximum of 24 hr of the reaction time. However, in many cases the yield was obtained even within 10 hr of the reaction time. The minimum reaction time needed to reach the 98% yield for the product 2-octanone from the corresponding *R*(-)2-octanol was 6 hr, whereas, the time required to obtain the similar yield from *S*(+)2-octanol was 24 hr. This shows higher affinity of the alcohol oxidase for *R*(-)2-octanol over *S*(+)2-octanol. The findings may

be correlated with the Michaelis–Menten constant (K_m) values 0.012- and 0.020- mM for the substrates *R*(-)2-octanol and *S*(+)2-octanol, respectively. This alcohol oxidase is, thus, suggested as potential biocatalyst for the kinetic resolution of chiral alcohols. The product yield from the aromatic alcohol substrates was significant but not very high. Although the reason for these low yields is not clearly known, a possible reason attributed to this fact is the low alcohol oxidase activity on these substrates as evident from the table 3.1. The high yield of the carbonyl compounds invariably obtained from the corresponding long chain alcohols during the biocatalytic conversion using this alcohol oxidase protein is intriguing. It is likely that the lipoidic nature of the alcohol oxidase protein, which was demonstrated in chapter 4, induces high binding affinity of this enzyme with those hydrophobic substrates through non-polar interaction, thus enhances the catalytic rate of the reactions and product yield. However, a detail kinetic investigation and structure-function relationship studies of this novel alcohol oxidase are warranted to interpret the observed yield of the products. Unlike other alcohol oxidases reported so far, the alcohol oxidase isolated from *A. terreus* showed poor enzymatic activity on the short chain alcohol (methanol, ethanol) substrates. The yield of the products from these short chain alcohol substrates was also found to be significantly low as compared to the other long chain alcohol substrates (Table 6.1). Since the enzyme is predominantly induced during the growth of the fungus on long chain alkane substrates, it is likely that the activity of the enzyme is primarily evolved to catalyze only the long chain alcohol substrates formed from the initial oxidation of such hydrocarbon substrates during the growth. The other interesting trait of this fungal alcohol oxidase observed by us is the sustained operational stability against *in-situ* generation of H_2O_2 during the enzyme catalysis. It was not required to supplement catalase or other H_2O_2 scavenger in the reaction mixture to prevent inactivation of the enzyme within the studied reaction time as evident from the high product yields. The inhibitory effect of H_2O_2 formed during the alcohol oxidase catalysis is generally neutralized by supplementing catalase to the reaction mixture, without which the oxidase is immediately denaturated by hydrogen peroxide [Chaabouni *et al.,* 2003]. Additional attractive feature of this fungal alcohol oxidase is that the conversion of secondary alcohol substrates to the corresponding carbonyl compounds could be increased by adding 1,12DCD as the activator in the reaction mixture as shown in the table 6.1.

The biocatalytic conversion of alcohols to the corresponding carbonyl compounds has been largely exploited for the production of optically pure alcohols useful in pharmaceutical and other industrial sectors [Edegger *et al.,* 2006]. The application of these biocatalysts in organic synthesis is also growingly focused [Dienys *et al.,* 2003]. Thus, considering the importance of this class of biocatalysts from the industrial perspective development of alcohol oxidase-based process technology guided by the tenet of green chemistry is advocated. The alcohol oxidase reported here is envisaged as stable potential green catalysts for industrial process due to its catalytic activity for such high product yields obtained under environmentally compatible conditions. The application potential of this enzyme for kinetic resolution of secondary alcohols is also foreseen with further optimization of the reaction parameters for the conversion.

6.4 FIGURES

Determination of Molar absorption coefficient for standard representative hydrazone derivatives of carbonyl compounds:

The detailed procedure of measurement was given in the methods section.

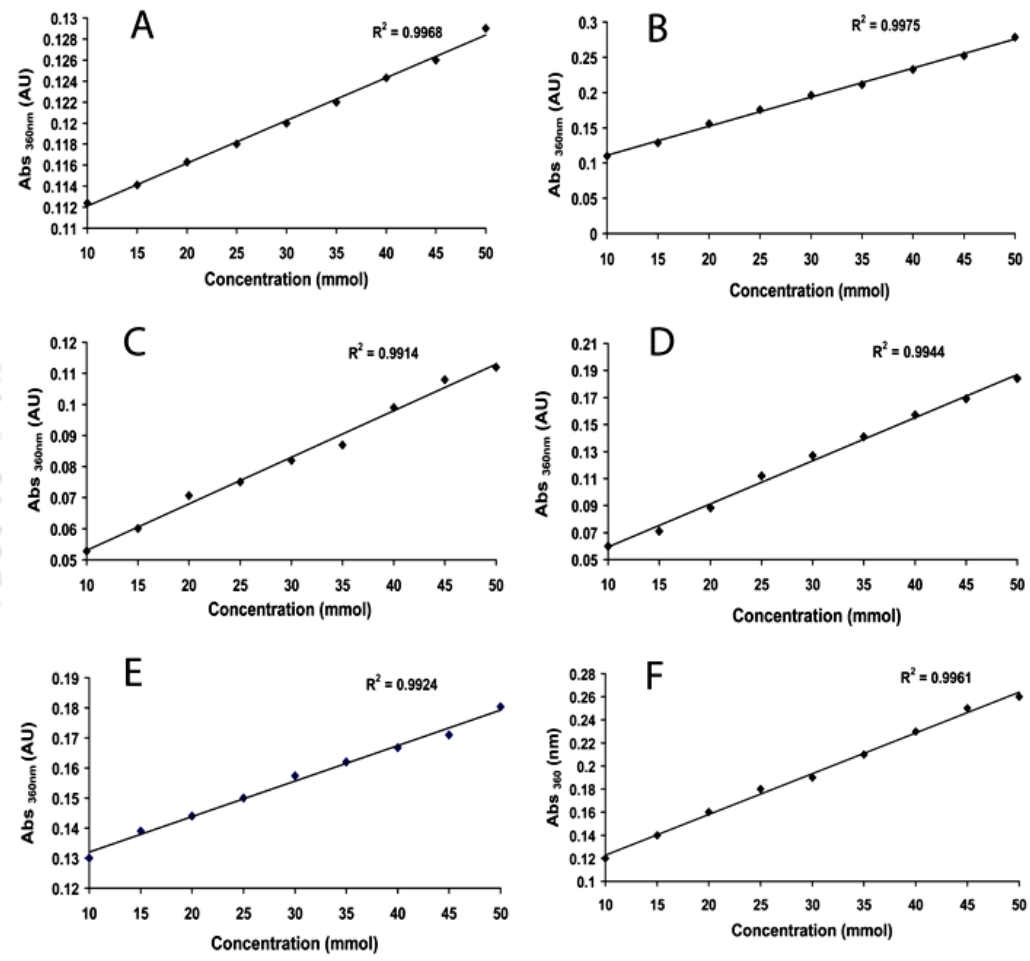

Figure 6.1: Hydrazone derivative of carbonyl compounds. [**A**] acetaldehyde, [**B**] hexanaldehyde, [**C**] dodecanaldehyde, [**D**] cyclooctanone, [**E**] benzaldehyde, and [**F**] cholestenone.

Mass spectrometric analysis of the purified hydrazones:

All the mass spectra of respective hydrazone derivatives of the carbonyl compounds were given below. All the mass calculations for the hydrazone derivatives obtained were based on the calibration of the instrument with the standard leucine enkaphalin. Leucine enkaphalin was used as lock mass and run simultaneously for all the compounds.

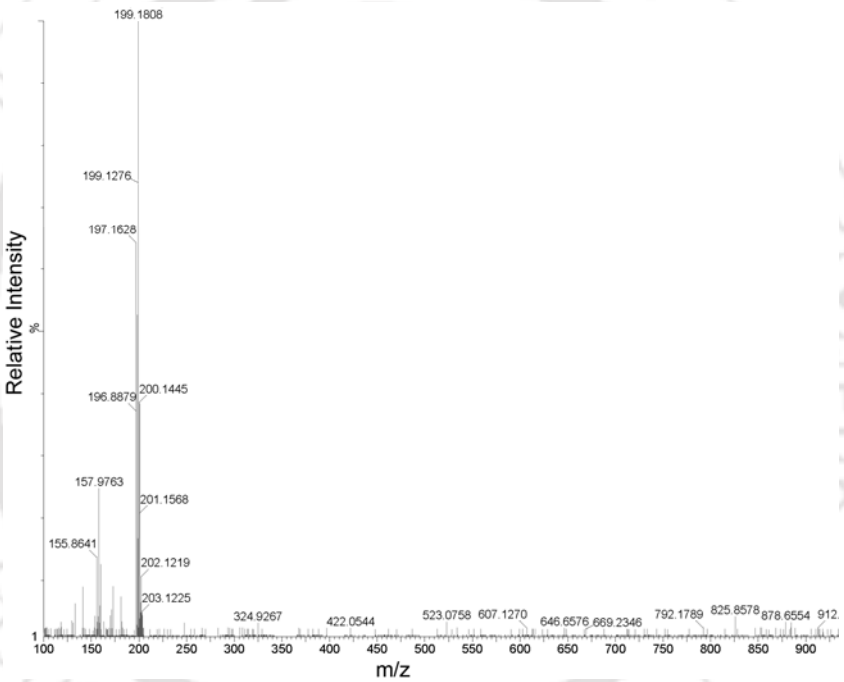

Figure 6.2: ESI-MS spectra of the 2,4-dinitro phenyl hydrazine (*m/z* 198.1362; [M^+ (the molecular ion)] M^++H,199.1808).

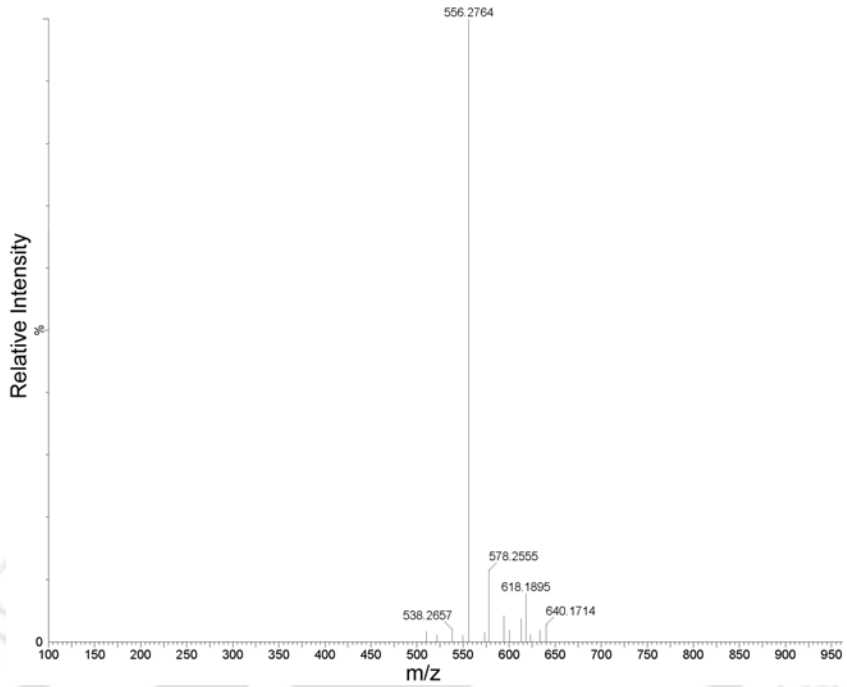

Figure 6.3: ESI-MS spectra of the standard leucine enkaphalin (*m/z* 555.2771; [M^+ (the molecular ion)] M^++H, 556.2764).

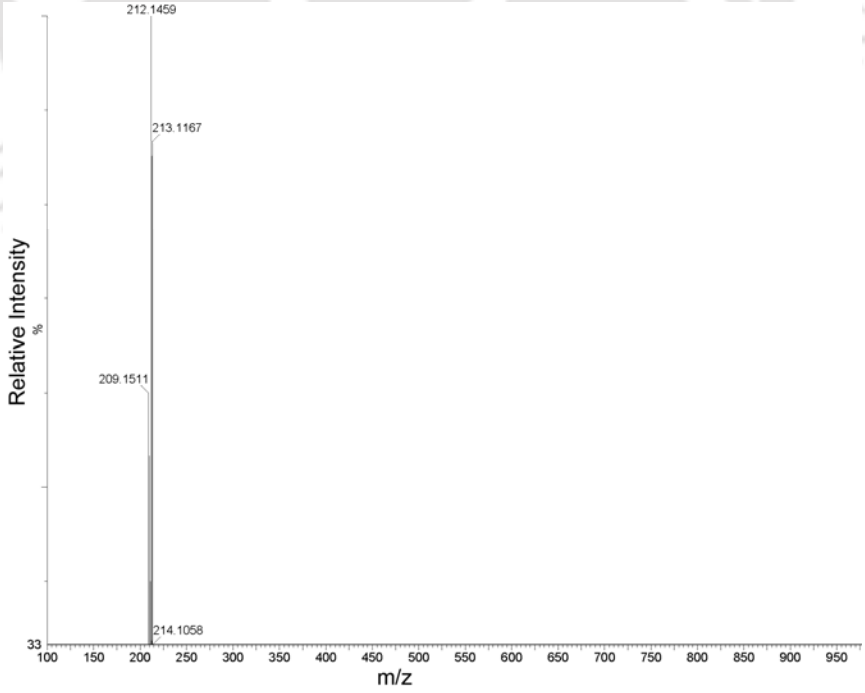

Figure 6.4: ESI-MS spectra of the hydrazone derivative of formaldehyde (*m/z* 211.1469; [M^+ (the molecular ion)] M^++H, 212.1459). Substrate used was methanol.

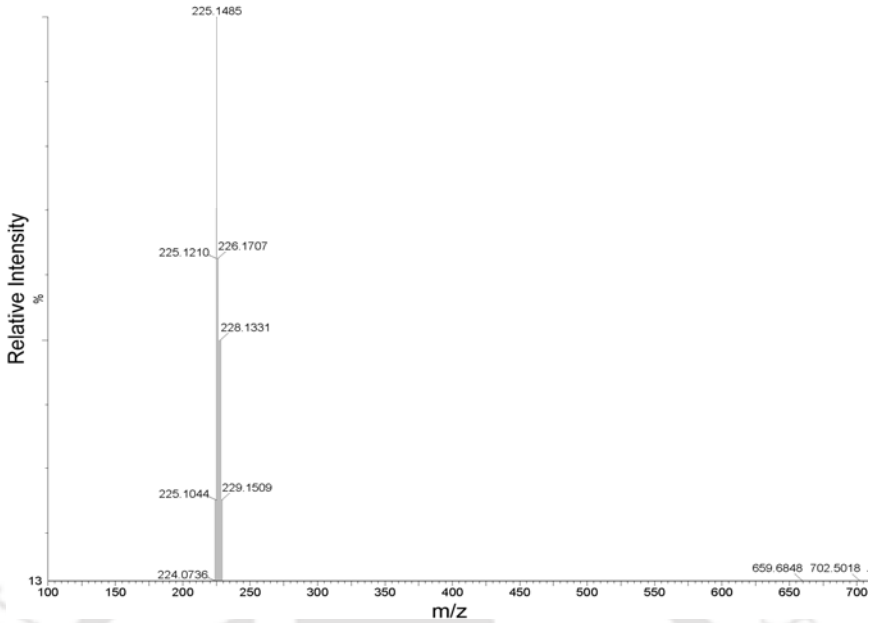

Figure 6.5: ESI-MS spectra of the hydrazone derivative of acetaldehyde (*m/z* 224.1735; [M^+ (the molecular ion)] M^++H, 225.1485). Substrate used was ethanol.

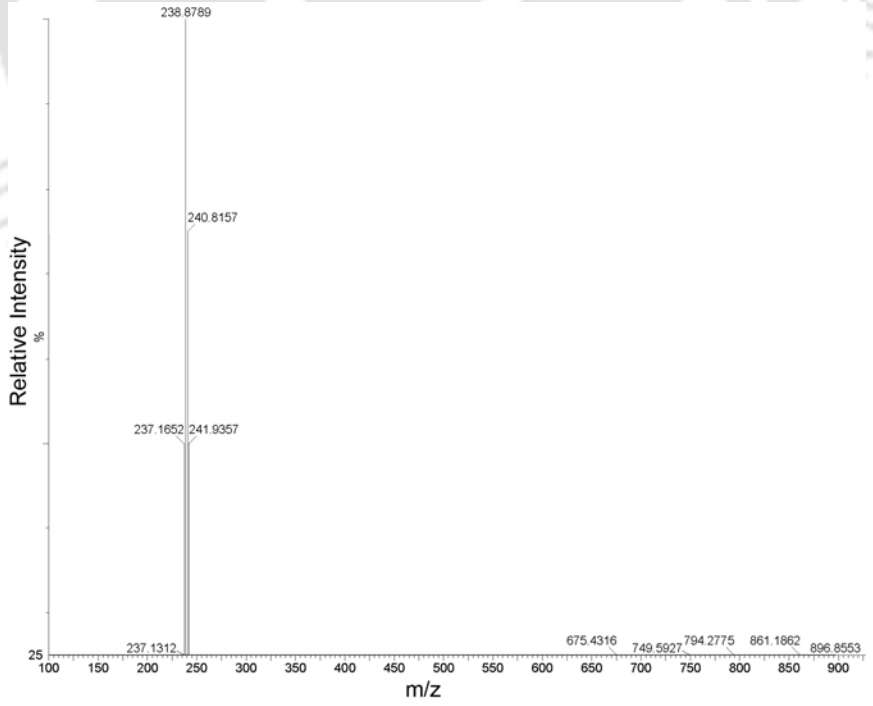

Figure 6.6: ESI-MS spectra of the hydrazone derivative of propanaldehyde (*m/z* 238.0702; [M^+ (the molecular ion)] M^++H, 238.8789). Substrate used was propanol.

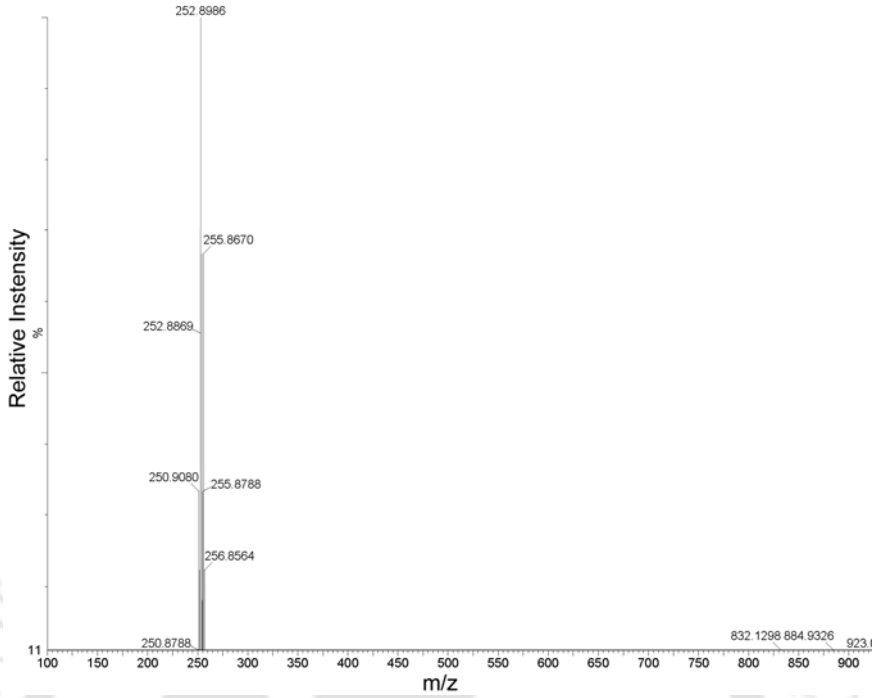

Figure 6.7: ESI-MS spectra of the hydrazone derivative of butanaldehyde (*m/z* 252.0859; [M^+ (the molecular ion)] M^++H, 252.8986). Substrate used was butanol.

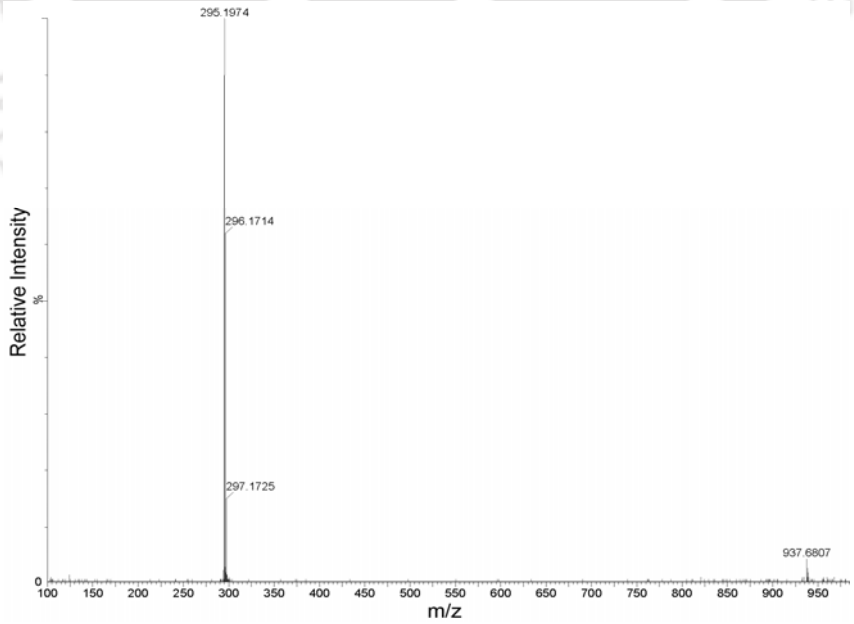

Figure 6.8: ESI-MS spectra of the hydrazone derivative of heptanaldehyde (*m/z* 294.1328; [M^+ (the molecular ion)] M^++H, 295.1974). Substrate used was heptanol.

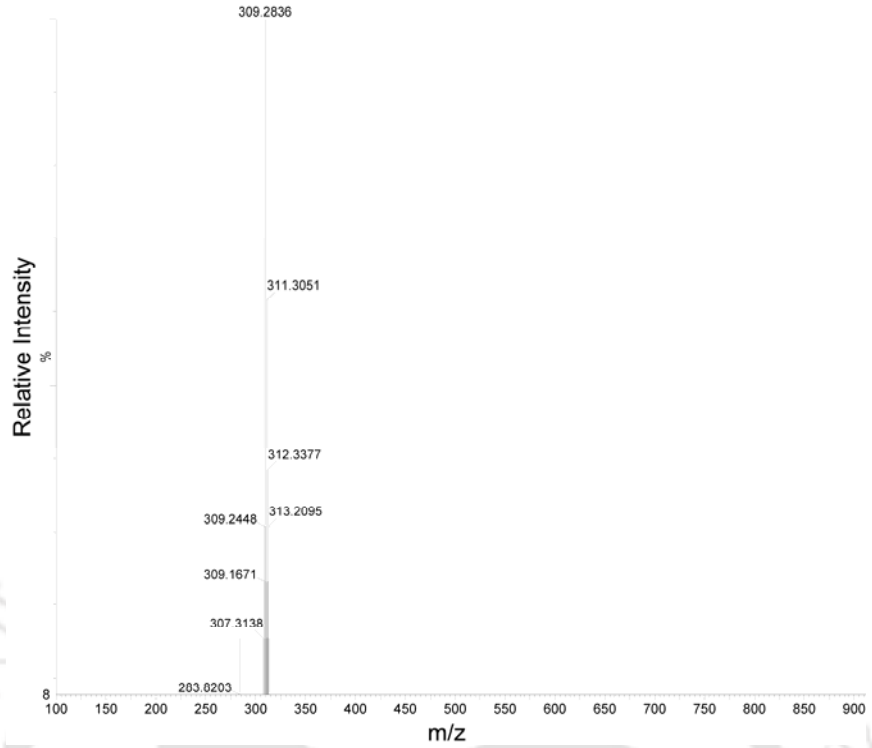

Figure 6.9: ESI-MS spectra of the hydrazone derivative of octanaldehyde (*m/z* 308.1485; [M^+ (the molecular ion)] M^++H, 309.2836). Substrate used was octanol.

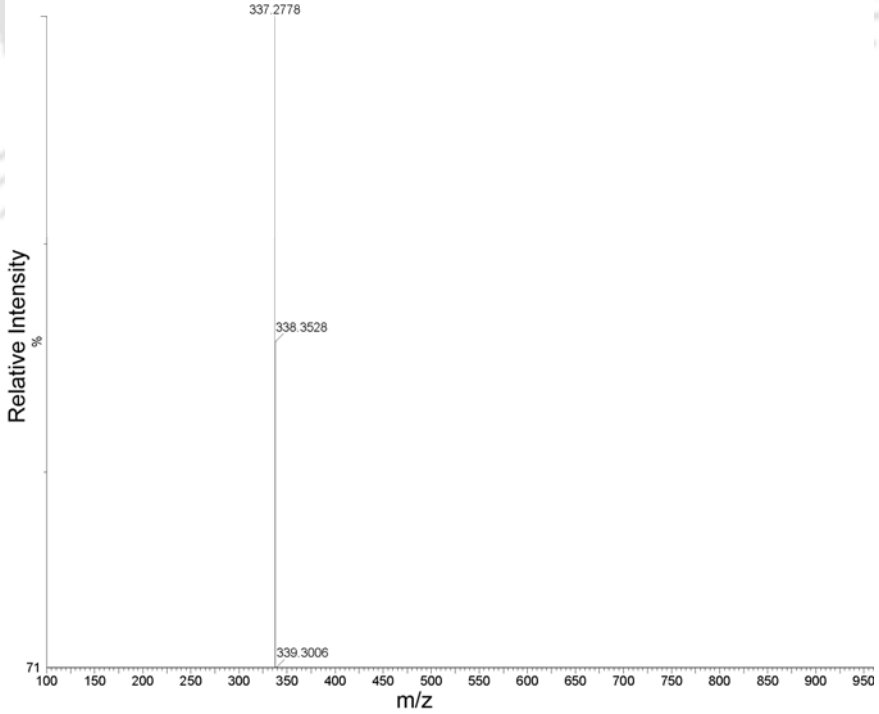

Figure 6.10: ESI-MS spectra of the hydrazone derivative of decanaldehyde (*m/z* 336.1798; [M^+ (the molecular ion)] M^++H, 337.2778). Substrate used was decanol.

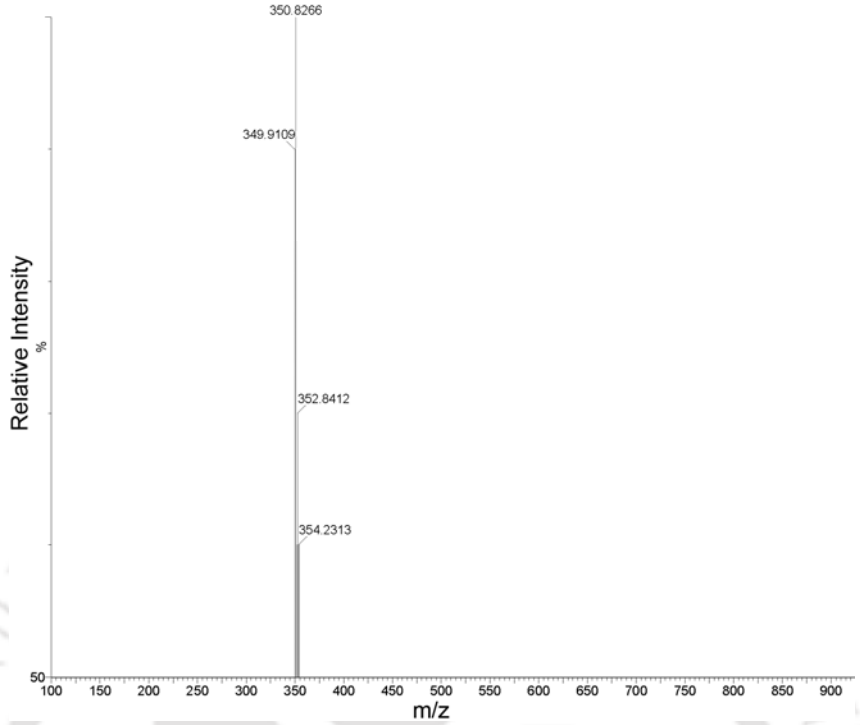

Figure 6.11: ESI-MS spectra of the hydrazone derivative of undecanaldehyde (*m/z* 350.1954; [M^+ (the molecular ion)] M^++H, 350.8266). Substrate used was undecanol.

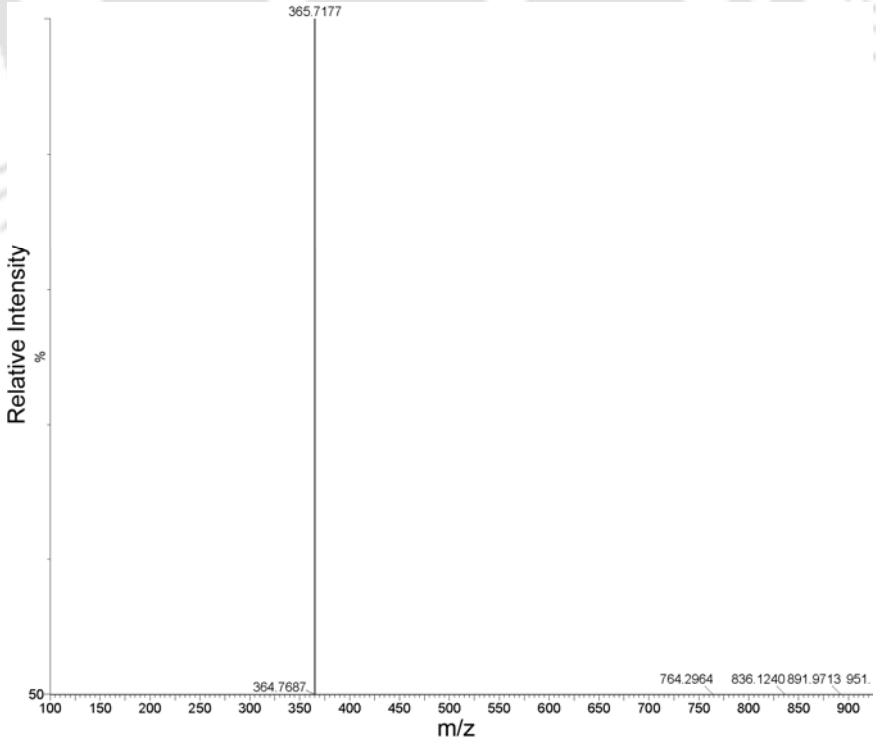

Figure 6.12: ESI-MS spectra of the hydrazone derivative of dodecanaldehyde (*m/z* 364.4393; [M^+ (the molecular ion)] M^++H, 365.7177). Substrate used was dodecanol.

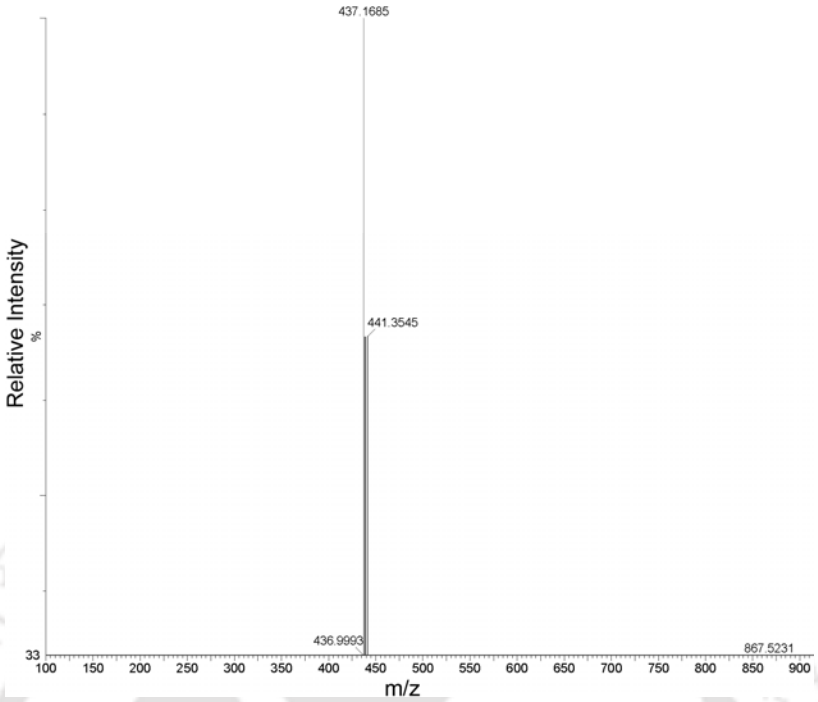

Figure 6.13: ESI-MS spectra of the hydrazone derivative of 16-0H hexadecanaldehyde (*m/z* 436.2686; [M^+ (the molecular ion)] M^++H, 437.1685). Substrate used was 1,16 hexadecane diol.

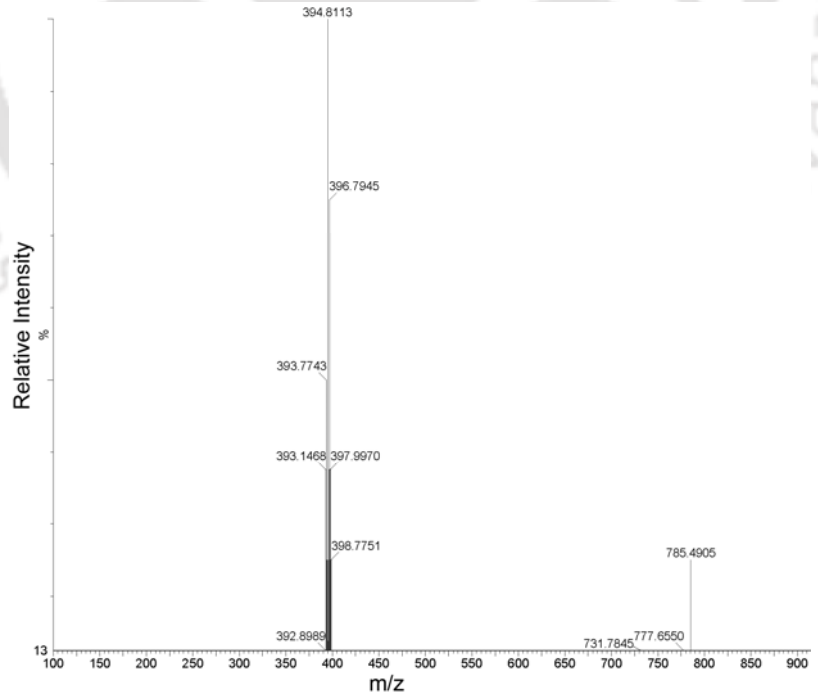

Figure 6.14: ESI-MS spectra of the hydrazone derivative of 11-formyl undecanoic acid (*m/z* 394.1852; [M^+ (the molecular ion)] M^++H, 394.8113). Substrate used was 12-hydroxy dodecanoic acid.

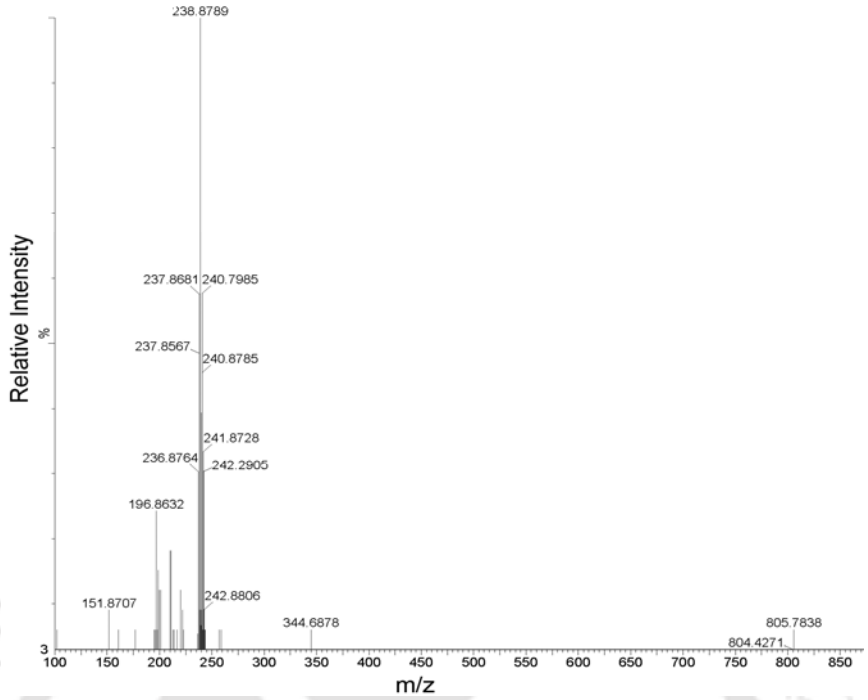

Figure 6.15: ESI-MS spectra of the hydrazone derivative of acetone (*m/z* 238.0702; [M^+ (the molecular ion)] M^++H, 238.8789). Substrate used was 2-propanol.

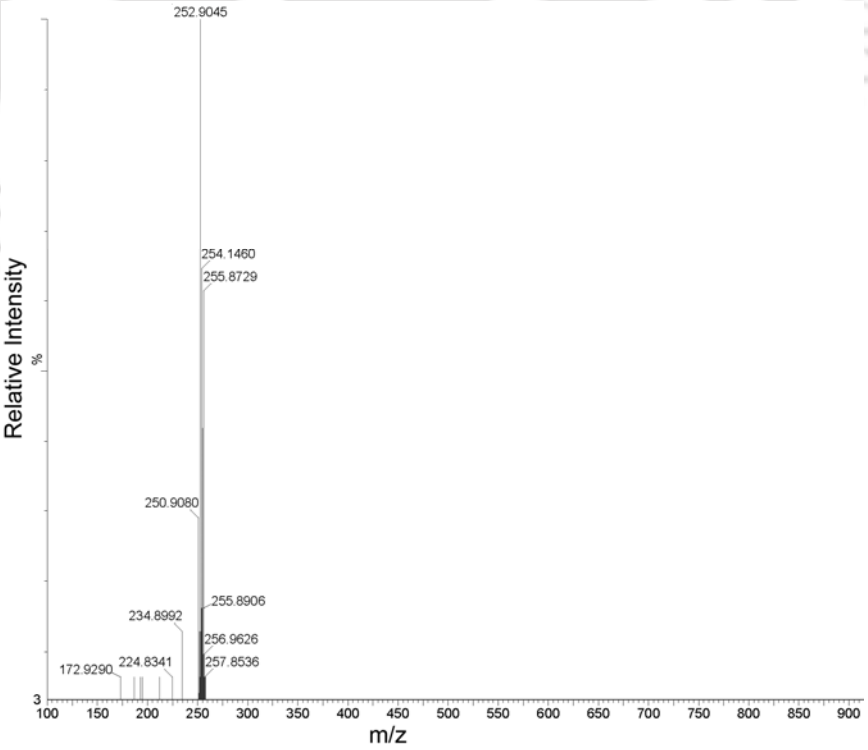

Figure 6.16: ESI-MS spectra of the hydrazone derivative of 2-butanone (*m/z* 252.0859; [M^+ (the molecular ion)] M^++H, 252.9045). Substrate used was 2-butanol.

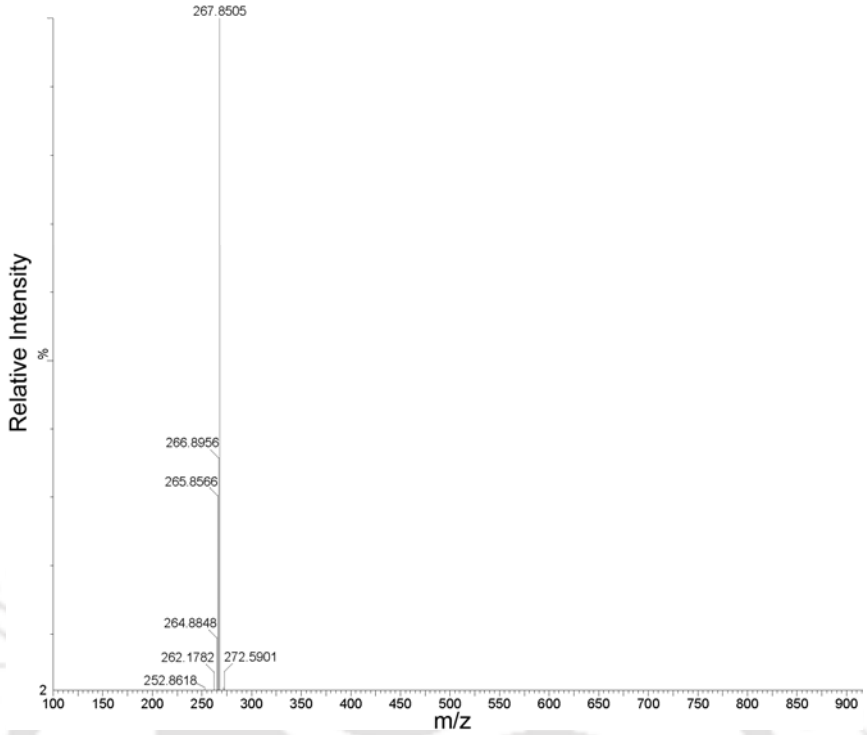

Figure 6.17: ESI-MS spectra of the hydrazone derivative of 3-methyl butanaldehyde (*m/z* 266.2533; [M^+ (the molecular ion)] M^++H, 267.8505). Substrate used was 3-methyl butanol.

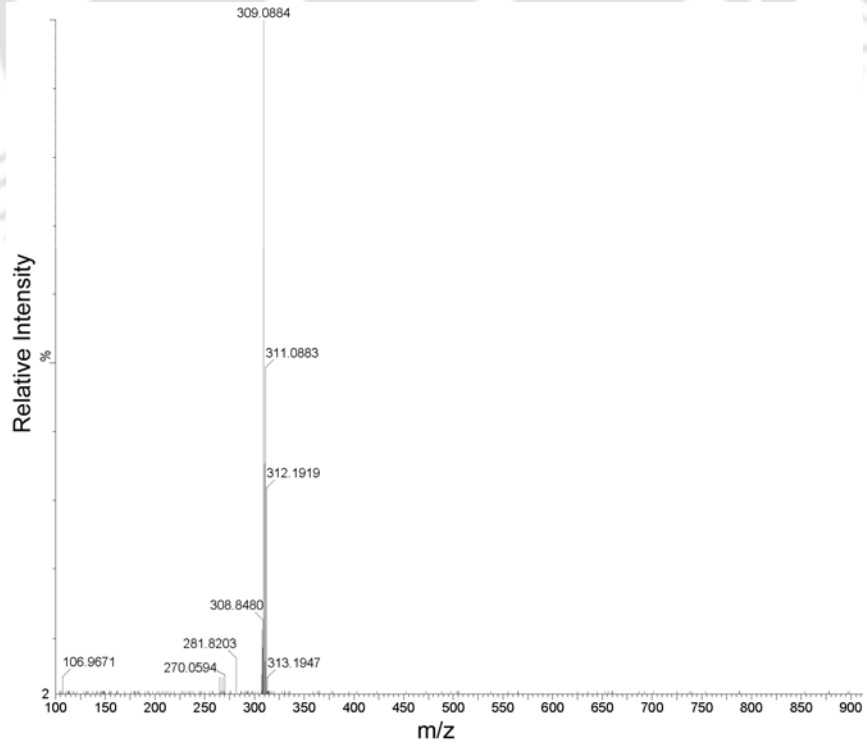

Figure 6.18: ESI-MS spectra of the hydrazone derivative of 3-octanone (*m/z* 308.1485; [M^+ (the molecular ion)] M^++H, 309.0884). Substrate used was 3-octanol.

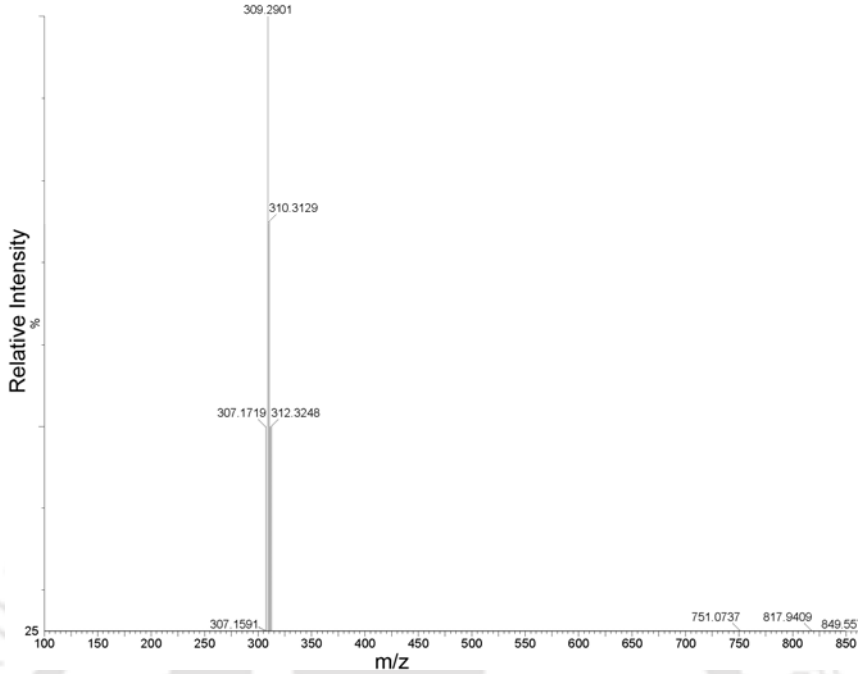

Figure 6.19: ESI-MS spectra of the hydrazone derivative of 2-octanone (*m/z* 308.1485; [M^+ (the molecular ion)] M^++H, 309.2901). Substrate used was *R*(-)2-octanol.

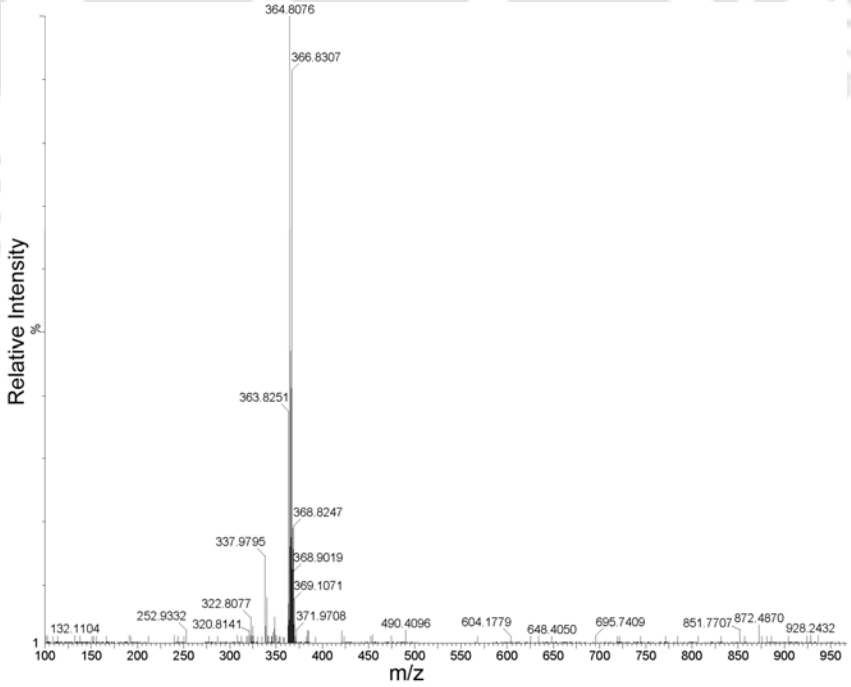

Figure 6.20: ESI-MS spectra of the hydrazone derivative of 2-dodecanone (*m/z* 364.2111; [M^+ (the molecular ion)] M^++H, 364.8076). Substrate used was 2-dodecanol.

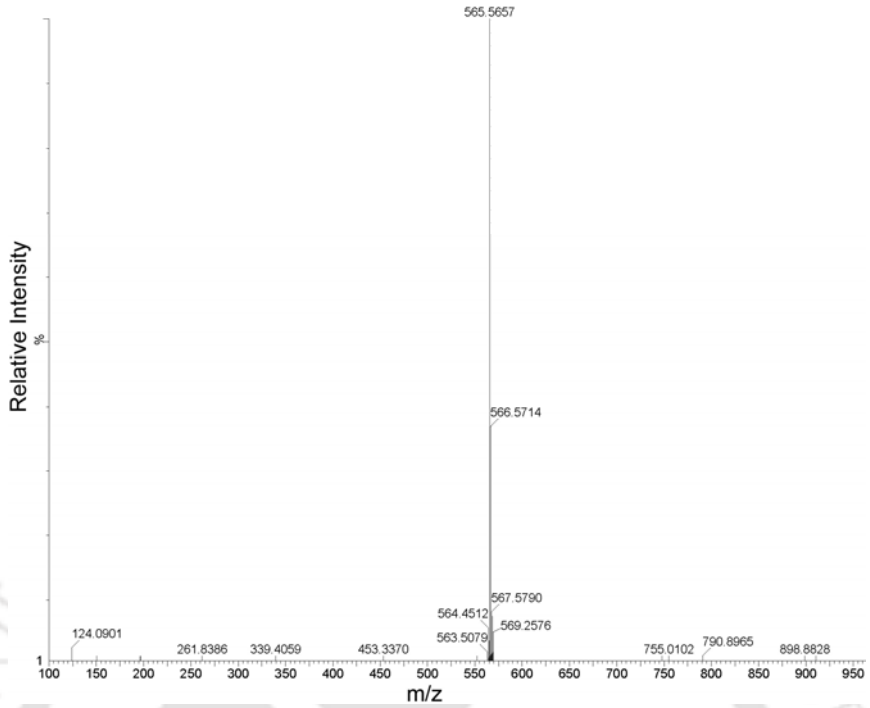

Figure 6.21: ESI-MS spectra of the hydrazone derivative of 4-cholesten-3-one (*m/z* 564.3676; [M^+ (the molecular ion)] M^++H, 565.5657). Substrate used was cholesterol.

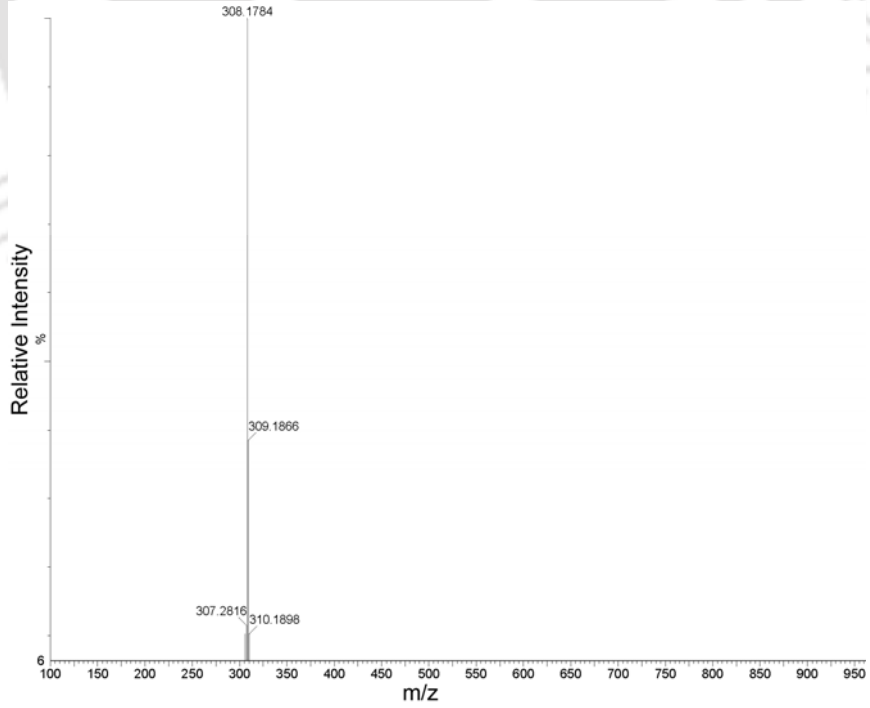

Figure 6.22: ESI-MS spectra of the hydrazone derivative of cyclo octanone (*m/z* 306.1328; [M^+ (the molecular ion)] M^++2H, 308.1784). Substrate used was cyclo octanol.

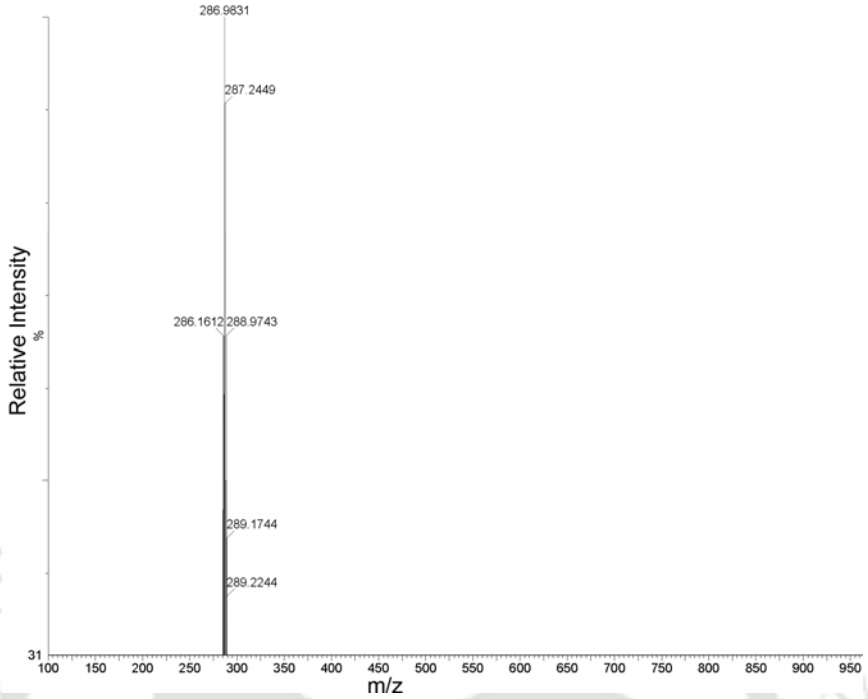

Figure 6.23: ESI-MS spectra of the hydrazone derivative of benzaldehyde (*m/z* 286.0702; [M^+ (the molecular ion)] M^++H, 286.9831). Substrate used was benzyl alcohol.

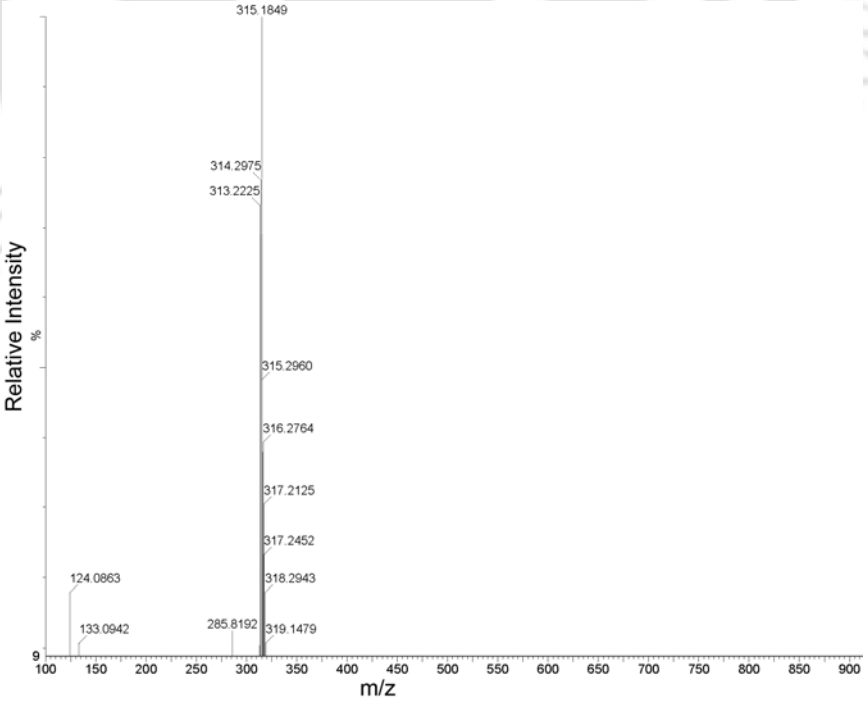

Figure 6.24: ESI-MS spectra of the hydrazone derivative of phenyl-3-propanone (*m/z* 314.1015; [M^+ (the molecular ion)] M^++H, 315.1849). Substrate used was phenyl-3-propanol.

6.5 TABLES

Table 6.1. AOX protein catalyzed conversion of various alcohols to corresponding carbonyl compounds

Sl No	Substrate	Product	Molar conversion (%)*	*m/z* (M^+ + H)
1			52	212.1459
2			70	225.1485
3			84	238.8789
4			77	252.8986
5			99[b]	295.1974
6			99[b]	309.2836
7			99	337.2778
8			98	350.8266
9			98	365.7177
10			96	437.1685
11			56	394.8113
12			80, 99[#]	238.8789
13			32	252.9045
14			90, 97[#]	267.8505
15			99[b]	309.0884
16			99	309.2901
17			96, 99[#]	364.8076
18			14, 25[#]	565.5657
19			80[a], 98	308.1784
20			9	286.9831
21			25	315.1849

*****The reaction mixture contained 10 mM of respective substrate and 0.15 mg AOX protein. The reaction was carried out at 25 ^{o}C for 24 hr. The products were isolated at different time periods: [a] 6 hr; [b] 10 hr, and molar absorption coefficient at $UV_{360\ nm}$ of representative corresponding aldehydes/ketones was obtained to calculate the molar conversion %.

[#] The molar conversion % was calculated after carrying out the reaction in presence of 30 mM 1,12-dichlorododecane at similar conditions mentioned above. M^+: The molecular ion.

Chapter 7

CONCLUSIONS AND SCOPE FOR FUTURE WORK

An *Aspergillus terreus* isolated from oil contaminated soil was found to degrade a wide range of petroleum hydrocarbons including the immediate oxidation products of hydrocarbons, like alkanols and alkanals. Maximum growth of the fungus was observed on *n*-hexadecane substrate amongst the various hydrocarbon substrates considered in this investigation. Assimilation of such highly hydrophobic hydrocarbon substrates by this filamentous fungus was appeared to occur through the sorption mechanism. There was a change of hyphal morphology during the growth on hydrocarbon substrates. Adaptation of the cells for up-taking such highly hydrophobic substrates through sorption mechanism and accumulation of high lipid content in the cells, as evident from nearly seven-fold more lipid production in *n*-hexadecane-grown cells than the glucose-grown cells, were the suggested reasons for the observed morphological change. The fatty acid analysis in the cellular lipid demonstrated the predominance of two saturated fatty acids namely, palmitic- and stearic acids in the hexadecane-grown cells. Contrary to this fact, the predominance of two unsaturated fatty acids namely, oleic- and linoleic acids in the glucose-grown cells was established. Among the total lipids isolated from the *n*-hexadecane-grown cells, palmitic acid with highest intensity was observed. This is the most probable product of terminal oxidation of *n*-hexadecane substrate catalyzed by the cell membrane associated redox enzymes. Nearly nine different fatty acids were additionally induced in the *n*-hexadecane-grown cells as compared to the corresponding glucose-grown cells. Long chain fatty acids with chain length C_{32} and C_{33} were detected for the first

time in *Aspergillus strains*. However, the fungal metabolism of these very long chain fatty acids is not clearly known from this organism.

A broad substrate specific alcohol oxidase activity in the microsome of the cells capable of oxidizing short chain-, long chain-, secondary- and aromatic alcohol substrates during growth of the fungi on *n*-hexadecane was detected. The preliminary characteristics showed that the pH and temperature optimum of the enzyme was 8.1 ± 0.5 and 27-33 ^{o}C, respectively. The stability of the alcohol oxidase was drastically decreased beyond 30 ^{o}C. The enzyme showed 33% enantiomeric excess for the *R*(-)2-octanol over *S*(+)2-octanol, which may be correlated with the lower K_m values of the enzyme for the *R*(-)2-octanol than the *S*(+)2-octanol. The fluorescence emission spectrum of the column chromatographically separated protein was similar to that obtained with authentic FAD, which indicates the presence of FAD as a cofactor in the alcohol oxidase protein. This cofactor was non-covalently but avidly associated with the alcohol oxidase protein. The alcohol oxidase was purified to homogeneity by ion exchange chromatography. The purified enzyme shows highest affinity for *n*-heptanol (K_m = 0.498 mM, K_{cat} = 2.7 x 10^2 s^{-1}). The functional characteristics of the purified protein showed the molecular mass of 269 ± 5kDa and the subunit molecular masses 85-, 63-, 43-, 27-, and 13-kDa, respectively. The isoelectric point of the alcohol oxidase protein (8.3-8.5) from *A. terreus* was entirely different from other sources. Chemical analysis showed the presence of oleic acid and palmitic acid at a ratio of 2:1 in the purified protein. This is the first report on the lipoprotein nature of alcohol oxidase enzyme from any sources. The high aggregating nature of the protein with an average particle size 180nm (radius) was also demonstrated. Peptide mass fingerprinting studies showed the presence of two FAD binding domains in 63kDa protein. Among these two domain sequences, only the YPVIDHEYDAVVV**G**A**G**GA**G**LR peptide shows 45-50% sequence similarity with the reported N-terminal sequences of other known alcohol oxidases. Non-redundant database search of 63- and 43-kDa subunits peptide sequences showed no sequence similarity with the other alcohol oxidase protein reported till now.

We have demonstrated a highly efficient method for dissociation and simultaneous deflavination of the alcohol oxidase protein using *β*-ME. The highly aggregated alcohol oxidase protein particles when incubated with 0.74 M *β*-ME for 8 h at 4 ^{o}C, the aggregated particles were dissociated to subunits and almost 87% of the FAD present in the native protein was simultaneously separated. This dissociation

process had traversed through two intermediate protein (IP) stages, IP_1 and IP_2, which were associated with the FAD. The IP_1 (size 10 nm) that contained the subunits 85-, 63-, 43-, 25-, 13-kDa was functionally active, whereas, the IP_2 (size 9 nm) that contained 85-, 63-, 25-, 13-kDa was inactive, which indicates the critical role of the 43kDa protein for the alcohol oxidase activity. The intermediate protein particle (IP_1) with molecular mass nearly equivalent to the native protein was considered as the building block for these highly aggregated multimeric protein particles of size 180 nm radius. A functionally inactive reconstituted apoprotein (P_R) with molecular mass and subunits similar to IP_1 was generated upon removal of *β*-ME from the subunit level dissociated proteins using simple dialysis technique. The re-associated protein was also successfully reconstituted with exogenous FAD to a functionally active alcohol oxidase holoenzyme. The solvent effect caused by the high concentration of the *β*-ME destabilized the conformation of the partially degraded (27kDa to 25kDa) multimeric protein, which was formed from the *β*-ME mediated intrapeptide disulphide bond breakage, is attributed to the observed dissociation and associated deflavination of these highly aggregated alcohol oxidase multimeric protein particles.

The potential applications of this approach on preparing apoprotein and its reassemble with FAD to a functional enzyme are envisaged in the preparation of enzyme electrodes for biosensor and biofuel cell applications. The biocatalytic application of the isolated alcohol oxidase was also explored to some extent. High yield conversion of different alcohols to the corresponding carbonyl compounds under room temperature, atmospheric pressure, aqueous environment, and in a single step was achieved by using this alcohol oxidase protein. This was evident from the yields of almost 95% products (aldehydes or ketones) from the corresponding alcohol substrates. The application potential of this enzyme for kinetic resolution of secondary alcohols is also foreseen with further optimization of the reaction parameters for the conversion.

The findings obtained through this investigation have revealed many interesting facts about this novel microsomal alcohol oxidase enzyme. However, at the same time many of the findings are enigmatic that need further investigations to understand this complex enzyme. The broad substrate specificity is identified as one of the fascinating fact for this multimeric alcohol oxidase. Conversely, specific activator and inhibitor for certain activity of the enzyme is intriguing. $MgCl_2$ increased the enzyme activity for both short chain-, and long chain alcohol substrates;

whereas, ferrocene increased the activity only for the short chain alcohol substrate. The 1,12DCD was identified as competitive inhibitor for long chain alcohol substrate. There was no inhibitory effect of 1,12DCD on the oxidation of short chain- and aromatic-alcohols, while, it was found to be an activator for secondary alcohols. The substrate induced catalytic activation of the reconstituted dissociated proteins and FAD infers likely cooperation among the subunit proteins that lead to the functionally active protein. However, the exact functional role of each individual subunits of this hetero-oligomeric protein is yet to be established and linked to the specificity of the enzyme. Investigation on the biogenesis of this alcohol oxidase multimeric protein on the microsome may provide answer to many of these critical questions. Complete molecular characterization, heterologous expression, and x-ray crystallographic study of this enzyme expected to furnish important information regarding the structural features, catalytic sites and assembly of the subunits in this holo-protein. This investigation has opened up new avenue on the research to explore the architecture of alcohol oxidase proteins from fungal sources including their structure-function relationship and potential applications.

BIBLIOGRAPHY

Adekunle AA, & Adebambo OA. (2007) Petroleum hydrocarbon utilization by fungi isolated from *Detarium senegalense* (J. F Gmelin) seeds. *J. Am. Sci.* 3: 69-76.

Ahmed SA, McPhie P, & Miles EW. (1996) Mechanism of activation of the tryptophan synthase $\alpha_2\beta_2$ Complex: solvent effects of the co-substrate β-mercaptoethanol. *J. Biol. Chem.* 271: 29100-29106.

Akyilmaz E, & Dinckaya E. (2000) A mushroom (*Agaricus bisporus*) tissue homogenate based alcohol oxidase electrode for alcohol determination in serum. *Talanta.* 53: 505–509.

Alvarado-Caudillo Y, Bravo Torres JC, Novoa VZ, Silva JH, Torres-Guzman JC, Gutierrez-Corona JF, & Zazueta-Sandoval R. (2002) Presence and physiologic regulation of alcohol oxidase activity in an indigenous fungus isolated from petroleum-contaminated soils. *Appl. Biochem. Biotech.* 98: 243-256.

Alhadeff EM, Salgado AM, Pereira N, & Valdman B. (2004) Development and application of an integrated system for monitoring ethanol content of fuels. *Appl. Biochem. Biotech.* 113: 125-136.

Annibale AD, Rosetto F, Leonardi V, Federici F, & Petruccioli M. (2006) Role of autochthonous filamentous fungi in bioremediation of a soil historically contaminated with aromatic hydrocarbons. *App. Environ. Microb.* 72: 28-36.

April TM, Foght JM, & Currah RS. (2000) Hydrocarbon-degrading filamentous fungi isolated from flare pit soils in northern and western Canada. *Can. J. Microbiol.* 46: 38-49.

Asada Y, Watanabe A, Ohtsu Y, & Kuwahara M. (1995) Purification and characterization of an aryl-alcohol oxidase from the lignin-degrading basidiomycete *Phanerochaete chrysosporium*. *Biosci. Biotech. Bioch.* 59: 1339-1341.

Ashin V, & Trotsenko Y. (2000) Alcohol oxidase of the methylotropic yeasts: new findings. *J. Mol. Catal. B-Enzym.* 10: 295-303.

Atlas RM (1981) Microbial degradation of petroleum hydrocarbons: an environmental perspective. *Microbiol. Rev.* 45: 180–209.

Azevedo AM, Prazeres DMF, Cabral JMS, & Fonseca LP. (2005) Ethanol biosensors based on alcohol oxidase. *Biosens. Bioelectron.* 21: 235–247.

Badea M, & Arsene ML. (1996) Catalytic properties of alcohol oxidase to oxidize aliphatic and aromatic alcohols. *Prog. Catal.* 5: 45-50.

Banthorpe DV, Cardemil E, Del C, & Contraras M. (1976) Purification and properties of alcohol oxidase from *Tanacetum vulgare*. *Phytochem.* 15: 391-394.

Barrasa JM, Gutierrez A, Escaso V, Guillen F, Martinez MJ, Martinez AT. (1998) Electron and fluorescence microscopy of extracellular glucan and aryl-alcohol oxidase during wheat-straw degradation by *Pleurotus eryngii*. *Appl. Environ. Microb.* 64: 325-332.

Barton AC, Collyer SD, Davis F, Gornall DD, Law KA, Lawrence ECD, Mills DW, Myler S, Pritchard JA, Thompson M, & Higson SPJ. (2004) Sonochemically fabricated microelectrode arrays for biosensors offering widespread applicability. Part I. *Biosens. Bioelectron.* 20: 328-337.

Billiar RB, Knappenberger M, & Little B. (1970) Xanthine oxidase for calibration of oxygen electrode apparatus. *Anal. Biochem.* 36: 101-104.

Blacklock TJ, Sohar P, Butcher JW, Lamanec T, & Grabowski EJJ. (1993) An enantioselective synthesis of the topically-active carbonic anhydrase inhibitor MK-0507:5,6-dihydro-(s)-4-(ethylamino)-(s)-6-mehtyl-4H-thieno[2,3-beta]thiopyran-2-sulfonamide 7,7-dioxide hydrochloride. *J. Org. Chem.* 58: 1672-1679.

Blasig R, Mauersberger S, Reige P, Schunck WH, Jockisch W, Franke P, & Muller HG. (1988) Degradation of long chain *n*-alkanes by the yeast *Candida maltosa*. Oxidation of *n*-alkanes and intermediates using microsomal membrane fractions. *Appl. Microbiol. Biot.* 28: 589-597.

Bokoch MP, Devadoss A, Palencsar MS, & Burgess JD. (2004) Steady-state oxidation of cholesterol catalyzed by cholesterol oxidase in lipid bilayer membranes on platinum electrodes. *Anal. Chim. Acta.* 519: 47-55.

Bormann C, & Sahm H. (1978) Degradation of microbodies in relation to activities of alcohol oxidase and catalase in *Candida boidinii*. *Arch. Microbiol.* 117: 67-72.

Bourbonnais R, & Paice MG. (1988) Veratryl alcohol oxidases from the lignin-degrading basidiomycete *Pleurotus sajor-caju*. *Biochem. J.* 255: 445-450.

Bradford MM. (1976) A rapid and sensitive method for the quantification of microgram quantities of protein utilizing the principle of protein dye binding. *Anal. Biochem.* 72: 248-254.

Branden CI, Jornvall H, Eklund H, & Perugren B. (1975) Alcohol dehydrogenases. In The Enzymes (Edited by BOYER PAUL D.), 3rd edn, Vol. 11, pp. 103-189. Academic Press, New York.

Bringer S, Sprey B, & Sahm H. (1979) Purification and properties of alcohol oxidase from *Poria contigua*. *Eur. J. Biochem.* 101: 563-570.

Britton LN. (1984) Microbial degradation of aliphatic hydrocarbons. *Microbial. Degradation. Organic. Compounds.* 5:181-252.

Bruckmann M, Termonia A, Pasteels JM, & Hartmann T. (2002) Characterization of an extracellular salicyl alcohol oxidase from larval defensive secretions of *Chrysomela populi* and *Phratora vitellinae* (Chrysomelina). *Insect. Biochem. Molec.* 32: 1517-1523.

Bushnell LD, & Haas FF. (1941) The utilization of certain hydrocarbons by microorganisms. *J. Bacteriol.* 41: 653-673.

Casalin P, Pollegioni L, Curti B, & Pilone MS. (1991) A study on apoenzyme from *Rhodotorula gracilis* D-amino acid oxidase. *Eur. J. Biochem.* 197: 513-517.

Castillo J, Gaspar S, Sakharov I, & Csoregi E. (2003) Bienzyme biosensors for glucose, ethanol and putrescine built on oxidase and sweet potato peroxidase. *Biosens. Bioelectron.* 18: 705-714.

Cavener DR. (1992) GMC oxidoreductases: A newly defined family of homologous protein from diverse catalytic activities. *J. Mol. Biol.* 223: 811-814.

Cerniglia CE, & Perry JJ. (1974) Effect of substrate on the fatty acid composition of hydrocarbon-utilizing filamentous fungi. *J. Bacteriol.* 118: 844-847.

Chaabouni MK, Pulvin S, Meziani A, Thomas D, Touraud D, & Kunz W. (2003) Biooxidation of *n*-hexanol by alcohol oxidase and catalase in biphasic and micellar systems without solvent. *Biotechnol. Bioeng.* 81: 27-32.

Cheng Q, Liu HT, Bombelli P, Smith A, & Slabas AR. (2004) Functional identification of AtFao3, a membrane bound long chain alcohol oxidase in *Arabidopsis thaliana*. *FEBS. Lett.* 574: 62-68.

Cheng Q, Sanglard D, Vanhanen S, Liu HT, Bombelli P, Smith A, & Slabas AR. (2005) Candida yeast long chain fatty alcohol oxidase is a c-type haemoprotein and plays an important role in long chain fatty acid metabolism. *Biochim. Biophys. Acta.* 1735: 192-203.

Christian TK, & Stadtlander H. (2005) Dehydration and rehydration issues in biological tissue processing for electron microscopy. *Microscopy. Today.* 32-34.

Christovaa N, Tulevaa B, & Nikolova-Damyanovab B. (2004) Enhanced hydrocarbon biodegradation by a newly isolated *Bacillus subtilis* strain. *Zeitschrift. Für. Naturforschung. C.* 59c: 205-208.

Cos O, Ramon R, Montesinos JL, & Valero F. (2006) Operational strategies, monitoring and control of heterologous protein production in the methylotrophic yeast *Pichia pastoris* under different promoters: A review. *Microbial. Cell. Factories.* 5: 17.

Couderc R, & Baratti J. (1980) Oxidation of methanol by the yeast, *Pichia pastoris*. Purification and properties of the alcohol oxidase. *Agric. Biol. Chem*. 44: 2279-2289.

Cregg JM, Madden KR, Barringer KJ, Thill GP, & Stillman CA. (1989) Functional characterization of the two alcohol oxidase genes from the yeast *Pichia pastoris. Mol. Cell. Biol.* 9: 1316-1323.

Cromartie TH. (1981) Sulfhydryl and histidinyl residues in the flavoenzyme alcohol oxidase from *Candida boidinii*. *Biochemistry.* 20: 5416-5423.

Cromartie TH. (1982) Irreversible inactivation of the flavoenzyme alcohol oxidase by cyclopropanone. *Biochem. Bioph. Res. Co.* 10: 5785-5790.

Dalzeil K. (1975) Kinetics and mechanisms of nicotinamide nucleotide-linked dehydrogenases. In The Enzymes (Edited by BOYER PAUL D.), 3rd edn, Vol. II, pp. 1-60. Academic Press, New York.

Daniel G, Volc J, Filonova L, Plihal O, Kubatova E, & Halada P. (2007) Characteristics of *Gloeophyllum trabeum* alcohol oxidase, an extracellular source of H_2O_2 in brown rot decay of wood. *Appl. Environ. Microb.* 73: 6241-6253.

Danneel HJ, Reichert A, & Giffhorn F. (1994) Production, purification and characterization of an alcohol oxidase of the lignolytic fungus *Peniophora gigantean. J. Biotechnol.* 33: 33-41.

Dashti N, Al-Awadhi H, Khanafer M, Abdelghany S, & Radwan S. (2008) Potential of hexadecane-utilizing soil-microorganisms for growth on hexadecanol, hexadecanal and hexadecanoic acid as sole sources of carbon and energy. *Chemosphere.* 70: 475–479.

Davidsson R, Johansson B, Passoth V, Bengtsson M, Laurell T, & Emneus J. (2004) Microfluidic biosensing systems. Part II. Monitoring the dynamic production of glucose and ethanol from microchip-immobilised yeast cells using enzymatic chemiluminescent micro-biosensors. *Lab. Chip.* 4: 488-494.

De Hoop MJ, Cregg J, Keizer-Gunnink I, Sjollema K, Veenhuis M, & Ab G. (1991) Overexpression of alcohol oxidase in *Pichia pastoris*. *FEBS. Lett.* 291: 299-302.

De Prada AG, Pena N, Mena ML, Reviejo AJ, & Pingarron JM. (2003) Graphite-teflon composite bienzyme amperometric biosensors for monitoring of alcohols. *Biosens. Bioelectron.* 18: 1279-1288.

Deziel E, Paquette G, Villemur R, Lepine F, & Bisaillon J. (1996) Biosurfactant production by a soil *Pseudomonas* strain growing on polycyclic aromatic hydrocarbons. *Appl. Environ. Microb.* 62: 1908–1912.

Dickinson FM, & Wadforth C. (1992) Purification and some properties of alcohol oxidase from alkane-grown *Candida tropicalis. Biochem. J.* 282: 325-331.

Dienys G, Jarmalavicius S, Budriene S, Itavicius DC, & Sereikaite J. (2003) Alcohol oxidase from the yeast *Pichia pastoris*- a potential catalyst for organic synthesis. *J. Mol. Catal. B-Enzym.* 21: 47-49.

Dmytruk KV, Smutok OV, Ryabova OB, Gayda GZ, Sibirny VA, Schuhmann W, Gonchar MV, & Sibirny AA. (2007) Isolation and characterization of mutated alcohol oxidases from the yeast *Hansenula polymorpha* with decreased affinity toward substrates and their use as selective elements of an amperometric biosensor. *BMC. Biotechnol.* 7: 33-39.

Domasch KH, Game W, & Anderson TH. (1980) Compendium of soil fungi. Academic Press, London.

Dyal SD, & Narine SS. (2005) Implications for the use of *Mortierella* fungi in the industrial production of essential fatty acids. *Food. Res. Int.* 38: 445-467.

Edegger K, Mang H, Faber K, Gross J, & Kroutil W. (2006) Biocatalytic oxidation of sec-alcohols via hydrogen transfer. *J. Mol. Cat. A: Chem.* 251: 66-70.

Eirich D, Craft LD, Steinberg L, Asif A, Eschenfeldt WH, Stols L, Donnelly MI, & Wilson CR. (2004) Cloning and characterization of three fatty alcohol oxidase genes from *Candida tropicalis* strain ATCC 20336. *Appl. Environ. Microb.* 70: 4872-4879.

Eriksson KE, & Nishida A. (1988) Methanol oxidase of *Phanerochaete chrysosporium. Methods. Enzymol.* 161: 322-326.

Ernst M, Kaup B, Muler M, Bringer-Meyer S, & Sahm H. (2005) Enantioselective reduction of carbonyl compounds by whole-cell biotransformation, combining a formate dehydrogenase and a (*R*)-specific alcohol dehydrogenase. *App. Microbiol. Biot.* 66: 629-634.

Evers ME, Titorenko VI, van der Klei IJ, Harder W, & Veenhuis M. (1994) Assembly of alcohol oxidase in peroxisomes of the yeast *Hansenula polymorpha* requires the cofactor flavin adenine dinucleotide. *Mol. Biol. Cell.* 5: 829-837.

Evers ME, Harder W, & Veenhuis M. (1995) Invitro dissociation and re-assembly of peroxisomal alcohol oxidases of *Hanensula polymorpha* and *Pichia pastoris. FEBS. Lett.* 368: 293-296.

Faber K. (2000) In Biotransformation in organic Chemistry, Springer, Heidelberg, 4th edn, pp. 226.

Farmer VC, Henderson MEK, & Russell JD. (1960) Aromatic-alcohol oxidase activity in the growth medium of *Polystictus versicolor*. *Biochem. J.* 74: 257-262.

Fernando LG, Lorena B, Aurelio H, Gisela DO, Cesar M, Roberto FL, & An Jose MG. (2007) Stabilization of different alcohol oxidases via immobilization and post immobilization techniques. *Enzyme. Microb. Tech.* 40: 278-284.

Ferreira P, Medina M, Guillen F, Martinez MJ, van Berkel WJH, & Martinez AT. (2005) Spectral and catalytic properties of aryl-alcohol oxidase, a fungal flavoenzyme acting on polyunsaturated alcohols. *Biochem. J.* 389: 731-738.

Folch J, Lees M, & Sloane Stanley GH. (1958) A simple method for the isolation and purification of total lipids from animal tissues. *J. Biol. Chem.* 497-500.

Fowler SD, & Greenspan P. (1985) Application of nile red, a fluorescent hydrophobic probe, for the detection of neutral lipid deposits in tissue sections: comparison with oil red 0'. *J. Histochem. Cytochem.* 33: 833-836.

Fraaije MW, Veeger C, & van Berkel WJ. (1995) Substrate specificity of flavin-dependent vanillyl-alcohol oxidase from *Penicillium simplicissimum*. Evidence for the production of 4-hydroxycinnamyl alcohols from 4-allylphenols. *Eur. J. Biochem.* 234: 271-277.

Geissler J, Ghisla S, & Kroneck PMH. (1986) Flavin-dependent alcohol oxidase from yeast. Studies on the catalytic mechanism and inactivation during turnover. *Eur. J. Biochem.* 160: 93-100.

Geissler J, & Hemmerich P. (1981) Yeast methanol oxidases: an unusual type of flavoprotein. *FEBS. Lett.* 126: 152-156.

Ghisla S, & Massey V. (1989) Mechanism of flavoprotein-catalyzed reactions. *Eur. J. Biochem.* 181: 1-17.

Goswami P, & Cooney JJ. (1999) Sub-cellular localization of enzymes involved in oxidation of *n*-alkane by *Cladosporium resinae. Appl. Microbiol. Biot.* 51: 860-864.

Goswami P, & Singh HD. (1991) Different modes of hydrocarbon uptake by two *Pseudomonas* species. *Biotechnol. Bioeng.* 37: 1-11.

Greenspan P, & Fowler SD. (1985) Spectrofluorometric studies of the lipid probe, nile red. *J. Lipid. Res.* 26: 781-789.

Grewal N, Parveen Z, Large A, Perry C, & Connock M. (2000) Gastropod mollusc aliphatic alcohol oxidase: subcellular localization and properties. *Comp. Biochem. Phys. B.* 125: 543-554.

Guillen F, Martinez AT, & Martinez MJ. (1990) Production of hydrogen peroxide by arylalcohol oxidase from the ligninolytic fungus *Pleurotus eryhgii*. *Appl. Microbiol. Biot.* 32: 465-469.

Guillen F, Martinez AT, & Martinez MJ. (1992) Substrate specificity and properties of the aryl-alcohol oxidase from ligninolytic fungus *Pleurotus eryngii. Eur. J. Biochem.* 209: 603-611.

Guiseppin MLF, van Eijk HML, & Bes BCM. (1988) Molecular regulation of alcohol oxidase in *Hansenula polymorpha* in continuous cultures. *Biotechnol. Bioeng.* 32: 577–583.

Gunkel K, van Dijk R, Veenhuis M, & van der Klei IJ. (2004) Routing of *Hansenula polymorpha* alcohol oxidase: an alternative peroxisomal protein sorting machinery. *Mol. Biol. Cell.* 15: 1347-1355.

Gurkan C, Symeonides SN, & Ellar DJ. (2004) High-level production in *Pichia pastoris* of an anti-p185HER-2 single chain antibody fragment using an alternative secretion expression vector. *Biotechnol. Appl. Bioch.* 39: 115-122.

Hack JB, Chiang WK, Howland MA, Patel H, & Goldfrank LR. (2000) The utility of an alcohol oxidase reaction test to expedite the detection of toxic alcohol exposures. *Academic. Emergency. Medicine.* 7: 294-297.

Hammes-Schiffer, Sharon & Benkoviv, & Stephen J. (2006) Relating protein motion to catalysis. *Annu. Rev. Biochem.* 75: 519-541.

Hargrove JL, Greenspan P, & Hartle K. (2004) Nutritional significance and metabolism of very long chain fatty alcohols and acids from dietary wax. *Exp. Biol. Med.* 229: 215-226.

Hartree EF. (1972) Determination of protein: a modification of the Lowry method that gives a linear photometric response. *Anal. Biochem.* 48: 422–427.

Hasunuma T, Kuwabata S, Fukusaki E, & Kobayashi A. (2004) Real-time quantification of methanol in plants using a hybrid alcohol oxidase-peroxidase biosensor. *Anal. Chem.* 76: 1500–1506.

Hedrick JL, & Smith AJ. (1968) Size and charge isomer separation and estimation of molecular weights of proteins by disc gel electrophoresis. *Arch. Biochem. Biophys.* 126: 155-164.

Henderson RF, & Henderson TR. (1970) Effects of D_2O on the association-dissociation equilibrium in subunit proteins. *J. Biol. Chem.* 245: 3733-3737.

Hirano J, Miyamoto K, & Ohta H. (2008) The green and effective oxidation of alcohols to carboxylic acids with molecular oxygen via biocatalytic reaction. *Tetrahedron. lett.* 49: 1217-1219.

Hjelmeland LM, & Chrambach A. (1984) Solubilization of functional membrane proteins. *Methods. Enzymol.* 104: 305-318.

Holzmann K, Schreiner E, & Schwab H. (2002) A *Penicillium chrysogenum* gene (aox) identified by specific induction upon shifting pH encodes for a protein which shows high homology to fungal alcohol oxidases. *Curr. Genet.* 40: 339-344.

Hommel R, & Ratledge C. (1990) Evidence fro two fatty alcohol exidases in the biosurfactant-producing yeast *Candida* (Torulopsis) *bombicola*. *FEMS Microbiol. Lett.* 70: 183-186.

Hortencia SJ, & Roberto ZS. (2005) Intracellular fate of hydrocarbons: Possible existence of specific compartments for their biodegradation. *Appl. Biochem. Biotech.* 121: 205-218.

Hounsell EF, Davies MJ, & Smith KD. (1997) Chemical methods of analysis of glycoproteins. Protein protocol handbook (Walker, J.M., Ed.), Humana press, Totawa, NJ, pp. 803-804.

http://www.brenda.uni-koeln.de/php/flat_result.php4?ecno=1.1.3.6

Hummel W. (1999) Large-scale applications of NAD(P)-dependent oxidoreductases: recent development. *Trends. Biotechnol.* 17: 487-491.

Hwang JS, Yamada K, Honda A, Nakade K, & Ishihama A. (2000) Expression of functional influenza virus RNA polymerase in the methylotrophic yeast *Pichia pastoris*. *J. Virol.* 74: 4074-4084.

Isobe K, Kato A, Ogawa J, Kataoka M, Iwasaki A, Hasegawa J, & Shimizu S. (2007) Characterization of alcohol oxidase from *Aspergillus ochraceus* AIU 031. *J. Gen. Appl. Microbiol.* 53: 177-183.

Janssen FW, Rerwin RM, & Ruelius HW. (1965) Alcohol oxidase, a novel enzyme from a basidiomycete. *Biochem. Biophys. Res. Co.* 20: 630-634.

Janssen FW, Kerwin RM, & Ruelius HW. (1975) Alcohol oxidase from basidiomycetes. *Methods. Enzymol*. 41B: 364-369.

Janssen FW, & Ruelius HW. (1968) Alcohol oxidase, a flavoprotein from several basidiomycetes species. Crystallization by fractional precipitation with polyethylene glycol. *Biochim. Biophys. Acta.* 151: 330-342.

Johansson K, Jonsson-Pettersson G, Gorton L, Marko-Varga G, Csoregi E. (1993) A reagentless amperometric biosensor for alcohol detection in column liquid chromatography based on coimmobilized peroxidase and alcohol oxidase in carbon paste. *J. Biotechnol.* 31: 301-316.

Jornvall H, Persson B, & Jeffery J. (1987) Characteristics of alcohol/polyol dehydrogenases. The zinc-containing long-chain alcohol dehydrogenases. *Eur. J. Biochem.* 167(2): 195-201.

Juhasz AL, & Naidu R. (2000) Bioremediation of high molecular weight polycyclic aromatic hydrocarbons: a review of the microbial degradation of benzo[*a*]pyrene. *Int. Biodeter. Biodegr***.** 45: 57–88.

Kanwar L, & Goswami P. (2002) Isolation of a *Pseudomonas* lipase produced in pure hydrocarbon substrate and its application in the synthesis of isoamyl acetate using membrane immobilized lipase. *Enzyme. Microb. Tech.* 31: 727-735.

Karlinski L, Ravnskov S, Kieliszewska-Rokicka B, & Larsen J. (2007) Fatty acid composition of various ectomycorrhizal fungi and ectomycorrhizas of Norway spruce. *Soil. Biol. Biochem.* 39: 854-866.

Kato N, Omori Y, Tani Y, & Ogata K. (1976) Alcohol oxidases of *Kloeckera sp.* and *Hansenula polymorpha*: Catalytic properties and subunit structures. *Eur. J. Biochem.* 64: 341-350.

Kawagoshi Y, & Fujita M. (1997) Purification and properties of polyvinyl alcohol oxidase with broad substrate range obtained from *Pseudomonas vesicularis var. povalolyticus PH*. *World. J. Microb. Biot.* 13: 273-277.

Kemp GD, Dickinson FM, & Ratledge C. (1988) Inducible long chain alcohol oxidase from alkane-grown *Candida tropicalis*. *Appl. Microbiol. Biot.* 29: 370-374.

Kemp GD, Dickinson FM, & Ratledge C. (1990) Light sensitivity of the *n*-alkane-induced fatty alcohol oxidase from *Candida tropicalis* and *Yarrowia lipolytica*. *Appl. Microbiol. Biot.* 32: 461-464.

Kemp GD, Dickinson FM, & Ratledge C. (1991) Activity and substrate specificity of the fatty alcohol oxidase of *Candida tropicalis* in organic solvents. *Appl. Microbiol. Biot.* 34: 441-445.

Kim SJ, Suzuki N, Uematsu Y, & Shoda M. (2001) Characterization of aryl alcohol oxidase produced by dye-decolorizing fungus, *Geotrichum candidum* Dec1. *J. Biosci. Bioeng.* 91: 166-172.

Kinderlerer JL. (1993) Fungal strategies for detoxification of medium chain fatty acids. *Int. Biodeter. Biodegr.* 32: 213-224.

Kirk PW, & Gordon AS. (1988) Hydrocarbon degradation by filamentous marine higher fungi. *Mycologia.* 80: 776-782.

Kirley TL. (1990) Inactivation of (Na^+, K^+)-ATPase by β-mercaptoethanol: Differential sensitivity to reduction of the three β subunit disulfide bonds. *J. Biol. Chem.* 265: 4227-4232.

Ko HS, Fujiwara H, Yokoyama Y, Ohno N, Amachi S, Shinoyama H, & Fujii T. (2005) Inducible production of alcohol oxidase and catalase in a pectin medium by *Thermoascus aurantiacus* IFO 31693. *J. Biosci. Bioeng.* 99: 290-292.

Komduur JA, Leao AN, Monastyrska I, Veenhuis M, & Kiel JA. (2002) Old yellow enzyme confers resistance of *Hansenula polymorpha* towards allyl alcohol. *Curr. Genet.* 41: 401-406.

Kondo T, Morikawa Y, & Hayashi N. (2008) Purification and characterization of alcohol oxidase from *Paecilomyces variotii* isolated as a formaldehyde-resistant fungus. *Appl. Microbiol. Biot.* 77: 995–1002.

Korpan YI, Gonchar MV, Sibirny AA, Martelet C, Elskaya AV, Gibson TD, & Soldatkin AP. (2000) Development of highly selective and stable potentiometric sensors for formaldehyde determination. *Biosens. Bioelectron.* 15: 77-83.

Kragl U, Kruse W, Hummel W, & Wandrey C. (1996) Enzyme engineering aspects of biocatalysis: Cofactor regeneration as example. *Biotechnol. Bioeng.* 52: 309-319.

Krauzova VI, II chenko AP, Sharyshev AA, & Lozinov AB. (1985) Possible pathways of the oxidation of higher alcohols by membrane fractions of yeast culture on hexadecane and hexadecanol. *Biochimie.* 50: 726-732.

Kroutil W, Mang H, Edegger K, & Faber K. (2004) Biocatalytic oxidation of primary and secondary alcohols. *Adv. Synth. Catal.* 346: 125-142.

Kumar AK, & Goswami P. (2006) Functional characterization of alcohol oxidases from *Aspergillus terreus* MTCC 6324. *Appl. Microbiol. Biot.* 72: 906-911.

Kumar AK, & Goswami P. (2008) Purification and properties of a novel broad substrate specific alcohol oxidase from *Aspergillus terreus* MTCC 6324. *BBA-Protein. Proteom.* (doi 10.1016/j.bbapap.2008.06.009).

Laemmli UK. (1970) Cleavage of structural proteins during the assembly of the head of bacteriophage T4. *Nature.* 227: 680-685.

Lahtinen P, Ahmad JU, Lankinen E, Pihko P, Leskel M, & Repo T. (2007) Organocatalyzed oxidation of alcohols to aldehydes with molecular oxygen. *J. Mol. Cat. A: Chem.* 275: 228-232.

Lanfranconi MP, Alvarez HM, & Studdert CA. (2003) A strain isolated from gas oil-contaminated soil displays chemotaxis towards gas oil and hexadecane. *Environ. Microbiol.* 5: 1002-1008.

Leahy JG, & Colwell RR. (1990) Microbial degradation of hydrocarbons in the environment. *Microbiol. Rev.* 54: 305–315.

Liden H, Vijayakumar AR, Gorton L, & Marko-Varga G. (1998) Rapid alcohol determination in plasma and urine by column liquid chromatography with biosensor detection. *J. Pharm. Biomed. Anal.* 17: 1111-1128.

Lin CC, & Yang MC. (2003) Cholesterol oxidation using hollow fiber dialyzer immobilized with cholesterol oxidase: preparation and properties. *Biotechnol. Prog.* 19: 361-364.

Li Z, Butikofer L, & Witholt B. (2004) A high-throughput measurement of enantiomeric excess of chiral alcohols by using two enzymes. *Angew. Chem.* 116: 1730-1734.

Luxova A, & Svatos A. (2006) Substrate specificity of membrane-bound alcohol oxidase from the tobacco hornworm moth (*Manduca sexta*) female pheromone glands. *J. Mol. Catal. B-Enzym.* 38: 37-42.

MacLachlan J, Wotherspoon ATL, Ansell RO, & Brooks CJW. (2000) Cholesterol oxidase: sources, physical properties and analytical applications, *J. Steroid. Biochem. Mol. Bio.* 72: 169-195.

Mainwaring MG, Lugo SD, Fingal RA, Kapp OH, & Vinogradov SN. (1986) The dissociation of the extracellular hemoglobin of *Lumbricus terrestris* at acid pH and its reassociation at neutral pH: A new model of its quaternary structure. *J. Biol. Chem.* 261: 10899-10908.

Mann V, Large A, Khan S, Malik Z, & Connock MJ. (1989) Aromatic alcohol oxidase: a new membrane-bound H_2O_2-generating enzyme in alimentary tiddues of the slug *Arion ater*. *J. Exp. Zool.* 251: 265-274.

Marzullo L, Cannio R, Giardina P, Santini MT, & Sannia G. (1995) Veratryl alcohol oxidase from *Pleurotus ostreatus* participates in lignin biodegradation and prevents polymerization of laccase-oxidized substrates. *J. Biol. Chem.* 270: 3823-3827.

Massey V, & Curti B. (1966) A new method of preparation of D-amino acid oxidase apoprotein and a conformational change after its combination with flavin adenine dinucleotide. *J. Biol. Chem.* 241: 3417-3423.

Mattevi A. (1998) The PHBH fold: not only flavoenzymes. *Biophys. Chem.* 70: 217-222.

Matthieu JM, & Quarles RH. (1973) Quantitative scanning of glycoproteins on polyacrylamide gels stained with periodic acid schiff Reagent (PAS). *Anal. Biochem.* 55: 313-316.

Mauersberger S, Kargel E, Matyashova RN, & Muller HG. (1987) Subcellular organization of alkane oxidation in the yeast *Candica maltosa*. *J. Basic. Microbiol.* 27: 565–582.

Miralles G, Grossi V, Acquaviva M, Duran R, Claude Bertrand J, & Cuny P. (2007) Alkane biodegradation and dynamics of phylogenetic subgroups of sulfate-reducing bacteria in an anoxic coastal marine sediment artificially contaminated with oil. *Chemosphere.* 68: 1327-1334.

Mitsubayashi K, Matsunaga H, Nishio G, Toda S, & Nakanishi Y. (2005) Bioelectronic sniffers for ethanol and acetaldehyde in breath air after drinking. *Biosens. Bioelectron.* 20: 1573–1579.

Molinari F. (2006) Oxidations with isolated and cell-bound dehydrogenases and oxidases. *Curr. Org. Chem.* 10: 1247-1263.

Moreau RA, & Huang AHC. (1979) Oxidation of fatty alcohol in the cotyledons of jojoba seedlings. *Arch. Biochem. Biophys.* 194: 422-430.

Moreau RA, & Huang AHC. (1981) Enzymes of wax ester catabolism in jojoba. *Methods. Enzymol.* 71: 804-813.

Morgan P, & Atlas RM. (1989) Hydrocarbon degradation in soils and methods for soil biotreatment. *Crit. Rev. Biotechnol.* 8: 305-333.

Morita M, & Watanabe Y. (1977) A secondary alcohol oxidase: a component of a polyvinyl alcohol degrading enzyme preparation. *Agric. Biol. Chem.* 41: 1535-1537.

Morita M, Hamada N, Sakai K, & Watanabe Y. (1979) Purification and properties of secondary alcohol oxidase from a strain of *Pseudomonas*. *Agric. Biol. Chem.* 43: 1225-1235.

Muheim A, Waldner R, Leisola MSA, & Fiechter A. (1990a) An extracellular aryl-alcohol oxidase from the white-rot fungus *Bjerkandera adusta*. *Enzyme. Microb. Tech.* 12: 204-209.

Muheim A, Leisola MSA, & Schoemaker HE. (1990b) Aryl-alcohol oxidase and lignin peroxidase from the white-rot fungus *Bjerkandera adusta. J. Biotechnol.* 13: 159-167.

Muncnerova & Augustin J. (1994) Fungal metabolism and detoxification of polycyclic aromatic hydrocarbons: a review. *Biores. Technol.* 48: 97–106.

Narvaez A, Suarez G, Popescu IC, Katakis I, & Dominguez E. (2000) Reagentless biosensors based on self-deposited redox polyelectrolyte oxidoreductases architectures. *Biosens. Bioelectron.* 15: 43-52.

Nemec T, Jernejc K, & Cimerman A. (1997) Sterols and fatty acids of different *Aspergillus* species. *FEMS. Microbiol. Lett.* 149: 201-205.

Nicolau E, Cabrera CR, & Berberena M. (2007) Immobilization of alcohol dehydrogenase on platinum surface by using self-assembly monolayer technique for biofuel cell applications. *J. Biotechnol.* 131: S125-S126.

Nichols CS, & Cromartie TH. (1980) Irreversible inactivation of the flavoenzyme alcohol, oxidase with acetylenic alcohols. *Biochem. Bioph. Res. Co.* 97: 216-221.

Nishida A, & Eriksson KE. (1987) Formation, purification, and partial characterization of methanol oxidase, a H_2O_2-producing enzyme in *Phanerochaete chrysosporium*. *Biotechnol. Appl. Bioc.* 9: 325-338.

Okamoto K, & Yanase H. (2002) Aryl alcohol oxidases from the white-rot basidiomycete *Pleurotus ostreatus*. *Mycoscience*. 43: 391-395.

Ozimek P, Veenhuis M, & van der Klei IJ. (2005) Alcohol oxidase: A complex peroxisomal, oligomeric flavoprotein. *FEMS. Yeast. Res.* 5: 975–983.

Ozimek P, van Dijk R, Latchev K, Gencedo C, Wang DY, van der Klei IJ, & Veenhuis M. (2003) Pyruvate carboxylase is an essential protein in the assembly of yeast peroxisomal oligomeric alcohol oxidase. *Mol. Biol. Cell.* 14: 786-797.

Patel RN, Hou CT, Laskin AI, & Derelanko P. (1981) Microbial oxidation of methanol: properties of crystallized alcohol oxidase from a yeast, *Pichia sp*. *Arch. Biochem. Biophys.* 210: 481-448.

Patrick MA, & Dugan PR. (1974) Influence of hydrocarbons and derivatives on the polar lipid fatty acids of an *Acinetobacter* isolate. *J. Bacteriol.* 119: 76-81.

Pedneault K, Angers P, Avis TJ, Gosselin A, & Tweddell RJ. (2007) Fatty acid profiles of polar and non-polar lipids of *Pleurotus ostreatus* and *P. cornucopiae* var. '*citrino-pileatus*' grown at different temperatures. *Mycol. Res.* 111: 1228-1234.

Pedrini N, Juarez MP, Crespo R, & de Alaniz MJ. (2006) Clues on the role of Beauveria bassiana catalases in alkane degradation events. *Mycologia.* 98: 528-534.

Pollegioni L, Wels G, Pilone MS, & Ghisla S. (1999) Kinetic mechanisms of cholesterol oxidase from *Streptomyces hygroscopicus* and *Brevibacterium sterolicum*. *Eur. J. Biochem.* 264: 140-151.

Pundir SCS. (2003) Co-immobilization of cholesterol esterase, cholesterol oxidase and peroxidase onto alkylamine glass beads for measurement of total cholesterol in serum. *Curr. Appl. Phys.* 3: 129–133.

Qian D, Du G, & Chen J. (2004) Isolation and culture characterization of a new polyvinyl alcohol-degrading strain: *Penicillium sp.* WSH02-21. *World. J. Microbiol. Biot.* 20: 587-591.

Radianingtyas H, & Wright PC. (2003) Alcohol dehydrogenases from thermophilic and hyperthermophilic archaea and bacteria. *FEMS. Microbiol. Rev.* 27: 593-616.

Radwan SS, & Sorkhoh NA. (1993) Lipids of *n*-alkane-utilizing microorganisms and their application potential. *Adv. Appl. Microbiol.* 39: 616-621.

Raibaud O, & Goldberg ME. (1976) The dissociated tryptophanase subunit is inactive. *J. Biol. Chem.* 251: 2820-2824.

Ram MK, Bertoncello P, Ding H, Paddeu S, & Nicolini C. (2001) Cholesterol biosensors prepared by layer-by-layer technique. *Biosens. Bioelectron.* 16: 849–856.

Ramanaviciusa A, Kausaitea A, & Ramanavicienea A. (2005) Biofuel cell based on direct bioelectrocatalysis. *Biosens. Bioelectron.* 20: 1962-1967.

Ramanaviciusa A, Kausaitea A, & Ramanavicienea A. (2008) Enzymatic biofuel cell based on anode and cathode powered by ethanol. *Biosens. Bioelectron.* doi:10.1016/j.bios.2008.06.048

Rangel-Aldao R, & Roseno OM. (1976) Dissociation and reassociation of the phosphorylated and non-phosphorylated forms of adenosine 3',5'-monophosphate-dependent protein kinase from bovine cardiac muscle. *J. Biol. Chem.* 251: 3375-3380.

Raper KB, & Fennel DT. (1977) *Aspergillus*. Robert E. Krieger Publishing Company, New York.

Raschke WC, Neiditch BR, Hendricks M, & Cregg JM. (1996) Inducible expression of a heterologous protein in *Hansenula polymorpha* using the alcohol oxidase 1 promoter of *Pichia pastoris*. *Gene.* 177: 163-167.

Recny MA, & Hager LP. (1982) Reconstitution of native *Escherichia coli* pyruvate oxidase from apoenzyme monomers and FAD. *J. Biol. Chem.* 257: 12878-12886.

Reid MF, & Fewson CA. (1994) Molecular characterization of microbial alcohol dehydrogenases. *Crit. Rev. Microbiol.* 20: 13-56.

Robelo CR, Novoa VZ, & Sandoval RZ. (2004) Effects of carbon source on expression of alcohol oxidase activity and on morphologic pattern of YR-1 strain, a filamentous fungus isolated from petroleum-contaminated soils. *Appl. Microbiol. Biot.* 113: 161-172.

Romanos MA, Scorer CA, & Clare J. (1992) Foreign gene expression in yeast: a review. *Yeast.* 8: 423-488.

Sahm H. (1977) Metabolism of methanol by yeasts. *Adv. Biochem. Eng.* 6: 77–103.

Sahm H, Schuette H, & Kula MR. (1982) Alcohol oxidase from *Candida boidinii*. *Methods. Enzymol.* 89: 424-428.

Sahm H, & Wanger F. (1973) Microbial assimilation of methanol. The ethanol and methanol oxidizing enzymes from the yeast *Candida boidinii*. *Eur. J. Biochem.* 36: 250-256.

Sakai K, Hamada N, & Watanabe Y. (1985) Purification and properties of secondary alcohol oxidase with an acidic isoelectric point. *Agric. Biol. Chem.* 49: 817-825.

Santos EO, Rosa CFC, Passos CT, Sanzo AVL, Burkert JFM, Kalil SJ, & Burkert CAV. (2008) Pre-screening of filamentous fungi isolated from a contaminated site in southern brazil for bioaugmentation purposes. *Afr. J. Biotechnol.* 7: 1314-1317.

Savitha J, & Ratledge C. (1991) Alcohol oxidase of *Aspergillus flavipes* grown on hexadecanol. *FEMS. Microbiol. Lett.* 80: 221-224.

Scopes RK. (1983) An iron-activated alcohol dehydrogenase. *FEBS. Lett.* 156: 303-306.

Scott TA, & Melvin EH. (1953) Determination of dextan with anthrone. *Anal. Biochem.* 25: 656-1660.

Segers G, Bradshaw N, Archer D, Blissett K, & Oliver RP. (2001) Alcohol oxidase is a novel pathogenic factor for *Cladosporium fulvum*, but aldehyde dehyrogenase is dispensible. *Mol. Plant. Microbe. In.* 13: 367-377.

Siebum A, van Wijk A, Schoevaart R, & Kiebooma T. (2006) Galactose oxidase and alcohol oxidase: Scope and limitations for the enzymatic synthesis of aldehydes. *J. Mol. Catal. B-Enzym*. 41: 141-145.

Shimao M, Nishimura Y, Kato N, & Sakazawa C. (1985) Localization of polyvinyl alcohol oxidase produced by a bacterial symbiont, *Pseudomonas sp.* strain VM15C. *Appl. Environ. Microbiol.* 49: 8-10.

Shimao M, Taniguchi Y, Shikata S, Kato N, & Sakazawa C. (1982) Production of polyvinyl alcohol oxidase by a symbiotic mixed culture. *Appl. Environ. Microb.* 44: 28-32.

Shimao M, Tsuda T, Takahashi M, Kato N, & Sakazawa C. (1983) Purification of membrane-bound polyinyl alcohol oxidase in *Pseudomonas sp*. VM15C. *FEMS. Microbiol. Lett*. 20: 429-433.

Slabas AR, Elborough K, Vanhanen S, West M, Cheng Q, Lindner N, Casey J, & Sanglard D. 23 September 1999. International patent application WO 99/47685.

Smith AG, & Brooks CJW. (1977) The substrate specificity and stereochemistry, reversibility and inhibition of the 3-oxo steroid Δ4-Δ5-isomerase component of cholesterol oxidase. *Biochem. J.* 167: 121-129.

Smith VJ, Green RA, & Hopkins TR. (2000) Determination of aspartame in beverages using an alcohol oxidase enzyme electrode. *J. Assoc. Off. Anal. Chem.* 72: 30-33.

Sofer W, & Presley MF. (1987) Analysis of alcohol dehydrogenase gene expression in Drosophila. *Annu. Rev*. 21: 203-225.

Stewart MQ, Esposito RD, Gowani J, & Goodman JM. (2001) Alcohol oxidase and dihydroxyacetone synthase, the abundant peroxisomal proteins of methylotrophic yeasts, assemble in different cellular compartments. *J. Cell. Sci.* 114: 2863-2868.

Sugiuchi H, Uji Y, Okabe H, Irie T, Uekama K, Kayahara N, & Miyauchi K, (1995) Direct measurement of high-density lipoprotein cholesterol in serum with polyethylene glycol-modifed enzymes and sulfated alpha-cyclodextrin. *Clin. Chem.* 41: 717-723.

Suzuki T. (1976) Purification and some properties of polyvinyl alcohol degrading enzyme produced by *Pseudomonas* O-3. *Agric. Biol. Chem.* 40: 497-504.

Suzuki T. (1978) Oxidation of secondary alcohols by polyvinyl alcohol degrading enzyme produced by *Pseudononas* O-3. *Agric. Biol. Chem.* 42: 1187-1194.

Suye SS. (1997) Purification and properties of alcohol oxidase from *Candida methanosorbosa* M-2003. *Curr. Microbiol.* 34: 374-377.

Szamecz B, Urban G, Rubiera R, Kucsera J, & Dorgai L. (2005) Identification of four alcohol oxidases from methylotrophic yeasts. *Yeast.* 22: 669-676.

Tahallah N, van den Heuvel RHH, van den Berg WAM, Maier CS, van Berkel WJH, & Heck AJR. (2002) Cofactor-dependent assembly of the flavoenzyme vanillyl-alcohol oxidase. *J. Biol. Chem.* 277: 36425-36432.

Tani Y, Miya T, & Ogata K. (1972a) The microbial metabolism of methanol. *Agric. Biol. Chem*. 36: 68-75.

Tani Y, Miya T, & Ogata K. (1972b) The microbial metabolism of methanol. Part II. Properties of crystalline alcohol oxidase from *Kloeckera sp*. No. 2201. *Agric. Biol. Chem*. 36: 76-83.

Thomas SM, DiCosimo R, & Nagarajan V. (2002) Biocatalysis: applications and potentials for the chemical industry. *Trends. Biotechnol.* 20: 238-242.

Van den Heuvel RHH, Fraaije MW, Mattevi A, Laane C, & van Berkel WJH. (2001) Vanillyl-alcohol oxidase, a tasteful biocatalyst. *J. Mol. Catal. B: Enzym.* 11: 185–188.

Van der Klei IJ, Bystryck LV, & Harder W. (1990) Alcohol oxidase from *Hansenula polymorpha* CBS 4732. *Methods. Enzymol.* 188: 420-427.

Van Der Klei IJ, Harder W, & Veenhuis M. (1991) Biosynthesis and assembly of alcohol oxidase, a peroxisomal matrix protein in methylotrophic yeasts: A review. *Yeast.* 7: 195-209.

Van Dijken JP, Otto R, & Harder W. (1976) Growth of *Hansenula polymorpha* in a methanol-limited chemostat. Physiological responses due to the involvement of

methanol oxidase as a key enzyme in methanol metabolism. *Arch. Microbiol.* 111: 137–144.

Van Hamme D, Singh A, & Ward OP. (2003) Recent advances in petroleum microbiology. *Microbiol. Mol. Biol. R.* 67: 503-549.

Vanhanen S, West M, Kroon JTM, Lindner N, Casey J, Cheng Q, Elborough KM, & Slabas AR. (2000) A consensus sequence for long-chain fatty-acid alcohol oxidases from Candida identifies a family of genes involved in lipid.omega-oxidation in yeast with homologues in plants and bacteria. *J. Biol. Chem.* 275: 4445-4452.

Varela E, Bockle B, Romero A, Martinez AT, & Martinez MJ. (2000) Biochemical characterization, cDNA cloning and protein crystallization of aryl-alcohol oxidase from *Pleurotus pulmonarius*. *Biochim. Biophys. Acta.* 1476: 129-138.

Varela E, Guillen F, Martinez AT, & Martinez MJ. (2001) Expression of *Pleurotus eryngii* aryl-alcohol oxidase in *Aspergillus nidulans*: purification and characterization of the recombinant enzyme. *Biochim. Biophys. Acta.* 1546: 107-113.

Vatsyayan P, Kumar AK, Goswami P, & Goswami P. (2008) Broad substrate cytochrome P450 monooxygenase activity in the cells of *Aspergillus terreus* MTCC 6324. *Biores. Technol.* 99: 68-75.

Veenhuis M, Sulter G, van der Klei I, & Harder W. (1989) Evidence for functional heterogeneity among microbodies in yeasts. *Arch. Microbiol.* 151: 105-110.

Veenhuis M, van Dijken JP, & Harder W. (1976) Cytochemical studies on the localization of methanol oxidase and other oxidases in peroxisomes of methanol grown *Hanensula polymorpha*. *Arch. Micbrobiol.* 111: 123-135.

Veenhuis M, van Dijken JP, & Harder W. (1983) The significance of peroxisomes in the metabolism of one-carbon compounds in yeasts. *Adv. Microb. Physiol.* 24: 1-82.

Visser NV, Wang D, Stanley WA, Groves MR, Wilmanns M, Veenhuis M, & van der Klei IJ. (2007) Octameric alcohol oxidase dissociates into stable, soluble monomers upon incubation with dimethylsulfoxide. *Arch. Biochem. Biophys.* 459: 208-213.

Walker JD, & Cooney JJ. (1973) Aliphatic hydrocarbons of *Cladosporium resinae* cultured on glucose, glutamic acid, and hydrocarbons. *Appl. Microbiol.* 26: 705-708.

Werner W, Rey HG, & Weilinger H. (1970) Uber die Eigenschaften eine neuen Chromogens fur die Blutzuckerbestimmung nach der GOD/POD Methode. *Z. Anal. Chem.* 254: 224-228.

Widdel F, Boetius A, & Rabus R. (2006) Anaerobic biodegradation of hydrocarbons including methane. *Prokaryotes.* 2: 1028-1049.

Willner EK & Buckmann AF. (2001) Self-powered enzyme-based biosensors. *J. Am. Chem. Soc.* 123**:** 10752-10753.

Yamada H, Shin KC, Kato N, Shimizu S, & Tani Y. (1979) Purification and characterization of alcohol oxidase from *Candida* 25-A. *Agric. Biol. Chem*. 43: 877-878.

Yuan SY, Wei SH, & Chang BV. (2000) Biodegradation of polycyclic aromatic hydrocarbons by a mixed culture. *Chemosphere.* 41: 1463-1468.

Zhan BZ, & Thompson A. (2004) Recent developments in the aerobic oxidation of alcohols. *Tetrahedron.* 60: 2917-2975.

LIST OF PUBLICATIONS

I. In Referred Journals

Kumar AK, & Goswami P. (2006) Functional characterization of alcohol oxidase from *Aspergillus terreus* MTCC 6324. *Appl. Microbiol. Biotechnol.* 72: 906-911.

Vatsyayan P, Kumar AK, Goswami P, & Goswami P. (2008) Broad Substrate Cytochrome-P450-monooxygenase activity in the cells of *Aspergillus terreus* MTCC 6324. *Biores. Technol.* 99: 68-75.

Kumar AK, & Goswami P. (2008) Purification and properties of a novel broad substrate specific alcohol oxidase from *Aspergillus terreus* MTCC 6324. *BBA- Protein. Proteom.*1784: 1552-1559.

Kumar AK, & Goswami P. (2009) Dissociation and reconstitution studies of a broad substrate specific multimeric alcohol oxidase protein produced by *A. terreus. J. Biochem.* 145: 259-265.

Kumar AK, Vatsyayan P, & Goswami P. (2009) High lipid production during growth of *Aspergillus terreus* on petroleum sludge (Communicated).

Kumar AK, & Goswami P. (2008) High yield conversions of different alcohols to carbonyl compounds catalyzed by a fungal alcohol oxidase (Communicated).

II. In Conferences

Kumar AK, & Goswami P. (2005) Alcohol Oxidases with novel catalytic properties from *A. terreus*. *Catalysis and Biocatalysis in Green Chemistry: Royal Society of Chemistry Conference*, Cambridge UK December 2005. (P-02).

Kumar AK, & Goswami P. (2005) Subcellular localization and partial characterization of alcohol oxidase produced by *Aspergillus terreus.* 46th Annual Conference, *MICROBIOTECH 2005*, Hyderabad. December 2005, Page no: 23 (Ind-5).

Vatsyayan P, Kumar AK, & Goswami P. (2005) Characterization of Alkane Oxygenase produced by *Aspergillus terreus.* 46th Annual Conference, *MICROBIOTECH 2005*, Hyderabad. December 2005, Page no: 103 (Ind-80).

Sushovan C, Lepakshi B, Kumar AK, Goswami P, & Goswami P. (2006) Trans esterification of lipid using immobilized *pseudomonas* lipase. Proceedings of International Conference on "*Bio-Fuel Vision* 2015", October.

Kumar AK, Vatsyayan P, & Goswami P. (2006) Purification and specific functional characterization of alcohol oxidases from *Aspergillus terreus* MTCC 6324. 75th Annual meeting of Society of Biological Chemists (INDIA), JNU, NewDelhi. December 2006, Page no: 69 (P-114).

Vatsyayan P, Kumar AK, Goswami P, & Goswami P. (2006) Localization and broad substrate Cytochrome-P450-monooxygenase activity in the cells of *Aspergillus terreus* MTCC 6324**.** 75th Annual meeting of Society of Biological Chemists (INDIA), JNU, NewDelhi. December 2006, Page no: 69 (P-115).

Vatsyayan P, Kumar AK, & Goswami P. (2006) Cytochrome-P450-monooxygenase of *Aspergillus terreus* MTCC 6324. BIND-06 Conference 2006, IIT Kanpur, UP. December 2006 (P-55).

Kumar AK, & Goswami P. (2007) Isolation and functional characterization of cholesterol oxidase produced by *Aspergillus terreus* MTCC 6324. International conference on New horizons in Biotechnology (NHBT-2007), Trivandrum. November 2007, Page no: 161 (IB-200).

Kumar AK, & Goswami P. (2007) Structure-function relationship studies of multimeric Alcohol oxidases from *Aspergillus terreus* MTCC 6324. 11th ADNAT Convention, Advances in Structural Biology & Structure Prediction, CCMB, Hyderabad. February 2007, Page no: 113 (P-40).

Kumar AK, & Goswami P. (2008) Dissociation, deflavination, reconstitution studies of a novel multimeric protein containing different alcohol oxidases produced by *Aspergillus terreus*. 33rd FEBS and 11th IUBMB conference, Athens. June 2008, Page no: 403 (PP8-66).

Vatsyayan P, Kumar AK, & Goswami P. (2008) A potential *Aspergillus terreus* strain for bioremediation of petroleum hydrocarbon. International Congress of Environmental Research, BITS Pilani, Goa.

III. Book Chapters

Sushovan C, Lepakshi B, Kumar AK, Goswami P, Dutta NN, & Goswami P. (2007) Transesterification of lipid using immobilized pseudomonas lipase. *Biodiesel. Production. Technologies.* 1st *ed*. Jaipur, Pointer Publishers. 2007. xviii, 206 p. ISBN: 8171325177.